OPEN ACCESS

African Journal of **Biotechnology**

June 2021
ISSN 1684-5315
DOI: 10.5897/AJB
www.academicjournals.org

ACADEMIC JOURNALS
expand your knowledge

About AJB

The African Journal of Biotechnology (AJB) is a peer reviewed journal which commenced publication in 2002. AJB publishes articles from all areas of biotechnology including medical and pharmaceutical biotechnology, molecular diagnostics, applied biochemistry, industrial microbiology, molecular biology, bioinformatics, genomics and proteomics, transcriptomics and genome editing, food and agricultural technologies, and metabolic engineering. Manuscripts on economic and ethical issues relating to biotechnology research are also considered.

Indexing

CAB Abstracts, CABI's Global Health Database, Chemical Abstracts (CAS Source Index) Dimensions Database, Google Scholar, Matrix of Information for The Analysis of Journals (MIAR), Microsoft Academic, Research Gate

Open Access Policy

Open Access is a publication model that enables the dissemination of research articles to the global community without restriction through the internet. All articles published under open access can be accessed by anyone with internet connection.

The African Journals of Biotechnology is an Open Access journal. Abstracts and full texts of all articles published in this journal are freely accessible to everyone immediately after publication without any form of restriction.

Article License

All articles published by African Journal of Biotechnology are licensed under the Creative Commons Attribution 4.0 International License. This permits anyone to copy, redistribute, remix, transmit and adapt the work provided the original work and source is appropriately cited. Citation should include the article DOI. The article license is displayed on the abstract page the following statement:

This article is published under the terms of the Creative Commons Attribution License 4.0
Please refer to https://creativecommons.org/licenses/by/4.0/legalcode for details
about Creative Commons Attribution License 4.0

Memberships and Standards

Academic Journals strongly supports the Open Access initiative. Abstracts and full texts of all articles published by Academic Journals are freely accessible to everyone immediately after publication.

All articles published by Academic Journals are licensed under the Creative Commons Attribution 4.0 International License (CC BY 4.0). This permits anyone to copy, redistribute, remix, transmit and adapt the work provided the original work and source is appropriately cited.

Crossref is an association of scholarly publishers that developed Digital Object Identification (DOI) system for the unique identification published materials. Academic Journals is a member of Crossref and uses the DOI system. All articles published by Academic Journals are issued DOI.

Similarity Check powered by iThenticate is an initiative started by CrossRef to help its members actively engage in efforts to prevent scholarly and professional plagiarism. Academic Journals is a member of Similarity Check.

CrossRef Cited-by Linking (formerly Forward Linking) is a service that allows you to discover how your publications are being cited and to incorporate that information into your online publication platform. Academic Journals is a member of CrossRef Cited-by.

Academic Journals is a member of the International Digital Publishing Forum (IDPF). The IDPF is the global trade and standards organization dedicated to the development and promotion of electronic publishing and content consumption.

Contact

Editorial Office: ajb@academicjournals.org

Help Desk: helpdesk@academicjournals.org

Website: http://www.academicjournals.org/journal/AJB

Submit manuscript online http://ms.academicjournals.org

Academic Journals
73023 Victoria Island, Lagos, Nigeria
ICEA Building, 17th Floor,
Kenyatta Avenue, Nairobi, Kenya.

Editor-in-Chief

Editorial Board Members

Table of Content

Vol. 20(6), pp.229-236, June 2021
DOI: 10.5897/AJB2021.17321
Article Number: 4D4E8F966969
ISSN: 1684-5315

http://www.academicjournals.org/AJB

ACADEMIC JOURNALS
expand your knowledge

African Journal of Biotechnology

Full Length Research Paper

Effect of VIUSID-Agro™ on the conversion of somatic embryos of coffee (*Coffea arabica* L.) cv. Red Caturra rojo-884

Laisyn Posada-Pérez[1*], Raúl Barbón Rodríguez[1], Alina Capote Pérez[1], Anabel Pérez Pérez[1], Yenny Padrón Montesino[1], Bulent Kukurtcu[2], Dion D. Daniels[3], Guillermo Reyes[4] and Rafael Gómez-Kosky[5]

[1]Instituto de Biotecnología de Las Plantas, Universidad Central "Marta Abreu" de Las Villas. Carretera a Camajuaní KM 5½, Santa Clara, Villa Clara, Cuba.
[2]Catalysis, S. L. Macarena, 14. 28016, Madrid, España, Spain.
[3]Faculty of Science and Technology, University of Belize, Hummingbird Avenue, Belmopan, Belize C.A., Belize.
[4]Facultad de Agronomía, Universidad Nacional Agraria (UNA), Managua, Nicaragua.
[5]Estación Territorial de Investigaciones de La Caña de Azúcar (ETICA Centro Villa Clara), Instituto de Investigaciones de La Caña de Azúcar (INICA), Autopista Nacional KM 246. Ranchuelo, Villa Clara, Cuba.

Received 3 February, 2021; Accepted 21 May, 2021

A critical factor in the *in vitro* propagation protocol via somatic embryogenesis of coffee is the survival and growth of plants under *ex vitro* conditions. The objective of this work was to determine the effect of VIUSID Agro™ during the conversion of somatic embryos of coffee cv. Red Caturra rojo-884 in semi-controlled culture conditions. Two solutions (0.5 and 0.8 mL L^{-1}) of the biostimulant were evaluated on *in vitro* plant. Applications were done twice daily for the first three days and thereafter once a day from day 7 to 90 days after transplanting. Survival rate at 15 days and morpho-physiological characteristics at 30, 60 and 90 days after transplanting were evaluated. All treatments with VIUSID-Agro™ and the control resulted in 100% survival. The concentration of 0.5 mL L^{-1} of VIUSID-Agro™ registered the better results in morpho-physiological variables. These results constitute the first report of the use of VIUSID Agro™ on *in vitro* plant of coffee during acclimatization phase.

Key words: Ex vitro acclimatization, coffee, conversion, somatic embryos, VIUSID Agro™.

INTRODUCTION

Coffee is one of the most important agricultural products. It ranks second in international trade after oil. As a crop, it covers approximately 10.2 million hectares in more than 80 countries, especially in the tropical and subtropical regions of Africa, Asia and Latin America. The economy of many coffee producing countries depends largely on the profits from this crop. More than 100 million people earn their income directly or indirectly from coffee

*Corresponding author. E-mail: laisyn@ibp.co.cu.

cultivated areas (Argoti and Belalcazar, 2017). In Cuba, the cultivation of coffee is an important aspect to increase the income of the national economy by concept of grain exportation. There are about 160,000 ha destined for cultivation (MINAG, 2018).

The economic importance of phyto-stimulants has grown in recent years, with market factors and the growing predominance of a culture of sustainability in economic development being the two main phenomena that drive the production and consumption of plant stimulants in the world. Plant biostimulants based on natural materials have received considerable attention by both the scientific community and commercial enterprises especially in the last two and a half decades (Yakhin et al., 2017). In view of this situation, the search for biological alternatives is necessary to solve the problems of fertilization of agricultural crops of agro-economic interest (Yu et al., 2004; Montano et al., 2007; Alarcón et al., 2012). Therefore, organic fertilization and phyto-stimulants are becoming increasingly important not only because of the yields that are usually achieved, but also because of the economic nature of their application and their contribution to the preservation of the environment (Núñez et al., 2010).

Foliar fertilization is a method by which nutrients are supplied to the plants through the leaves, basically in aqueous solutions in order to complement the fertilization performed in the soil, or to correct specific deficiencies in the same period of crop development. Physiologically speaking, all nutrients can be absorbed via foliar with greater or lesser speed at different times. This is so that theoretically the complete nutrition of the plant could be satisfied via foliar, but in practice it is not possible because of the high cost of numerous applications that would be necessary in order to meet the total requirements (Peña et al., 2015).

VIUSID Agro™ is another of the formulations that are used as plant growth stimulants. This has the particularity that all its components are subjected to the molecular activation technique, a procedure that leads to a considerable increase in the biological action of the substance. In addition, the product has been shown not to affect the environment and the health of the population. VIUSID Agro™ is a product that essentially contains *Ascophyllum nodosum* (algae extract), Potassium Phosphate, Malic Acid, Glucosamine, Aspartic acid, Arginine, Glycine, Tryptophan, Ascorbic acid, Zinc sulfate, Calcium Pantothenate, Pyridoxine, Folic acid, Cyanocobalamin, Monoammonium Glycyrrhizinate, Sodium Benzoate and Potassium Sorbateamino (Catalysis, 2019).

Gomez-Kosky et al. (2020) were the first researchers to study the effects of VIUSID Agro™ with reported very good results during *ex vitro* acclimatization of sugarcane (*Saccharum* spp.) *in vitro* plants in Cuba. The objective of this research is to study the effects of VIUSID Agro™ on the conversion of coffee somatic embryos.

MATERIALS AND METHODS

Plant materials

A total of 56 *in vitro* plants obtained by somatic embryogenesis of coffee (*C. arabica* L. cv. Red Caturra rojo-884) with 3 pairs of true leaves, 2.5–3.5 cm height and with radical development according to the protocol developed by Ortiz et al. (2017) were used by treatment. Before acclimatization, plants were washed with running water. They were subsequently placed in black polypropylene trays of 28 holes with a capacity of 200 cm^3 each, with a substrate composed of compost from bagasse (remains of the sugarcane industry), to which zeolite was added in proportion of 3:1 (v/v).

Effect of VIUSID Agro™ on *ex vitro* acclimatization of *in vitro* plants

Two solutions of VIUSID Agro™ (Catalysis, Spain) (0.5 and 0.8 mL L^{-1}) were prepared and applied on the leaves during the first 3 days after transplanting. These applications were done twice a day; at 9:00 am and at 4:00 pm. After one week in the *ex vitro* acclimatization phase, applications were reduced to a weekly basis up until 90 days under these conditions. These were carried out with a 16-L capacity backpack sprayer (Matabi, Spain), with flood nozzle (flood-jet) Lurmark AN 2.5, according to its technical parameters. *In vitro* plants from somatic embryos were used as control to which no applications of the biostimulant were made.

Survival rate, defined as the number of plants that survived, was assessed at 7 and 15 days. At 30, 60 and 90 days the height of the plants (cm) from the base to the apex, the number of leaves, length of the main root, and number of roots were evaluated. In addition, the fresh weight (gFW), the dry weight (gDW) and the total chlorophyll content (SPAD units) were evaluated as well.

Determination of fresh and dry weight

For the determination of fresh and dry weight, 10 plants from treatments were taken at 30, 60 and 90 days of cultivation in the shade house. The roots were washed with water to remove substrates. The fresh weight was determined with an analytical balance (SCALTEC, model SPD 54). Subsequently, for the determination of the dry weight, the plant material was dried in an oven (MERMERT) at a temperature of 70°C for 48 h and the weight was determined on an analytical balance (SCALTEC, model SPD 54).

Determination of total chlorophylls

The total chlorophyll content was determined using the SPAD-502 chlorophyll detector (Minolta, Japan). SPAD units are recorded through the chlorophyll meter that measures the relative concentration of chlorophyll by means of transmitted light through the leaf at 650 nm (photosynthetically active wavelength) and 940 nm (Piekielek et al., 1995).

Culture conditions

The trays with the in vitro plants were placed in a shade house, with black shade mesh (Saran) that allowed the light intensity to be reduced to 70%. Other environmental conditions in the shade

Table 1. Effect of VIUSID-Agro™ on the growth of *in vitro* coffee plants (*Coffea arabica* L.) cv. Red Caturra rojo-884 at 30 days of culture under *ex vitro* acclimatization conditions.

VIUSID (mL L^{-1})	Height (cm)	Number of leaves	Chlorophyll content (SPAD)	Fresh weight (gFW)	Dry weight (gDW)	Number of roots	Length of main root (cm)
0 (control)	2.18[b]	13.9[a]	19.03[a]	0.33[a]	0.07[a]	2.9[a]	2.51[a]
0.5	2.58[a]	15.6[a]	20.28[a]	0.33[a]	0.07[a]	3.0[a]	2.61[a]
0.8	2.72[a]	14.5[a]	21.52[a]	0.31[a]	0.06[b]	2.8[a]	2.62[a]
M±SE	2.49±0.05	14.6±0.35	20.27±0.56	0.32±0.01	0.06±0.002	2.9±0.14	2.58±0.12

Means with different letters within the same column differ statistically according to Tukey's test for $p < 0.05$ (n = 40).

house include an average daytime temperature of 27 ± 5°C, relative humidity of 70% and light intensity that ranged between 224 and 457 µmol m^{-2} s^{-1} measured with a LM 76 Light Meter luxmeter (Paris, France). An automated micro sprinkler irrigation system was used. The frequency of the irrigation was four times a day for two minutes.

Experimental design and statistical analysis

The experimental design used was completely randomized. The Shapiro-Wilk test and the homogeneity of variance by Levene were used in the analysis of normality of the variables. For the comparison between the means, a variance analysis (simple ANOVA) was applied and the difference between the means was determined by the Tukey test. The SPSS Statistical Package version 23.0 of 2015 for Windows was used. In all cases, the significant differences were established for $p \leq 0.05$. All experiments were carried out twice.

RESULTS AND DISCUSSION

Effect of VIUSID Agro™ on *ex vitro* acclimatization of *in vitro* plants

In vitro plants in both concentrations of VIUSID-Agro™ and in the control registered 100% of survival at 7 and 15 days after transplanting. However, a positive effect of VIUSID-Agro™ on the morphology and growth of *in vitro* plants of *C. arabica* L. cv. Red Caturra rojo was observed in relation the control. The highest heights of the plants were recorded in the treatments with VIUSID-Agro™ with no significant differences between both concentrations. At 30 days of cultivation in the *ex vitro* acclimatization phase there were significant differences between the treatments with VIUSID-Agro™ and the control only for plant height (Table 1).

There was no significant difference between the treatment with 0.5 mL L^{-1} of VIUSID-Agro™ and the control in dry weight, but both were significantly different to the treatment with 0.8 mL L^{-1}. There were no differences between the treatments and the control in number of leaves, chlorophyll content, fresh weight, number of roots and the length of the main root at 30 days of cultivation. A good morphological development of the plants was observed in all the treatments (Figure 1).

At 60 days after transplanting *in vitro* plants developed in treatment with 0.5 mL L^{-1} of VIUSID-Agro™ registered the highest values in all variables. The VIUSID-Agro™ treatments developed plants with no significant between them, but both were significant different to the control.

The treatments with VIUSID-Agro™ were statistical similar in number of leaves, but only the treatment with 0.5 mL L^{-1} of VIUSID-Agro™ was significant superior to the control (Table 2). However, no significant differences were found in total chlorophyll content, number of roots and the length of the main root between VIUSID Agro™ and the control.

The treatment with 0.5 mL L^{-1} solution of VIUSID Agro™ obtained value of fresh weight and dry weight was statistically superior to the treatment with 0.8 mL L^{-1} solution of VIUSID Agro™ and the control. Plants developed in treatment control registered the lowest fresh weight and dry weight, which indicates that it did not have an efficient growth compared to the treatments where VIUSID-Agro™ was applied. The height difference among the treatments can be observed in Figure 2.

No information was found to date on the use of VIUSID Agro™ in the *in vitro* propagation of coffee. There is not any published research in the last phase of the process (*ex vitro* acclimatization), which is where high survival and growth of in vitro plants must be guaranteed so that they can be taken to the field.

At 90 DAP, the treatment with 0.5 mL L^{-1} of VIUSID-Agro™ registered the highest values of plant height, number of leaves, fresh weight and dry weight were obtained with significant differences with the other treatments in the *ex vitro* acclimatization phase (Table 3). The height of the *in vitro* plants at 90 days after transplanting showed stimulatory effects on their growth by the biostimulant. This aspect is of utmost importance since it allows shortening their time period in the acclimatization phase, which is a crucial cost-saving component of the production process.

Another aspect to note that shows the positive effect of VIUSID-Agro™ is the SPAD absorbance values of chlorophyll reached at 90 days of cultivation. In the case of treatments with the application of this biostimulant,

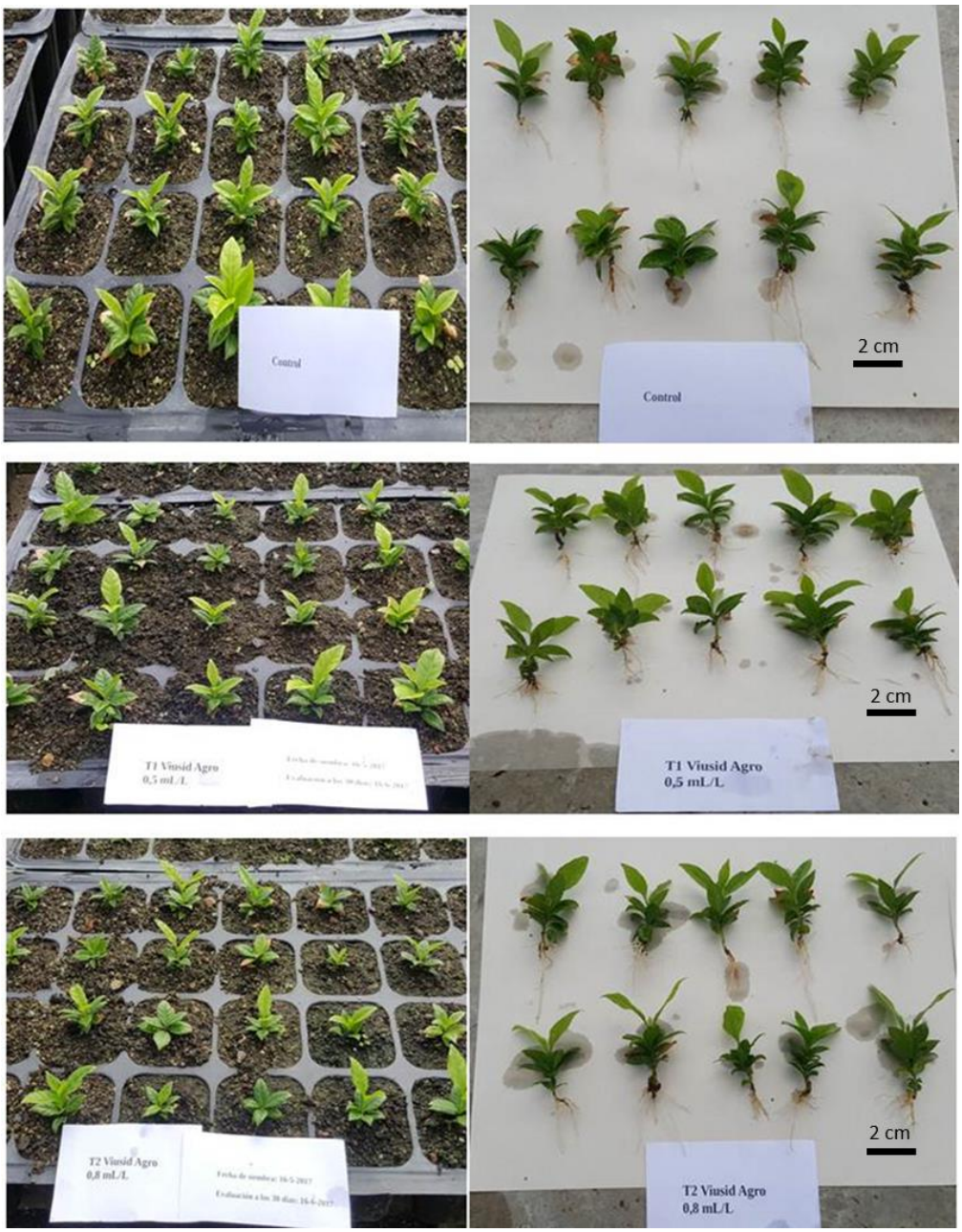

Figure 1. Somatic embryogenesis-derived *in vitro* coffee plants (*C. arabica* cv Caturra rojo-884) at 30 days after transplanting in *ex vitro* acclimatization phase with applications of 0.5 and 0.8 mL L^{-1} of VIUSID-Agro™.

higher values of SPAD (total chlorophyll) were obtained in relation to the control (Table 3). Gómez-Kosky et al., (2020) reported similar results using *in vitro* plant of sugarcane during the ex vitro acclimatization phase with the same biostimulant.

With regards to the number of roots, there were no significant differences between the control and 0.5 mL L^{-1} of VIUSID Agro™, but with the solution of 0.8 mL L^{-1} after 90 days. The two treatments and control were the same with respect to the length of the main root. The superiority of the results of 0.5 mL L^{-1} of VIUSID Agro™ could be observed over the other treatments with greater growth and development of plants (Figure 3). Accordingly, Pospisilova et al. (2007) noted that the fundamental aspect is that *in vitro* plants develop good rooting system because their nutrition depends largely on the

Table 2. Effect of VIUSID Agro™ on the growth of *in vitro* coffee plants (*Coffea arabica* L.) cv. Red Caturra rojo-884 at 60 days after transplanting under *ex vitro* acclimatization conditions.

VIUSID (mL L^{-1})	Height (cm)	Number of leaves	Chlorophyll content (S PAD)	Fresh weight (gFW)	Dry weight (gDW)	Number of roots	Length of main root (cm)
0 (control)	2.67[b]	13.6[b]	19.36[a]	0.43c	0.08c	3.3[a]	3.33[a]
0.5	3.85[a]	16.6[a]	20.58[a]	0.69[a]	0.15[a]	3.3[a]	3.93[a]
0.8	3.67[a]	15.6[ab]	21.65[a]	0.56[b]	0.13[b]	3.1[a]	3.29[a]
M±SE	3.39±0.09	15.26±0.41	20.53±0.98	0.56±0.02	0.12±0.01	3.23±0.08	3.51±0.17

Means with different letters within the same column differ statistically according to Tukey's test for $p<0.05$ (n = 40).

Figure 2. *In vitro* coffee plants (*C. arabica* cv. Red Caturra rojo -884) at 60 days after transplanting in *ex vitro* acclimatization phase with the application of VIUSID-Agro™. T-1 0.5 mL L^{-1} of VIUSID-Agro™ and T-2 0.8 mL L^{-1} of VIUSID-Agro™.

Table 3. Effect of VIUSID Agro™ on the growth of *in vitro* coffee plants (*Coffea arabica* L.) cv. Red Caturra rojo-884 at 90 days after transplanting in *ex vitro* acclimatization conditions.

VIUSID (mL L^{-1})	Height (cm)	Number of leaves	Chlorophyll content (SPAD)	Fresh weight (g FW)	Dry weight (gDW)	Number of roots	Length of main root (cm)
0 (control)	3.81[b]	18.3[b]	14.64[b]	3.98[b]	0.21[b]	3.70[a]	6.60[a]
0.5	7.48[a]	20.3[a]	26.45[a]	5.16[a]	0.48[a]	3.30[a]	6.55[a]
0.8	4.25[b]	16.4[b]	20.81[a]	3.79[b]	0.20[b]	2.50[b]	5.81[a]
M±SE	5.18±0.27	18.33±0.38	20.63±0.96	4.31±0.02	0.30±0.08	3.16±0.13	6.32±0.35

Means with different letters within the same column differ statistically according to Tukey's test for $p < 0.05$ (n = 40).

Figure 3. *In vitro* coffee plants (*C. arabica* cv. Red Caturra rojo-884) at 90 days after transplanting in *ex vitro* acclimatization phase with application of VIUSID-Agro™. T-1 0.5 mL L^{-1} of VIUSID-Agro™ and T-2 0.8 mL L^{-1} of VIUSID-Agro™.

functionality of the roots, as well as on nutrients accumulated in the seedlings before reaching *ex vitro* conditions.

Leaves play an important role in the development of *in vitro* plants. It was observed in this study that the biostimulant at 0.5 mL L^{-1} increased the number of leaves in the different treatments. In sugarcane (*Saccharum* spp cv. C90-469), Gómez-Kosky et al. (2020) reported that VIUSID Agro™ at 0.5 and 0.8 mL L^{-1} applied to *in vitro* plant during *ex vitro* acclimatization lead to leaf length and fresh weight exceeding those of the control.

Leaves produced *in vitro* are used for storage of carbon compounds, which are used in growth and development of the seedlings. When *in vitro* plants are transferred to *ex vitro* conditions, they maintain this function until new leaf emission. The first pair of leaves emitted in *ex vitro* conditions have autotrophic characteristics and temporarily accumulate photosynthate; where one part of these is retained by the leaf for growth and metabolism and the other part is exported outside the leaf to non-photosynthetic tissues and organs (Hazarika, 2003).

The results obtained in our study can be attributed to the composition of the VIUSID Agro™ formulation, which contains potassium phosphate that is necessary for the transfer and storage of energy in plants. In addition, it favors the formation of carbohydrates. The biostimulant also contains zinc sulfate that influences the creation and development of new tissues. Another component is glycine, which is a vital amino acid for growth, structural pillar of cytochromes and chlorophyll. This favors the formation of leaf tissue according to Catalysis (2019).

Besides, VIUSID Agro™ contains a group of amino acids, which are assimilated by plants through their leaves (Catalysis, 2019). The effects that can be produced when applying products with amino acids are of three types, one of which is hormonal: when amino acids enter plants, they stimulate the formation of chlorophyll, the auxin indole-3-acetic acid (IAA) and the production of vitamins and synthesis of numerous enzymatic systems (Simbaña and Carla, 2011). Another component of no less importance is folic acid that acts as a transporter of compounds. It is also a very important coenzyme in the metabolism of amino acids and in the synthesis of nitrogenous bases required for the formation of new tissues. Hence it positively influences growth of vegetative organs (Azcón-Bieto and Talón, 2008).

As reported by Catalysis (2019), the VIUSID Agro™ growth promoter was subjected to a biocatalytic process of molecular activation to improve its biological activity and the biochemical reactivity of all its molecules. It is an innovative liquid that, due to its components subjected to a biocatalytic process of molecular activation, make it different from the rest of the other products that can be similar to it on the market, since this process increases its effectiveness without altering its properties, producing a series of benefits when treating crops. The biocatalytic process of molecular activation greatly improves the biological activity and the biochemical reactivity of all antioxidant molecules. This activation method has been much more effective when applied to a much broader spectrum of water-soluble molecules.

Molecular activation is a process that increases the energy of molecules. This is possible due to the accumulation of additional electrons in the outer orbits of the molecules. Each component is activated separately following a specific protocol. This is what leads to its positive effects of growth and development in plants and hence an increase in yields.

Conclusion

VIUSID-Agro™ positively influenced *ex vitro* acclimatization of coffee plants. The greatest growth and development of plants from somatic embryos was achieved in the treatment with 0.5 mL L^{-1} of VIUSID-Agro™.

CONFLICT OF INTERESTS

The authors have not declared any conflict of interests.

REFERENCES

Alarcón A, Barreiro P, Alarcón A, Díaz SY (2012). Efecto del Biobras 16 y el Fitomas E en algunos indicadores del crecimiento y el rendimiento del tomate (*Solanum lycopersicum* L.) variedad 'Vyta'. Revista Granma Ciencia 1:1-10.

Argoti CA, Belalcazar BN (2017). El mercado del café en los contextos mundial, nacional y regional. Revista UNIMAR 35(2):325-348.

Azcón-Bieto J, Talón M (2008). Fundamentos de Fisiología Vegetal. Segunda Edición. 638 p.

Catalysis (2019). VIUSID Agro, promotor del crecimiento. http://www.catalysisagrovete.com. Accessed March 2019.

Gómez-Kosky R, Núñez DJ, Reyes CE, Bernal AV, Bermúdez MC, Machado PA, Álvarez JF, Pineda ER, Kukurtcu B, Daniels DD (2020). Effect of VIUSID Agro and FitoMas-E on the ex vitro acclimatization of sugarcane plants (Saccharum spp.) cultivar C90-469. Sugar Tech 22:42-51. https://doi.org/10.1007/s12355-019-00752-7

Hazarika B (2003). Acclimatization of tissue cultured plants. Current Science 85(12):1704-1712. https://doi.org/10.1007/s10529-010-0290-0

MINAG (2018). Estadísticas oficiales del Ministerio de la Agricultura. La Habana, Cuba. Jan. 2019.

Montano R, Zuaznabar R, García A, Viñals M, Villar J (2007). FitoMas E, bionutriente derivado de la industria azucarera: Instituto Cubano de Investigaciones de los Derivados de la Caña de Azúcar (ICIDCA) sobre los derivados de la industria azucarera. La Habana 41(3):14-21.

Núñez M, Mazorra LM, Martínez M (2010). Los brasinoesteroides y las respuestas de las plantas a estrés abióticos. Una visión actualizada. Cultivos Tropicales 31(2):17-21.

Ortiz N, Barbón R, Capote A, Pérez A, Robaina M (2017). Caracterización morfológica en vivero de plantas de *Coffea arabica* L. cv Caturra rojo J-884 obtenidas por embriogénesis somática. Biotecnología Vegetal 17(4):251-257.

Peña CK, Rodríguez FJC, Meléndrez JF (2015). Efecto de un promotor del crecimiento activado molecularmente sobre la germinación y la producción de frijol (*Phaseolus vulgaris* L.). Infociencia 19(3):1-12.

Piekielek W, Fox R, Toth JD, Macneal KE (1995). Use of a chlorophyll meter at the early dent stage of corn to evaluate nitrogen sufficiency. Agronomy Journal 87(3):403-408.

Pospisilova J, Synkova H, Haisel D, Semoradova S (2007). Acclimatization of plantles to *ex vitro* conditions: effects of air, humidity, irradiance, CO_2 concentration and abscisic acid. Acta Horticulturae 748:29-39.

Simbaña C, Carla L (2011). Estudio de las propiedades físicas y funcionales de un hidrolizado enzimático de proteína a escala piloto y su aplicación como fertilizante. http://bibdigital.epn.edu.ec/bitstream/15000/3762/1/CD-3535.pdf. Accessed, May 2019.

Yakhin OI, Lubyanov AA, Yakhin IA, Brown PH (2017). Biostimulants in Plant Science: A Global Perspective. Frontiers in Plant Science 7(2049):1-32. https://doi.org/10.3389/fpls.2016.02049.

Yu JQ, Feng LH, Hai WH, Hong YZ, Hua WM, Feng SY, Nogués S (2004). A role for brassinosteroids in the regulation of photosynthesis in *Cucumis sativus*. Journal of Experimental Botany 55(399):1135-1143.

Vol. 20(6), pp.237-250, June, 2021
DOI: 10.5897/AJB2021.17344
Article Number: 553C6AD67024
ISSN: 1684-5315

http://www.academicjournals.org/AJB

ACADEMIC JOURNALS
expand your knowledge

African Journal of Biotechnology

Review

CRISPR/Cas genome editing: A frontier for transforming precision cassava breeding

Bicko Steve Juma[1], Cecilia Mweu[1], Mathew Piero[2] and Wilton Mbinda[3,4*]

[1]Instutute for Biotechnology Research, Jomo Kenyatta University of Agriculture and Technology, Juja, Kenya.
[2]Department of Biochemistry, Microbiology and Biotechnology, Kenyatta University, Nairobi, Kenya.
[3]Department of Biochemistry and Biotechnology, Pwani University, Kilifi, Kenya.
[4]Pwani University Bioscience Research Centre (PUBReC), Pwani University, Kilifi, Kenya.

Received 1 April 2021; Accepted 25 May, 2021

Improved agricultural production of essential crops through advanced breeding is important for increasing access to nutritious food for the world's rapidly growing population, which is expected to reach 9.8 billion by 2050. Recent advancements in the clustered regularly interspaced short palindromic repeats/CRISPR-associated protein9 (CRISPR/Cas9) genome editing process, which uses single-guide RNA for genome editing, have made it easy, stable and efficient tool for targeted gene mutations, knockout and knock-in/replacement to boost crop yield. The CRISPR/Cas method is constantly being improved, and its applications have greatly expanded. It can be used to modify the genome sequence of any organism, including plants like cassava, to achieve the desired trait. As a result, CRISPR/Cas is regarded as a game-changing technology in plant biology. Here, we discuss the principles of operation, implementations and future prospects of CRISPR/Cas9 for efficient processing of individual genes in cassava cultures. Recent work on cassava crop with regards to the use of CRISPR/Cas9 for the plant improvement was also addressed.

Key words: *Manihot esculenta*, CRISPR/Cas9, genome editing, gRNA, protospacer adjacent motif (PAM).

INTRODUCTION

With a predicted global population of 9.8 billion people by 2050, the agri-food industry would need to double crop production rates (Clarke and Zhang, 2013; Ray et al., 2013). The ability to feed this rapidly growing population will soon become a critical issue that society, especially agricultural scientists, must address (Savary et al., 2019; Kumar et al., 2020). However, the five key crops that produce almost two-thirds of agricultural calories: maize, wheat, soybean, cassava and rice, currently have the production rates of 1.6, 0.9, 2.2, 1.3 and 1.0%, respectively, as compared to the expected rate of 2.4% (Ray et al., 2013; FAO, 2020). Again, developing new varieties in any crop takes time because it is dependent on the crop's generation cycle. Factors such as diminishing cultivable land, climate change, water scarcity, and increased demand for biofuels aggravate the situation (Ricroch, 2019). Climate change has an impact on crop production by hastening ecological stresses such as soil salinity, drought, and the emergence of new pathogens and insect pests, in

*Corresponding author. E-mail: w.mbinda@pu.ac.ke.

addition changing weather patterns (Godfray et al., 2010; Bhatta and Malla, 2020). Crops with higher yields, greater adaptability to changing climates, tolerance to biotic and abiotic stresses, improved nutrition, and lower resource requirements are being developed to meet this anticipated demand (Li and Xia, 2020).

Present day agriculture has evolved into an massive and complex production chain with ever increasing reliance on crop optimization via soil, water, postharvest management employing sophisticated machinery and facilities (Xingliang et al., 2018). Via self-pollination, cross-pollination, or clonal propagation, traditional breeding technologies have been used to improve crop production for important crops. Despite their use, these techniques have only been applied to a small number of crops, such as wheat and maize, which are widely grown in temperate regions around the world (Al-Khayri et al., 2015; Ansari et al., 2017), and limited diversity have further confined the amount of crop improvement that can be achieved through this process (Li et al., 2020). While conventional plant breeding is an extremely critical tool, it has its own constraints as well. To begin with, breeding can only take place between two plants that are sexually compatible. Secondly, numerous traits, including those that have negative effects on the yield potential, are transferred along with the traits of interest during crossing (ISAAA, 2020). Furthermore, in terms of edible crop crops, the incorporation of transgenes via these techniques is non-specific and is a matter of public concern. Finally, in terms of adapting elite varieties to local environmental conditions, these techniques remain time-consuming, resource-intensive, and expensive (Ghogare et al., 2020). As a result, breeding technological advancements are critical to overcoming the shortcomings of conventional breeding (Haque et al., 2018). Artificial mutagenesis, such as chemical mutagenesis, irradiation, and other modern methods, such as insertional mutagenesis by T-DNA insertion or transposon labeling, have been used to achieve these results (Xingliang et al., 2016). These modern mutagenesis have also encountered issues ranging from the random nature of induced mutations, low efficiency, time-consuming, laborious to being costly (Arora and Narula, 2017). Targeted gene technology based on homologous recombination has recently been developed, which allows for precise mutations, but they provide edits to limited number of species (Razzaq et al., 2019).

Speed breeding, also known as accelerated plant breeding cycle, has also risen to prominence in recent years as a modern and exciting breeding method that promises to grow new crop varieties faster, bringing hope to global food security (Ghosh et al., 2018a). This method involves growing plants in regulated growth chambers or greenhouses with optimal light intensity and quality (20 - 22 h), which speeds up various physiological processes in plants, particularly photosynthesis and flowering, and thus shortens the time of generation (Ghosh et al., 2018b). Rapid breeding techniques can involve any combination of the following methods: plant growth environment optimization (e.g., plant density, photoperiod, and temperature), flowering pathway genetic engineering, grafting juvenile plants to mature rootstocks, use of plant growth regulators, and early seed harvest (O'Connor et al., 2013; Ceballos et al., 2017). The method has been applied to produce 4 to 6 generation per year as compared to 2 to 3 generations per year for conventional breeding technologies under standard conditions (Nocker and Gardiner, 2014). This strategy is being applied in many orphaned crops, and standardization protocols are being developed for many perennial crops including apple (Chiurugwi et al., 2019). These techniques have not been utilized to the fullest as far cassava crop production is concerned, leading to the need for a fast, precise and simple methods for cassava crop improvement to alleviate the problem of food insecurity which is be brought about by the growing world population.

Advanced genome editing technology revolutionization has shown potential improvements in crops in recent years, making it easier to produce new varieties (Abdelrahman et al., 2018). These gene-specific genome editing technologies, zinc finger nucleases (ZFNs), transcriptional activator-like effector nucleases (TALENs), and more recently, clustered regularly interspaced short palindromic repeats (CRISPR), are important because they are fast, effective, and technically straightforward to use (Peisach et al., 2001; Christian et al., 2010; Georges and Ray, 2017). In the target DNA, the nucleases trigger double-stranded breaks. The DNA is then repaired using one of two pathways: nonhomologous end-joining repair (NHEJ) or homology guided repair (HDR); the former is the most common, resulting in insertions/deletions and substitution mutations in the target DNAs, resulting in insertions/deletions and substitution mutations in the target DNAs (Figure 1) (Savic et al., 2017). These tools also sparked the development of new transgene-free crop varieties that are difficult to differentiate from those developed using conventional breeding methods (Sharma et al., 2017). Clustered regularly interspaced short palindromic repeats (CRISPR)/CRISPR-associated proteins genome editing technology has shown greater promise in addressing agricultural challenges than its predecessors due to its ease, versatility, and effectiveness (Gupta and Musunuru, 2014; Mohan, Shibao and Silva., 2019). This technology can be used to alter virtually any genomic sequence in species, including plants, to achieve the desired characteristics since it only requires the presence of the protospacer adjacent motif (PAM) sequence (Mekler et al., 2020).

UNDERSTANDING CRISPR/CAS GENOME EDITING

CRISPR/Cas is a form of adaptive immunity discovered

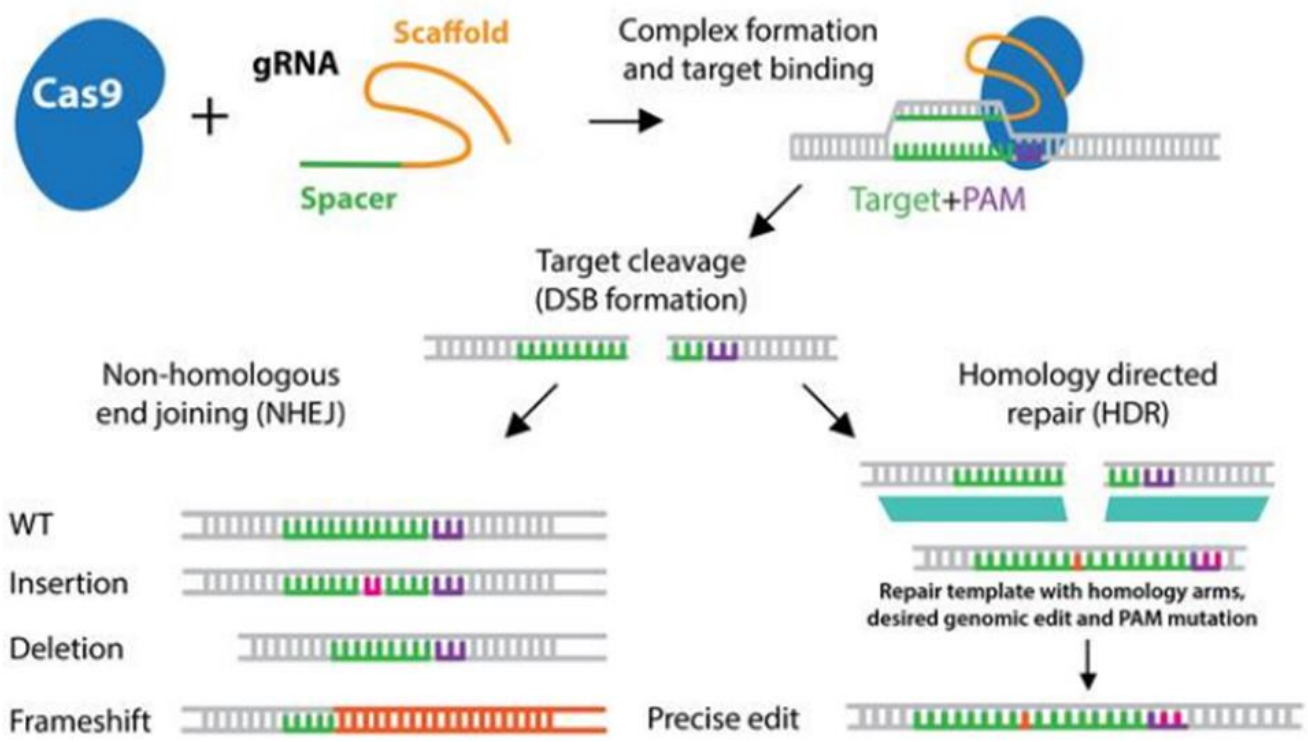

Figure 1. CRISPR/Cas9 for DSBs and NHEJ or HDR.
Source: Savic et al. (2017)

in prokaryotes in 1987 by Atsuo Nakata's group in Japan while researching the *iap* enzyme involved in isozyme conversion of alkaline phosphate in *Escherichia coli* (Ishino et al., 1987). It was not until 2005 that the CRISPR spacers were discovered to be extremely homologous with exogenous bacterial plasmids and phages enabling them to cleave foreign DNA (Watters, 2018). All at the same, the CRISPR-associated (Cas gene) genes were discovered (Jansen et al., 2002), and yields the Cas proteins (Barrangou and Horvath, 2017). CRISPR/Cas, a critical site-specific gene editing tool, was later developed in 2013, as described by two scientists named Jennifer Duodna and Emmanuelle Charpenteir, who demonstrated that CRISPR can be used to alter human genes outside the body (Jinek et al., 2012; Doudna and Charpentier, 2014). To cleave complex DNA sequences, the CRISPR-Cas system employs a combination of proteins and short RNAs (Hoffmann et al., 2019). Protospacers from foreign DNA sequences are collected by the bacteria, inserted into their genome, and used to make short guide RNAs, which are then used by the CRISPR-Cas system to kill any DNA sequences that match the protospacers (Musunuru, 2017).

CRISPR/Cas is faster, cheaper, and more effective at multiplexing genome editing than other previously developed genome editing tools like ZFNs and TALENs (Wang et al., 2018). CRISPR/Cas operations are rapidly expanding as a result of these benefits (Nakayama et al., 2013). In the not-too-distant future, genome editing technologies will have a tremendous impact on agriculture, because they will allow for direct and rapid genetic modification of various crops in the field (Xuejun et al., 2017). Between 1987 and 2002, several clusters of signature CRISPR-associated (Cas) genes were discovered to be conserved and usually adjacent to repeat components, laying the groundwork for the future classification of the CRISPR/Cas system into two major classes based on effector module design principles: class I and class II, which are further divided into six categories (Makarova et al., 2011, 2015). Classifications are based on the phylogeny, sequence, locus, organizations and contents of the CRISPR array. Class 1 systems have multi-subunit effector complexes made up of several Cas proteins with uneven stoichiometry, whereas class 2 systems have a single large multi-domain protein found almost exclusively in bacteria as an effector (Yoshizumi et al., 2018).

Each of the two CRISPR-Cas classes is divided into three categories, with types I, III, and IV belonging to class 1 and types II, V, and VI in class 2. Each type is distinguished by distinct effector module architectures that include distinct signature proteins (Shmakov et al., 2015). The presence of distinct signature proteins distinguishes types I, II, and III: Cas3 for type I, Cas9 for

type II, and Cas10 for type III (Rouillon et al., 2013). The CRISPR-associated complex for antiviral defense (CASCADE) and the Csm/Cmr RAMP complexes are multimeric effector complexes of type I and type III systems, respectively, that are architecturally identical and evolutionarily related (Young et al., 2019; Molina et al., 2020). Type III systems are thought to target both DNA and RNA, while type I and II systems are thought to target only DNA (Shmakov et al., 2017a). The signature protein, Cas10, is contained in type III CRISPR-Cas systems. The functionally uncharacterized type IV systems, unlike all other developed CRISPR-Cas systems, lack the adaptation module, which consists of the nucleases Cas1 and Cas2 (Makarova et al., 2015; Pinilla-Redondo et al., 2020). Spacers produced by type I systems are known to be used in the effector modules of subtype III-B systems, demonstrating the modularity of CRISPR-Cas systems (Garrett et al., 2011). While majority of the genomes encoding type IV systems do not carry recognizable CRISPR loci, it is not excluded that crRNAs from different CRISPR arrays are used by type IV systems, similar to subtype III-B systems, once they become available (Shmakov et al., 2015). Finally, based on additional signature genes and characteristic gene arrangements, each type is subdivided into several subtypes (I-A to F and U and III-A to D in class 1; II-A to C, V-A to E and U, and VI-A to C in class 2) (Shmakov et al., 2017b).

Much of the study currently focuses on type II CRISPR/Cas9 concepts and implementations, primarily because it has a drastically reduced number of Cas proteins (Yin et al., 2015). To change genes, the CRISPR/Cas9 system employs the CRISPR-associated 9 proteins, the CRISPR RNA (crRNA) set, which encodes the guide RNA, transactivating crRNA (tracrRNA), which aids in crRNA processing, and ribonuclease III (RNase III). The use of type II CRISPR/Cas9 has resulted in significant crop improvement (Williams and Warman, 2017). The rapid production of the CRISPR/Cas9 genome editing system in plants has been addressed in many reviews (Ma et al., 2016; Liu et al., 2017; Georges and Ray, 2017; Haque et al., 2018; Manghwar et al., 2019). This paper presents a summary of recent CRISPR/Cas9 method innovations and applications in the cassava plant. Furthermore, it addresses the CRISPR/Cas method's potential growth and challenges, as well as its value for cassava crop research and enhancement.

MECHANISM OF CRISPR/CAS GENOME EDITING

CRISPR/Cas genome editing technology is a third (next)-generation genome editing method that was first used in plants in 2013 and is now the most commonly used tool for gene editing. It was found to be an RNA-guided adaptive immune system for bacteria and archaea against invasive nucleic acids (DNA or RNA) from viruses or plasmids (Carter and Wiedenheft, 2015). The CRISPR system is operated in three stages. The first being acquisition of Spacer, the second is the processing of crRNA, and the third is the degradation of interference and targets. The CRISPR/Cas device accomplishes this by identifying and killing invading foreign DNA. By inserting fragments of the invader's genetic material into their CRISPRs and spacer arrays, these systems recall the invasion history. The CRISPR/Cas system accomplishes this by identifying and destroying invading foreign DNA. These systems recall the invasion history by inserting fragments of the invader's genetic material into their CRISPRs and spacer arrays. By inserting fragments of the invader's genetic material into their CRISPRs and spacer arrays, these systems recall the invasion history (Zhang et al., 2018). It was a landmark moment in the use of CRISPR/Cas9 when Cong et al. (2013) engineered two CRISPR/Cas9 systems and demonstrated that short RNAs could direct Cas nucleases to induce precise cleavage at endogenous loci in animals.

The CRISPR/Cas9 system is based on the type II CRISPR system, which has three main components: the CRISPR-associated protein (Cas9) and two noncoding CRISPR RNAs (tracrRNA and precursor CRISPR RNA) (pre-crRNA) (Walsh and Hochedlinger, 2013). Cas9 is an endonuclease protein derived from *Streptococcus pyogenes* that has an HNH nuclease domain in the middle and a RuvC-like nuclease domain at the amino terminus. It is responsible for crRNA maturation and the introduction of targeted DSBs, which is coordinated by tracrRNA and double-stranded RNA specific RNA III (Peng et al., 2016). The HNH domain cuts the crRNA's complementary strands, while the RuvC-like domain cleaves the double-stranded DNA's opposite strand (Jinek et al., 2014; Zuo et al., 2019). In the engineered type II CRISPR/Cas9 system, two noncoding CRISPR RNAs are fused to form a synthetic dimer, single guide RNA (sgRNA). crRNA is useful for directing the nucleolytic activity of the Cas9 enzyme to degrade the target nucleic acids (Hussain et al., 2018). The molecule of sgRNA is approximately 100 nucleotides long. It has a 20-nt reference sequence at the 5' end that helps identify the target sequence, as well as the protospacer adjacent motif (PAM) sequence, which is normally the consensus NGG sequence (Tsai et al., 2015). The PAM flanking the 3'-end of the DNA target site helps Cas9 in dictating the DNA target search process and promoting self-versus non-self-discrimination because direct repeats lack PAM sites (Xiaonan et al., 2020). The loop structure at the 3' end of the sgRNA anchors the target sequence by the guide sequence and forms a complex with Cas9, which cleaves the double-stranded DNA and forms a double-stranded break (DSB) at this site (Ueta et al., 2017).

Following the formation of DSBs, the DNA repair mechanism can be activated using either error-prone

nonhomologous end-joining (NHEJ) or homology directed repair (HDR) (Figure 1) (Symington and Gautier, 2011; Stinson et al., 2020). In most cases, NHEJ is used to repair DSBs in the absence of homologous DNA, and it is a simple way to generate mismatches and gene insertions/deletions (indels), which frequently result in frameshift mutations if they occur in the coding sequence of a gene, effectively creating a gene knockout (Zaidi et al., 2018). HDR triggers unique gene replacement or foreign DNA knock-ins when an exogenous homology repair template is present (Fauser et al., 2014). These processes allow CRISPR/Cas9 to edit the genomes of a wide variety of organisms, including plants (Schenke and Cai, 2020). Numerous crops have had their genomes edited using the CRISPR/Cas9 technique, such as rice (Zhou et al., 2014; Macovei et al., 2018), tobacco (Gao et al., 2015), maize (Doll et al., 2019; Lee et al., 2019), wheat (Bhowmik et al., 2018; Okada et al., 2019), *Arabidopsis* (Zhang et al., 2018; Li et al., 2018), potato (Andersson et al., 2018), sorghum (Che et al., 2018; Char et al., 2020), tomato (Tashkandi et al., 2018), cotton (Li et al., 2019; Qin et al., 2020), soybean (Li et al., 2015), cucumber, rapeseed (Braatz et al., 2017), barley (Lawrenson et al., 2015) and cassava (Odipio et al., 2017; Gomez et al., 2019), for trait improvement.

While the CRISPR/Cas system has been used to boost food security in a variety of crops, is yet to be extensively utilized in cassava, a crop that is considered a potential food reserve. Cassava is among crops that survives in poor soils and can withstand the unfavourable climate change. This makes it a crop importance to curb the problem of food security in the world. The crop is affected by both abiotic and biotic stresses, in which utilization of CRISPR/Cas technology can be utilized to silence or knockout genes which are responsible for their expression. This review provides insight to works that have been done in regards to improving cassava plant.

CELLULAR DNA REPAIR MECHANISMS USING CRISPR/CAS9

CRISPR/Cas systems, particularly CRISPR/Cas9, have been widely used to edit genomes. The CRISPR-Cas9 mechanism induces a Cas9-mediated double-strand break (DSB) in prokaryotes, which is directed by two small RNAs, a CRISPR RNA (crRNA) and a trans-acting crRNA (tracrRNA), or a chimeric single guide RNA (sgRNA). Homologous recombination (HR) and non-homologous end-joining (NEJ) are the two main competing and partially overlapping pathways for repairing DSBs (NHEJ) (Khoury et al., 2018; Jayavaradhan et al., 2019). NHEJ is a flaw-prone repair pathway that can result in frameshift and non-sense mutations by insertion and/or deletion of short DNA sequences at the DSB site, a mechanism widely exploited in recently developed CRISPR-based gene editing technology (Chhotaray et al., 2018). NHEJ is known as the canonical homology-independent pathway because it only involves the alignment of one to a few complementary bases at most for the re-ligation of two ends (Pardo et al., 2009). HR, on the other hand, is a conservative mechanism that results in the reciprocal exchanging of genetic information between two homologous DNA sequences or, typically, in the unidirectional conversion of genes. The dominance of these two repair mechanisms differs by species, cell type, cell cycle stage, and even end DNA resection, with NHEJ dominant in most somatic cells and HR dominating in yeast, germline, and mammalian embryonic stem cells (Sansbury et al., 2019).

In contrast to single-stranded annealing and breakage-induced replication, which involve short sequence homology, HR requires greater sequence homology when exchanging DNA segments. HR has a high degree of fidelity but a low rate of occurrence (Jasin and Rothstein, 2013). HR requires donor sequences that are homologous for insertion accuracy or substitution at the target site of integration into plant genomes at the DSB site (Shimada, 1978). It only occurs during the S and G2 phases of the cell cycle. HR requires that genetic modification performance be improved by inhibiting enzymes associated with the NHEJ pathway, such as DNA ligase IV (Schmidt et al., 2019). The use of ribonucleoprotein in conjunction with endonucleases can increase the efficiency of HR-mediated repair by a factor of 2 to 6. Injection efficiency is also increased by adjusting the delivery time in complexes that affect the cell cycle (Tang et al., 2019). Controlling endonuclease delivery during the cell cycle can also improve HR performance (Nambiar et al., 2019).

As previously demonstrated in maize and *Arabidopsis*, NHEJ is essential for DSB plant repair (Palareti et al., 2016). NHEJ does not occur naturally during the S/G2 phase of the cell cycle due to the lack of homologous DNA near the DSB, whereas HR does. NHEJ comes in two varieties: (i) Canonical nonhomologous end-joining (C-NHEJ) and (ii) Alternative nonhomologous end-joining (A-NHEJ) pathways (A-NHEJ). The C-NHEJ is ku-dependent, and both are prone to errors. C-NHEJ involves three steps: (1) the ku-protein recognizes and binds the DSBs in a sequence-independent manner; (2) the damaged ends of the DNA are enzymatically processed; and (3) DNA ligase IV ligation at the DSB ends (Shen et al., 2017).

Because NHEJ is prone to mistakes, using it to modify pathways in order to generate targeted knockouts frequently results in deletions or insertions (indels) (Malzahn et al., 2017). In plants, the leading pathway for repairing DNA DSBs is not dependent on a homologous donor (Bernheim et al., 2017). Because NHEJ's non-specificity in the genome reduces its effectiveness in gene targeting, the NHEJ pathway must be inhibited, while the HR pathway for gene editing must be improved,

and spontaneous incorporation of donor molecules and mutagenic off-target effects must be reduced (Li et al., 2017).

NHEJ involves the mechanism of partial end-restriction and promotion of direct ligation of enormous DSBs' free ends, while HR removes breaks and leaves no errors (McFarlane et al., 2018). Because of evolutionary requirements to ensure genome integrity as part of genome complexity, NHEJ in plant somatic cells remains highly subjective (Ye et al., 2018). HR repair involves substitution, chromosome rearrangement, gene disruption, correction, and insertion, while NHEJ repair involves insertions and deletions; thus, biologists must understand each repair pathway and the factors involved in these pathways in order to design experimental designs for genome modification in plants (Devkota, 2018).

For the works that have been done in respect to cassava, the DSBs repair mechanism which has been used commonly in the error-prone NHEJ pathway. For example, Mehta et al., (2018) stated that CRISPR systems failed to confer virus resistance during glasshouse inoculation, resulting in frame-shift mutations. Further analysis showed that there were viral escapes associated with NHEJ method of DNA repair.

DELIVERY OF CRISPR/CAS REAGENTS TO CASSAVA

The delivery of editing reagents to plants and the production of editing events are crucial steps in genome editing in plants. To introduce CRISPR-mediated reagents such as DNA, RNA, and ribonucleoproteins (RNPs) into plant cells, protoplast transfection, *Agrobacterium*-mediated transfer DNA (T-DNA) transformation, or particle bombardment may all be used (Hui-Li et al., 2014). Particle bombardment and *Agrobacterium*-mediated transformation are the two main methods for producing stable edited plants, while protoplast transfection is typically used for transfection expression (McFarlane et al., 2018).

CRISPR/Cas DNA genome editing with stable expression

CRISPR/Cas DNA is delivered into recipient cells via *Agrobacterium*-mediated transformation or particle bombardment and, by selecting for a marker gene, the DNA is integrated into the plant genome and expressed to achieve genome editing (Hui-Li et al., 2014; McFarlane et al., 2018). This strategy has been used in most types of plant genome editing, including cassava. Almost all of the genome editing work done in cassava using the CRISPR system has used the *Agrobacterium*-mediated delivery system for the reagents. The technique of delivery has been perceived to result into transgene mutants and is time-consuming since it involves the selection stages using the herbicide and/or antibiotics, hence has not been appreciated by the larger public population (Adhikari and Poudel, 2020).

CRISPR constructs and marker genes, on the other hand, have the potential to become incorporated into the genome and trigger side effects such as increased off-target changes, potentially limiting commercial applications. These issues can be avoided by obtaining transgene-free derivatives via genetic segregation via selfing and crossing. Another interesting strategy involves using the suicide genes CMS2 and BARNASE to remove transgene-containing pollen and embryos developed by the T0 plant (He et al., 2018). While genetic segregation is a good way to get transgene-free mutants, it cannot be used on asexually propagated crops like potatoes, bananas (*Musa* species), and cassava (*Manihot esculenta*). Furthermore, a fragment of the DNA build can be integrated into previously unknown locations. In researches involving cassava, these problems can be solved by the use of transient expression methods such as the use of protoplast transfection. The technique is fast as in does not requiring the selection step and produces transgene free mutants (Bhowmik et al., 2018).

Genome editing by transient expression of CRISPR/Cas DNA

Transient gene expression of CRISPR reagents provide an alternative delivery method for transgene-free editing. This approach eliminates canonical selection measures involving herbicides or antibiotics, enabling some of the regenerated plants to be edited without introducing foreign DNA into the genome. This method was first documented in wheat via protoplast transformation (Bhowmik et al., 2018). A CRISPR/Cas9 plasmid was delivered into immature wheat embryos via protoplast transfection, and the resulting plants were regenerated without selection pressure, cutting the time required for tissue culture regeneration by 3 to 4 weeks. The frequency of mutations was comparable to that of the conventional DNA-integration procedure, which employs tissue culture selection pressure. Importantly, transgenes were undetectable in up to 86.8% of T0 mutants. This technique could also be applied to cassava. Because the majority of cassava research using the CRISPR/Cas9 method employs an *Agrobacterium*-mediated delivery system, protoplast transfection may be the best option because it produces transgene-free products and eliminates the tissue culture selection phase.

ADVANTAGES OF CRISPR/CAS9 SYSTEM

Cas9 protein in CRISPR/Cas9 targets the foreign DNA through base pairing mechanism of guide RNAs. This identifies the target sequence upstream the PAM, this is in contrast with ZFNs or TALENs, which targets the DNA

using the protein. Hence, the DNA recognition is more accurate with less off-target effects and lower cytotoxicity (Gaj et al., 2013).

The CRISPR/Cas9 system research community follows an open access policy. In comparison to ZFN's proprietary platform, this has aided in the widespread adoption and use of this technology. https://chopchop.cbu.uib.no/, https://www.benchling.com/crispr/, and http://crispor.tefor.net/ are some of the tools available on the platform for selecting gRNA sequences and predicting specificity (Liu et al., 2017; Concordet and Haeussler, 2018; Labun et al., 2019). New researchers have been motivated to embrace the new technologies and contribute to the rapid understanding of the device and its applications as a result of this. Finally, the simplicity with which CRISPR/key Cas9 can be multiplexed is a practical benefit. DSB induction may be used to knock out genes or parallel pathways in an organism by simultaneously editing several genes at multiple sites (Mao et al., 2013). The strategy can also be used to induce deletions or insertions. Multiplexing using CRISPR/Cas9 requires a monomeric Cas9 protein and any different sequence specific gRNA (Li et al., 2012). CRISPR/Cas9 has also been used to modify multiplex genomes, allowing multiple traits to be stacked in an elite array (Wang et al., 2018). This can be accomplished in one of two ways: by assembling multiple sgRNAs into a single vector or by assembling multiple gRNA expression cassettes in separate vector assemblies.

DISADVANTAGES OF CRISPR/CAS SYSTEM

Off-target effects

These can alter a gene's function and cause genomic instability, reducing its capacity and functionality in even the most complex applications. Off-target effects can be reduced using a range of techniques, such as Bowte alignment, which allows for just three mismatches, and BWA tools, which allow for up to five (Hatem et al., 2011); SgRNA must recognize the specific protospacer adjacent motif (PAM) sequence in order for the CRISPR/Cas9 framework to work. In the absence of the PAM, the Cas9 endonuclease protein does not generate double-stranded breaks in the target DNA region. The SpCas9 variant needs a 5'-NGG-3' PAM just after the 20-nt target sequence, and it only recognizes the NGG PAM site, limiting the CRISPR/Cas9 system's effectiveness. The Agrobacterium-mediated transformation process is time-consuming and labor-intensive, and it causes spontaneous somatic mutations, making it ineffective (Manghwar et al., 2019); and public acceptance is the main setback it faces as far as the agricultural products are concerned. Since foreign DNA can causes side effects in many crops, regulatory authorities have imposed restrictions on modified crops to prevent the implementation of the CRISPR/Cas9 system (Adhikari and Poudel, 2020).

PROSPECTIVE APPLICATIONS OF CRISPR SYSTEM IN CASSAVA BREEDING

This approach is a promising tool for site-specific genome editing, and it is expected to have a larger impact on plant biology and crop breeding in the future. Genome editing techniques, as opposed to backcrossing in conventional breeding methods, enable elite cultivars to be precisely changed, resulting in cost savings. Since then, the CRISPR/Cas9 method has been used to improve a variety of traits in nearly 20 crop varieties, including yield and biotic and abiotic stress tolerance. It is expected that there will be a food shortage as the world's population grows, resulting in increased demand for food. Furthermore, pathogenic microorganism-induced biotic stresses account for up to 50% of possible yield loss. Many technologies, such as TALENs, ZFNs, and sequence specific nucleases (SSNs), have been developed by the research community to increase crop yield. As a result of predicted climate change, crops like cassava will be needed to withstand harsh weather conditions and grow well in low-fertility soils.

Cassava (*M. esculenta*) is a very important crop which is not only vital to food security in tropics and subtropics, but also a predominant raw material of starch industry (Zhou et al., 2013). Cassava is grown globally for the calories, of which it provides up to 50% (Bredeson et al., 2016) intake of calories for over 800 million people worldwide thus an important staple food (Prochnik et al., 2012). The crop tolerates periods of unpredicted drought (Tomlinson et al., 2018), grows well in poor soils, and can be harvested anytime of the year (Nassar, 2002). The tubers can be retained in the soil for up to two years without rotting (Siritunga and Sayre, 2003). However, there are only few studies on the validity of the CRISPR technique in cassava compared to other crops like rice. Several genome editing projects involving the CRISPR/Cas9 method have recently been completed to increase the yield of cassava, a drought reserve crop, including disease resistance, rapid flowering, herbicide tolerance, and reduced cyanide content in the leaves and roots (Table 1) (Odipio et al., 2017; Hummel et al., 2018; Bull et al., 2018; Mehta et al., 2018; Gomez et al., 2019).

CASSAVA GENOME EDITING WITH CRISPR/CAS9 FOR RESISTANCE TO BIOTIC AND ABIOTIC STRESS

The loss of cassava yield due to disease-causing pathogens is much higher. The two most common diseases affecting cassava crop yield are African cassava mosaic virus (ACMV) and cassava brown streak disease (CBSD). They result in up to 50% crop yield loss

Table 1. Applications of CRISPR/Cas9 in cassava crop breeding.

Target gene	Technology	Method of transformation	Function of the gene	Phenotype (knock-in/knockout)	Repair pathway	References
Phytoene desaturase (MePDS)	CRISPR/Cas9 system	Agrobacterium-mediated delivery	Green pigmentation	Albino (knockout of MePDS)	NHEJ	Odipio et al. (2017)
Viral AC2 gene	CRISPR/Cas9 system	Agrobacterium-mediated delivery	Responsible for the expression of ACMV	Normal (knockout of AC2 gene)	NHEJ	Mehta et al. (2018)
PTST-1 and GBSS	CRISPR/Cas9 system	Agrobacterium-mediated delivery	Integration of flowering locus T of Arabidopsis to accelerate flowering	Accelerated flowering	NHEJ	Bull et al. (2018)
EPSPS	CRISPR/Cas9 system	Agrobacterium-mediated delivery	Activate tolerance to glyphosate (herbicide) in cassava	Normal	NHEJ and HDR	Hummel et al. (2018)
Multiple TFL1-like Floral Repressor	CRISPR/Cas9 system	Agrobacterium-mediated delivery	Floral repression	Activated flowering in cassava	NHEJ	Odipio et al. (2018)
eIF4E isoforms nCBP-1 and nCBP-2	CRISPR/Cas9 system	Agrobacterium-mediated delivery	Suppression of the symptoms of cassava brown streak disease	Normal	NHEJ	Gomez et al. (2019)
MeSSIII	CRISPR/Cas9 system	Agrobacterium-mediated delivery	Regulation of the synthesis of amylopectin glycan	Normal	NHEJ	Zhan et al. (2020)
MeSWEET10a	CRISPR/Cas9 system	Agrobacterium-mediated delivery	CBB susceptibility (S) gene	Visualization of the CBB infection *in vivo*	HDR	Veley et al. (2021)

in cassava. So many attempts have been developed to make disease resistant varieties. Gomez et al. (2019) pioneered the work of targeted mutation using Cas9/gRNA. The two isoforms of eIF4E, nCBP-1 and nCBP-2, were edited at the same time, resulting in heritable delayed and suppressed CBSD aerial symptoms, as well as reduced severity and frequency of storage root necrosis. By interference of the ACMV in cassava by the knockout of AC2 gene has led to transgenic lines of cassava offered at least 33 to 48% evolution of the gene resulting into resistance to ACMV. From the results, it was reported by Mehta et al., (2018) that this CRISPR system did not provide effective virus resistance during the glasshouse inoculations.

CRISPR/Cas9-mediated gene insertion and replacement has largely been used to create herbicide-resistant crop varieties. A crucial amino acid in the conserved domain of 5-enolpyruvylshikimate-3-phosphate synthase can be substituted to confer resistance to glyphosate-based herbicides (EPSPS). A process that uses the HR and NHEJ DNA repair pathways was used to improve herbicide resistance in cassava (Hummel et al., 2018). This method created phenotypically normal glyphosate tolerant cassava and demonstated the potential of gene editing for further improvement of cassava (Xuan Liu et al., 2017).

Furthermore, Veley et al., (2021) recently described the development of cassava that can be used to visualize the early stages of CBB infection *in vivo*. Plants with scarless nisertion of GFP at the 3' end of the CBB susceptibility (S) gene MeSWEET10a were created using CRISPR-mediated homolgy-directed repair (HDR). At the transcriptional and translational stages, this was successfully visualized.

TRAIT IMPROVEMENT VIA CRISPR/CAS9

By simultaneously developing *MESSIII-1* and *MESSIII-2* mutants isolated from *MESSIII* genes of cassava crop using CRISPR/Cas9 system resulted into cassava with edited genes related to starch synthesis pathway (Zhan Li et al., 2020). This research led to an examination of the role of genes in the regulation of amylopectin glucan

synthesis in cassava. Bull et al., (2018) showed that CRISPR/Cas9-mediated targeted mutagenesis of the two amylose synthesis genes, PTST1 and GBSS, can reduce or remove amylose content in root starch. It was also discovered that incorporating the *Arabidopsis* FLOWERING LOCUS T gene into the genome editing cassette accelerated cassava flowering, which is unusual in glasshouse conditions (Tyagi et al., 2021). By the use of CRISPR/Cas9 mediated disruption of Multiple TFL-like Floral Repressors, Odipio et al., (2018) was also able to achieve activated acceleration of flowering in cassava.

Since the mutants were phenotypically albino during cotyledon-stage somatic embryogenesis, researchers were able to understand the gene's role in the plant using CRISPR/Cas9-mediated genome editing technology to target the phytoene desaturase (MePDS) gene in cassava. This eliminated the need for gene sequencing to establish that a mutation had occurred at the target gene (Odipio et al., 2017). As a result, it served as a valuable forum for testing and optimizing the CRISPR/Cas9 process and other genome editing technologies in cassava.

FUTURE PERSPECTIVES FOR CRISPR/CAS9 IN CASSAVA BREEDING AND RESEARCH

Although CRISPR/Cas9-based genome editing technology has come a long way in recent years, it still faces a number of challenges, including off-target effects, CRISPR/Cas9 delivery methods, side effects on neighboring genes, and regulatory concerns. Even though the CRISPR/Cas9 system is still affected by these issues, it will undoubtedly revolutionize and resolve the majority of them. The CRISPR/Cas9 approach has sparked a surge of interest in genome editing in the scientific community. This quick, dependable, scalable, and low-cost method is expected to be widely used to boost crop performance and address food security in the near future. Cassava is one of these crops.

There have been several attempts to minimize the amount of cyanogenic glycosides in cassava. Attempts have been made to silence the genes responsible for the biosynthesis of cyanogenic glycosides in cassava, including the use of RNAi intervention as reported by Piero, (2013). In the future, this could be done by using the CRISPR/Cas9 method to knockout the cytochrome P450 genes (CYP79D1 and CYP79D2), which encode the enzymes valine monooxygenase I and valine monooxygenase II, which catalyze the dedicated first step in the biosynthesis of cyanogenic glycosides (Mikkelsen and Halkier, 2003).

The system's ability to deliver CRISPR/Cas9 machinery has always been a major obstacle. The latest cassava crop delivery systems are *Agrobacterium*-mediated and protoplast transfection using tissue culture methods, both of which are labor-intensive and time-consuming (Kivrak et al., 2021). As a result, improved *Agrobacterium*-mediated transformation could extend the delivery system's reach. This will necessitate further advances in genotype-dependent, tissue-free delivery via plant germlines or meristematic cells. Novel delivery systems based on nanotechnology and virus particle-like structures can also improve crop yield (Liu et al., 2009). Carbon nanotubes and polyethylenimine-mediated delivery, for example, have a lot of potential for expanding CRISPR/Cas9's usage because they cause little cellular damage, are low in toxicity, and yield higher transformation efficiencies (Kivrak et al., 2021).

One of the problems that prevents CRISPR/Cas9 from being commonly used is off-target activity. In order to achieve target precision and of the frequency of off-target performance, the Cas9 enzyme has undergone numerous attempts and modifications. Cas9 nuclease fused with FokI, for example, can be inactivated to increase specificity. Inactivation of Cas9 nuclease and double nicking with nickase also improve target activity. The method's specificity can also be improved by changing the PAM to a non-canonical NAG or NGA instead of the regular NGG. The use of a longer protospacer adjacent motif was previously the technique for reducing off-target cleavages. Off-target effects have been reduced by employing a variety of techniques, including Bowte alignment, which allows for only three mismatches, and BWA tools, which allow for up to five mismatches (Hatem et al., 2011). However, these tools are insufficient to solve the problem of off-targets. Increasing the applications of CRISPR/Cas9 by increasing the specificity of Cas9-linked base editors by extending gRNA sequences, linking with APOBEC1 with Cas9-HF1, and delivering base editors via RNPs (Martin et al., 2019).

CRISPR/SpCas9 has a wide range of potential applications in plant pathogens as a result of its growth. The ability to change the genomes of plant pathogens opens the door to disease resistance phenotypes. Although research is progressing to grow cassava crops resistant to the most common disease casing viruses, such as African cassava mosaic virus and cassava brown streak virus, these studies are still in the early stages. The CRISPR/Cas9 genome editing technique should be used to its full potential in the future for knockout genes, AC2 genes, and nCBP genes that confer plant pathogens (Mehta et al., 2018; Gomez et al., 2019).

CONCLUSION AND RECOMMENDATIONS

Food shortages would be exacerbated by the rise in global population to 9.8 billion by 2050, which will be followed by negative climate change. CRISPR/Cas9 has also come at a time when conventional breeding technology is struggling to keep up with the food demand. This possible genome editing has provided the scientific

community with the ability to precisely and quickly insert the desired traits than other conventional breeding techniques due to its versatility, durability, and robustness. In the near future, researchers will be interested in using this genome editing method to boost cassava crop production, quality, cyanogenic glycoside content in leaves and roots, biotic and abiotic stress tolerance, and other traits. Over the last four years, CRISPR/Cas9 has been extensively used in the cassava crop to combat both biotic and abiotic stresses, as well as to develop other essential agronomic traits. CRISPR/Cas9 is mainly used for genome editing and transcriptional control at the moment. CRISPR/Cas9 has also not been used in plants, despite the fact that it has been used for DNA labeling and epigenome editing. CRISPR/Cas9 may be used in plant DNA labeling with fluorescent-labeled Cas9 protein and optimized gRNA in the future, as well as epigenome editing through DNA methylation or histone modifications. The discovery of CRISPR/Cas9 core functions in genome editing has tremendous potential in medicinal plant science and opens up a multitude of new scientific avenues for gene function study. While CRISPR/Cas9 can be used to edit plant genomes, there are still some obstacles to overcome, such as reducing off-target rates, elucidating the mechanism behind this reduction, and optimizing Cas9 work. More research is required to enhance CRISPR/experimental Cas9's application in order to facilitate the potential growth of its basic and applied skill.

CONFLICT OF INTERESTS

The authors have not declared any conflict of interests.

REFERENCES

Abdelrahman M, Al-Sadi AM, Pour-Aboughadareh A, Burritt DJ, Tran LSP (2018). Genome editing using CRISPR/Cas9-targeted mutagenesis: An opportunity for yield improvements of crop plants grown under environmental stresses. Plant Physiology and Biochemistry 131:31-36. https://doi.org/10.1016/j.plaphy.2018.03.012

Adhikari P, Poudel M (2020). CRISPR-Cas9 in agriculture: Approaches, applications, future perspectives, and associated challenges. Malaysian Journal of Halal Research 3(1):6-16. https://doi.org/10.2478/mjhr-2020-0002

Al-Khayri JM, Jain SM, Johnson DV (2015). Advances in plant breeding strategies: Breeding, biotechnology and molecular tools. Advances in Plant Breeding Strategies: Breeding, Biotechnology and Molecular Tools (Vol. 1). https://doi.org/10.1007/978-3-319-22521-0

Andersson M, Turesson H, Olsson N, Fält AS, Ohlsson P, Gonzalez MN, Hofvander P (2018). Genome editing in potato via CRISPR-

Cas9 ribonucleoprotein delivery. Physiologia Plantarum 164(4):378-384. https://doi.org/10.1111/ppl.12731

Ansari A, Wang C, Wang J, Wang F, Liu P, Gao Y, Zhao K (2017). Engineered dwarf male-sterile rice: A promising genetic tool for facilitating recurrent selection in rice. Frontiers in Plant Science 8:1-11. https://doi.org/10.3389/fpls.2017.02132

Arora L, Narula A (2017). Gene editing and crop improvement using CRISPR-cas9 system. Frontiers in Plant Science 8:1932. https://doi.org/10.3389/fpls.2017.01932

Barrangou R, Horvath P (2017). A decade of discovery: CRISPR functions and applications. Nature Microbiology 2(7):1-9. https://doi.org/10.1038/nmicrobiol.2017.92

Bernheim A, Calvo-Villamañán A, Basier C, Cui L, Rocha EPC, Touchon M, Bikard D (2017). Inhibition of NHEJ repair by type II-A CRISPR-Cas systems in bacteria. Nature Communications 8(1):25-28. https://doi.org/10.1038/s41467-017-02350-1

Bhatta BP, Malla S (2020). Improving horticultural crops via crispr/cas9: Current successes and prospects. Plants 9(10):1-19. https://doi.org/10.3390/plants9101360

Bhowmik P, Ellison E, Polley B, Bollina V, Kulkarni M, Ghanbarnia K, Kagale S (2018). Targeted mutagenesis in wheat microspores using CRISPR/Cas9. Scientific Reports 8(1):1-10. https://doi.org/10.1038/s41598-018-24690-8

Braatz J, Harloff HJ, Mascher M, Stein N, Himmelbach A, Jung C (2017). CRISPR-Cas9 targeted mutagenesis leads to simultaneous modification of different homoeologous gene copies in polyploid oilseed rape (*Brassica napus*). Plant Physiology 174(2):935-942. https://doi.org/10.1104/pp.17.00426

Bredeson JV, Lyons JB, Prochnik SE, Wu GA, Ha CM, Edsinger-Gonzales E, Rokhsar DS (2016). Sequencing wild and cultivated cassava and related species reveals extensive interspecific hybridization and genetic diversity. Nature Biotechnology 34(5):562-570. https://doi.org/10.1038/nbt.3535

Bull SE, Seung D, Chanez C, Mehta D, Kuon JE, Truernit E, Vanderschuren H (2018). Accelerated ex situ breeding of GBSS- and PTST1-edited cassava for modified starch. Science Advances 4(9): eaat6086 https://doi.org/10.1126/sciadv.aat6086

Carter J, Wiedenheft B (2015). Snapshot: CRISPR-RNA-guided adaptive immune systems. Cell 163(1):260-260.e1. https://doi.org/10.1016/j.cell.2015.09.011

Ceballos H, Jaramillo J, Salazar S, Pineda L, Calle F, Setter T (2017). Induction of flowering in cassava through grafting. Journal of Plant Breeding and Crop Science 9(2)19-29. https://doi.org/10.5897/jpbcs2016.0617

Char SN, Wei J, Mu Q, Li X, Zhang ZJ, Yu J, Yang B (2020). An Agrobacterium-delivered CRISPR/Cas9 system for targeted mutagenesis in sorghum. Plant Biotechnology Journal 18(2):319-321. https://doi.org/10.1111/pbi.13229

Che P, Anand A, Wu E, Sander JD, Simon MK, Zhu W, Jones TJ (2018). Developing a flexible, high-efficiency Agrobacterium-mediated sorghum transformation system with broad application. Plant Biotechnology Journal 16(7):1388-1395. https://doi.org/10.1111/pbi.12879

Chiurugwi T, Kemp S, Powell W, Hickey LT (2019). Speed breeding orphan crops. Theoretical and Applied Genetics 132(3):607-616. https://doi.org/10.1007/s00122-018-3202-7

Christian M, Cermak T, Doyle EL, Schmidt C, Zhang F, Hummel A, Voytas DF (2010). Targeting DNA double-strand breaks with TAL effector nucleases. Genetics 186(2):756-761. https://doi.org/10.1534/genetics.110.120717

Clarke JL, Zhang P (2013). Plant biotechnology for food security and bioeconomy. Plant Molecular Biology 83(1-2):1-3. https://doi.org/10.1007/s11103-013-0097-1

Concordet JP, Haeussler M (2018). CRISPOR: Intuitive guide selection for CRISPR/Cas9 genome editing experiments and screens. Nucleic Acids Research 46(W1):W242-W245. https://doi.org/10.1093/nar/gky354

Devkota S (2018). The road less traveled: Strategies to enhance the frequency of homology-directed repair (HDR) for increased efficiency of CRISPR/Cas-mediated transgenesis. BMB Reports 51(9):437-443. https://doi.org/10.5483/BMBRep.2018.51.9.187

Doll NM, Gilles LM, Gérentes MF, Richard C, Just J, Fierlej Y, Widiez T (2019). Single and multiple gene knockouts by CRISPR-Cas9 in maize. Plant Cell Reports 38(4):487-501. https://doi.org/10.1007/s00299-019-02378-1

Doudna JA, Charpentier E (2014). The new frontier of genome engineering with CRISPR-Cas9. Science 346(6213). https://doi.org/10.1126/science.1258096

Fauser F, Schiml S, Puchta H (2014). Both CRISPR/Cas-based nucleases and nickases can be used efficiently for genome engineering in Arabidopsis thaliana. Plant Journal 79(2):348-359. https://doi.org/10.1111/tpj.12554

Gaj T, Gersbach CA, Barbas CF (2013). ZFN, TALEN, and CRISPR/Cas-based methods for genome engineering. Trends in Biotechnology 31(7)397-405 https://doi.org/10.1016/j.tibtech.2013.04.004

Gao J, Wang G, Ma S, Xie X, Wu X, Zhang X, Xia Q (2015). CRISPR/Cas9-mediated targeted mutagenesis in Nicotiana tabacum. Plant Molecular Biology 87(1-2):99-110. https://doi.org/10.1007/s11103-014-0263-0

Garrett RA, Vestergaard G, Shah SA (2011). Archaeal CRISPR-based immune systems: Exchangeable functional modules. Trends in Microbiology 19(11):549-556. https://doi.org/10.1016/j.tim.2011.08.002

Georges F, Ray H (2017). Genome editing of crops: A renewed opportunity for food security. GM Crops and Food 8(1):1-12. https://doi.org/10.1080/21645698.2016.1270489

Ghogare R, Williamson-Benavides B, Ramírez-Torres F, Dhingra A (2020). CRISPR-associated nucleases: the Dawn of a new age of efficient crop improvement. Transgenic Research 29:1-35 https://doi.org/10.1007/s11248-019-00181-y

Ghosh S, Watson A, Gonzalez-Navarro OE, Ramirez-Gonzalez RH, Yanes L, Mendoza-Suárez, M, Hickey LT (2018a). Speed breeding in growth chambers and glasshouses for crop breeding and model plant research. Nature Protocols 13(12):2944-2963. https://doi.org/10.1038/s41596-018-0072-z

Ghosh S, Watson A, Gonzalez-Navarro OE, Ramirez-Gonzalez RH, Yanes L, Mendoza-Suárez, M, Hickey LT (2018b). Speed breeding in growth chambers and glasshouses for crop breeding and model plant research. Nature Protocols 13(12):2944-2963 *BioRxiv*. https://doi.org/10.1101/369512

Godfray HCJ, Beddington JR, Crute IR, Haddad L, Lawrence D, Muir JF, Toulmin C (2010). Food security: The challenge of feeding 9 billion people. Science 327(5967):812-818. https://doi.org/10.1126/science.1185383

Gomez MA, Lin ZD, Moll T, Chauhan RD, Hayden L, Renninger K, Bart RS (2019). Simultaneous CRISPR/Cas9-mediated editing of cassava eIF4E isoforms nCBP-1 and nCBP-2 reduces cassava brown streak disease symptom severity and incidence. Plant Biotechnology Journal 17(2):421-434. https://doi.org/10.1111/pbi.12987

Gupta RM, Musunuru K (2014). The emergence of genome-editing technology. The Journal of Clinical Investigation 124(10):4154-4161. https://doi.org/10.1172/JCI72992.transcription

Haque E, Taniguchi H, Hassan MM, Bhowmik P, Karim M R, Śmiech M, Islam T (2018). Application of CRISPR/Cas9 genome editing technology for the improvement of crops cultivated in tropical climates: Recent progress, prospects, and challenges. Frontiers in Plant Science 9:617. https://doi.org/10.3389/fpls.2018.00617

Hatem A, Bozdağ D, Çatalyürek ÜV (2011). Benchmarking short sequence mapping tools. Proceedings - 2011 IEEE International Conference on Bioinformatics and Biomedicine, BIBM 2011, 109-113. https://doi.org/10.1109/BIBM.2011.83

He Y, Zhu M, Wang L, Wu J, Wang Q, Wang R, Zhao Y (2018). Programmed Self-Elimination of the CRISPR/Cas9 Construct Greatly Accelerates the Isolation of Edited and Transgene-Free Rice Plants. Molecular Plant 11(9):1210-1213. https://doi.org/10.1016/j.molp.2018.05.005

Hoffmann MD, Aschenbrenner S, Grosse S, Rapti K, Domenger C, Fakhiri J, Niopek D (2019). Cell-specific CRISPR-Cas9 activation by microRNA-dependent expression of anti-CRISPR proteins. Nucleic Acids Research 47(13):e75 https://doi.org/10.1093/nar/gkz271

Hui-Li X, D L, Wang Z, Zhang H, Han C, Liu B, Chen Q (2014). A CRISPR/Cas9 toolkit for multiplex genome editing in plants. Plant Biology 1(1):3-13. https://doi.org/10.1111/j.1439-0418.1914.tb01110.x

Hummel AW, Chauhan RD, Cermak T, Mutka AM, Vijayaraghavan A, Boyher A, Taylor NJ (2018). Allele exchange at the EPSPS locus confers glyphosate tolerance in cassava. Plant Biotechnology Journal 16(7):1275-1282. https://doi.org/10.1111/pbi.12868

Hussain B, Lucas SJ, Budak H (2018). CRISPR/Cas9 in plants: at play in the genome and at work for crop improvement. Briefings in Functional Genomics 17(5):319-328. https://doi.org/10.1093/bfgp/ely016

Ishino Y, Shinagawa H, Makino K, Amemura M, Nakatura A (1987). Nucleotide sequence of the iap gene, responsible for alkaline phosphatase isoenzyme conversion in Escherichia coli, and identification of the gene product. Journal of Bacteriology 169(12):5429-5433. https://doi.org/10.1128/jb.169.12.5429-5433.1987

Ishino, Yoshizumi, Krupovic, M, Forterre P (2018). History of CRISPR-Cas from Encounter with a Mysterious. Journal of Bacteriology 200(7):e00580-17.

Jansen R, Van Embden JDA, Gaastra W, Schouls LM (2002). Identification of genes that are associated with DNA repeats in prokaryotes. Molecular Microbiology 43(6):1565-1575. https://doi.org/10.1046/j.1365-2958.2002.02839.x

Jasin M, Rothstein R (2013). Repair of strand breaks by homologous recombination. Cold Spring Harbor Perspectives in Biology 5(11):1-18. https://doi.org/10.1101/cshperspect.a012740

Jayavaradhan R, Pillis DM, Goodman M, Zhang F, Zhang Y, Andreassen PR, Malik P (2019). CRISPR-Cas9 fusion to dominant-negative 53BP1 enhances HDR and inhibits NHEJ specifically at Cas9 target sites. Nature Communications 10(1):1-13. https://doi.org/10.1038/s41467-019-10735-7

Jinek M, Chylinski K, Fonfara I, Hauer M, Doudna JA, Charpentier E (2012). A Programmable Dual-RNA - Guided 337(6096):816-821.

Jinek M, Jiang F, Taylor DW, Sternberg SH, Kaya E, Ma E, Doudna JA (2014). Structures of Cas9 endonucleases reveal RNA-mediated conformational activation. Science 343(6176):2-18. https://doi.org/10.1126/science.1247997

Khoury LYE, Campbell JM, Clark KJ (2018). The transition of zebrafish functional genetics from random mutagenesis to targeted integration. Molecular-Genetic and Statistical Techniques for Behavioral and Neural Research. Elsevier Inc. https://doi.org/10.1016/B978-0-12-804078-2.00017-9

Kivrak E, Pauzaite T, Copeland NA, Hardy JG, Kara P, Firlak M, Ozsoz M (2021). Detection of CRISPR-Cas9-Mediated Mutations Using a Carbon Nanotube-Modified Electrochemical Genosensor. Biosensors 11(1):17. https://doi.org/10.3390/bios11010017

Labun K, Montague TG, Krause M, Torres Cleuren YN, Tjeldnes H, Valen E (2019). CHOPCHOP v3: Expanding the CRISPR web toolbox beyond genome editing. Nucleic Acids Research *47*(W1):W171-W174. https://doi.org/10.1093/nar/gkz365

Lawrenson T, Shorinola O, Stacey N, Li C, Østergaard L, Patron N, Harwood W (2015). Induction of targeted, heritable mutations in barley and Brassica oleracea using RNA-guided Cas9 nuclease. Genome Biology 16(1):1-13. https://doi.org/10.1186/s13059-015-0826-7

Lee K, Zhang Y, Kleinstiver BP, Guo JA, Aryee MJ, Miller J, Wang K (2019). Activities and specificities of CRISPR/Cas9 and Cas12a nucleases for targeted mutagenesis in maize. Plant Biotechnology Journal 17(2):362-372. https://doi.org/10.1111/pbi.12982

Li C, Chen C, Chen H, Wang S, Chen X, Cui Y (2018). Verification of DNA motifs in Arabidopsis using CRISPR/Cas9-mediated mutagenesis. Plant Biotechnology Journal 16(8):1446-1451. https://doi.org/10.1111/pbi.12886

Li G, Zhang X, Zhong C, Mo J, Quan R, Yang J, Wu Z (2017). Small molecules enhance CRISPR/Cas9-mediated homology-directed genome editing in primary cells. Scientific Reports 7(1):1-11. https://doi.org/10.1038/s41598-017-09306-x

Li J, Manghwar H, Sun L, Wang P, Wang G, Sheng H, Zhang X (2019). Whole genome sequencing reveals rare off-target mutations and considerable inherent genetic or/and somaclonal variations in CRISPR/Cas9-edited cotton plants. Plant Biotechnology Journal, 17(5):858-868. https://doi.org/10.1111/pbi.13020

Li Q, Sapkota M, van der Knaap E (2020). Perspectives of CRISPR/Cas-mediated cis-engineering in horticulture: unlocking the neglected potential for crop improvement. Horticulture Research 7(1). https://doi.org/10.1038/s41438-020-0258-8

Li S, Xia L (2020). Precise gene replacement in plants through CRISPR/Cas genome editing technology: current status and future perspectives. ABIOTECH 1(1):58-73. https://doi.org/10.1007/s42994-019-00009-7

Li T, Liu B, Spalding MH, Weeks DP, Yang B (2012). High-efficiency TALEN-based gene editing produces disease-resistant rice. Nature Biotechnology 30(5):390-392. https://doi.org/10.1038/nbt.2199

Li, Zhan, Wang, Y, Lu X, Li, R, Liu J, Fu S, Yao Y (2020). Construction and Verification of CRISPR/Cas9 Gene Editing Vector for Cassava *MeSSIII* Gene. Molecular Plant Breeding 11(17):1-8. https://doi.org/10.5376/mpb.2020.11.0017
Li, Zhongsen, Liu, Z. Bin, Xing, A., Moon, B. P., Koellhoffer, J. P., Huang, L, Cigan, A. M. (2015). Cas9-guide RNA directed genome editing in soybean. Plant Physiology 169(2):960-970. https://doi.org/10.1104/pp.15.00783
Liu H, Ding Y, Zhou Y, Jin W, Xie K, Chen LL (2017). CRISPR-P 2.0: An Improved CRISPR-Cas9 Tool for Genome Editing in Plants. Molecular Plant 10(3):530-532. https://doi.org/10.1016/j.molp.2017.01.003
Liu Q, Chen B, Wang Q, Shi X, Xiao Z, Lin J, Fang X (2009). Carbon nanotubes as molecular transporters for walled plant cells. Nano Letters 9(3):1007-1010. https://doi.org/10.1021/nl803083u
Liu, Xuan, Wu, S, Xu J, Sui C, Wei J (2017). Application of CRISPR/Cas9 in plant biology. Acta Pharmaceutica Sinica B 7(3):292-302. https://doi.org/10.1016/j.apsb.2017.01.002
Liu, Xuejun, Xie C, Si, H, Yang J (2017). CRISPR/Cas9-mediated genome editing in plants. Methods 121-122:94-102. https://doi.org/10.1016/j.ymeth.2017.03.009
Xiaonan M, Zhang X, Liu H, Li Z (2020). Highly efficient DNA-free plant genome editing using virally delivered CRISPR-Cas9. Nature Plants 6(7):773-779. https://doi.org/10.1038/s41477-020-0704-5
Xingliang M, Mau M, Sharbel TF (2018). Genome Editing for Global Food Security. Trends in Biotechnology 36(2):123-127. https://doi.org/10.1016/j.tibtech.2017.08.004
Xingliang M, Zhu Q, Chen Y, Liu YG. (2016). CRISPR/Cas9 Platforms for Genome Editing in Plants: Developments and Applications. Molecular Plant 9(7):961-974. https://doi.org/10.1016/j.molp.2016.04.009
Macovei A, Sevilla NR, Cantos C, Jonson GB, Slamet-Loedin I, Čermák T, Chadha-Mohanty P (2018). Novel alleles of rice eIF4G generated by CRISPR/Cas9-targeted mutagenesis confer resistance to Rice tungro spherical virus. Plant Biotechnology Journal 16(11):1918-1927. https://doi.org/10.1111/pbi.12927
Makarova KS, Haft DH, Barrangou R, Brouns SJJ, Charpentier E, Horvath P, Koonin EV (2011). Evolution and classification of the CRISPR-Cas systems. Nature Reviews Microbiology 9(6):467-477. https://doi.org/10.1038/nrmicro2577
Makarova KS, Wolf YI, Alkhnbashi OS, Costa F, Shah SA, Saunders SJ, Koonin EV (2015). An updated evolutionary classification of CRISPR-Cas systems. Nature Reviews Microbiology 13(11):722-736. https://doi.org/10.1038/nrmicro3569
Malzahn A, Lowder L, Qi Y (2017). Plant genome editing with TALEN and CRISPR. Cell and Bioscience 7(1):1-18. https://doi.org/10.1186/s13578-017-0148-4
Manghwar H, Lindsey K, Zhang X, Jin S (2019). CRISPR/Cas System: Recent Advances and Future Prospects for Genome Editing. Trends in Plant Science 24(12):1102-1125. https://doi.org/10.1016/j.tplants.2019.09.006
Mao Y, Zhang H, Xu N, Zhang B, Gou F, Zhu JK (2013). Application of the CRISPR-Cas system for efficient genome engineering in plants. Molecular Plant 6(6):2008-2011. https://doi.org/10.1093/mp/sst121
Martin AS, Salamango DJ, Serebrenik AA, Shaban NM, Brown WL, Harris RS (2019). A panel of eGFP reporters for single base editing by APOBEC-Cas9 editosome complexes. Scientific Reports 9(1):1-8. https://doi.org/10.1038/s41598-018-36739-9
McFarlane GR, Whitelaw CBA, Lillico SG (2018). CRISPR-Based Gene Drives for Pest Control. Trends in Biotechnology 36(2):130-133. https://doi.org/10.1016/j.tibtech.2017.10.001
Mehta D, Stürchler A, Hirsch-Hoffmann M, Gruissem W, Vanderschuren H (2018). CRISPR-Cas9 interference in cassava linked to the evolution of editing-resistant geminiviruses. BioRxiv pp. 1-10. https://doi.org/10.1101/314542
Mekler V, Kuznedelov K, Severinov K (2020). Quantification of the affinities of CRISPR-Cas9 nucleases for cognate protospacer adjacent motif (PAM) sequences. Journal of Biological Chemistry 295(19):6509-6517. https://doi.org/10.1074/jbc.RA119.012239
Mikkelsen MD, Halkier BA (2003). Metabolic engineering of valine- and isoleucine-derived glucosinolates in arabidopsis expressing CYP79D2 from cassava. Plant Physiology 131(2):773-779. https://doi.org/10.1104/pp.013425
Molina R, Sofos N, Montoya G (2020). Structural basis of CRISPR-Cas Type III prokaryotic defence systems. Current Opinion in Structural Biology 65:119-129. https://doi.org/10.1016/j.sbi.2020.06.010
Musunuru K (2017). The hope and hype of CRISPR-Cas9 genome editing: A review. JAMA Cardiology 2(8):914-919. https://doi.org/10.1001/jamacardio.2017.1713
Nakayama T, Fish MB, Fisher M, Oomen-Hajagos J, Thomsen GH, Grainger RM (2013). Simple and efficient CRISPR/Cas9-mediated targeted mutagenesis in Xenopus tropicalis. Genesis 51(12):835-843. https://doi.org/10.1002/dvg.22720
Nambiar TS, Billon P, Diedenhofen G, Hayward SB, Taglialatela A, Cai K, Ciccia A (2019). Stimulation of CRISPR-mediated homology-directed repair by an engineered RAD18 variant. Nature Communications 10(1):1-13. https://doi.org/10.1038/s41467-019-11105-z
Nassar NMA (2002). Cassava, Manihot esculenta Crantz, genetic resources: Origin of the crop, its evolution and relationships with wild relatives. Genetics and Molecular Research 1(4):298-305. https://doi.org/0045 [pii]
Nocker S Van, Gardiner SE (2014). Breeding better cultivars, faster: Applications of new technologies for the rapid deployment of superior horticultural tree crops. Horticulture Research 1(1):1-8. https://doi.org/10.1038/hortres.2014.22
O'Connor DJ, Wright GC, Dieters MJ, George DL, Hunter MN, Tatnell JR, Fleischfresser DB (2013). Development and Application of Speed Breeding Technologies in a Commercial Peanut Breeding Program. Peanut Science 40(2):107-114. https://doi.org/10.3146/ps12-12.1
Odipio J, Alicai T, Ingelbrecht I, Nusinow DA, Bart R, Taylor NJ (2017). Efficient CRISPR/cas9 genome editing of phytoene desaturase in cassava. Frontiers in Plant Science 8:1780. https://doi.org/10.3389/fpls.2017.01780
Odipio J, Alicai T, Nusinow D, Bart R, Taylor N (2018). CRISPR/Cas9-mediated Disruption of Multiple TFL1-like Floral Repressors Activates Flowering in Cassava. In In Vitro Cellular and Developmental Biology-Animal 54:S47-S47. 233 Spring St, New York, NY 10013 Usa: Springer.
Okada A, Arndell T, Borisjuk N, Sharma N, Watson-Haigh NS, Tucker EJ, Whitford R (2019). CRISPR/Cas9-mediated knockout of Ms1 enables the rapid generation of male-sterile hexaploid wheat lines for use in hybrid seed production. Plant Biotechnology Journal 17(10):1905-1913. https://doi.org/10.1111/pbi.13106
Palareti G, Legnani C, Cosmi B, Antonucci E, Erba N, Poli D, Tosetto A (2016). Comparison between different D-Dimer cutoff values to assess the individual risk of recurrent venous thromboembolism: Analysis of results obtained in the DULCIS study. International Journal of Laboratory Hematology 38(1):42-49. https://doi.org/10.1111/ijlh.12426
Pardo B, Gómez-González B, Aguilera A (2009). DNA double-strand break repair: How to fix a broken relationship. Cellular and Molecular Life Sciences 66(6):1039-1056. https://doi.org/10.1007/s00018-009-8740-3
Piero Peisach E, Carl P, Robert G (2001). Design And Selection Ofnovel Cys2his2 Zinc Finger Proteins. Annual Review of Biochemistry 70(1):291-321.
Peng R, Lin G, Li J (2016). Potential pitfalls of CRISPR/Cas9-mediated genome editing. FEBS Journal 283(7):1218-1231. https://doi.org/10.1111/febs.13586
MN (2013). Regeneration and RNAi-mediated downregulation of cyano-glycoside biosynthesis in cassava 167. Retrieved from https://ir-library.ku.ac.ke/handle/123456789/9082
Pinilla-Redondo R, Mayo-Muñoz D, Russel J, Garrett RA, Randau L, Sørensen SJ, Shah SA (2020). Type IV CRISPR-Cas systems are highly diverse and involved in competition between plasmids. Nucleic Acids Research 48(4):2000-2012. https://doi.org/10.1093/nar/gkz1197
Prochnik S, Marri PR, Desany B, Rabinowicz PD, Kodira C, Mohiuddin M, Rounsley S (2012). The Cassava Genome: Current Progress, Future Directions. Tropical Plant Biology 5(1):88-94. https://doi.org/10.1007/s12042-011-9088-z
Qin L, Li J, Wang Q, Xu Z, Sun L, Alariqi M, Jin S (2020). High-efficient and precise base editing of C•G to T•A in the allotetraploid cotton

(*Gossypium hirsutum*) genome using a modified CRISPR/Cas9 system. Plant Biotechnology Journal 18(1):45-56. https://doi.org/10.1111/pbi.13168
Ray DK, Mueller ND, West PC, Foley JA (2013). Yield Trends Are Insufficient to Double Global Crop Production by 2050. PLoS ONE 8(6):e66428. https://doi.org/10.1371/journal.pone.0066428
Razzaq A, Saleem F, Kanwal M, Mustafa G, Yousaf S, Arshad HMI, KhanJoyia FA (2019). Modern trends in plant genome editing: An inclusive review of the CRISPR/Cas9 Toolbox. International Journal of Molecular Sciences 20(16). https://doi.org/10.3390/ijms20164045
Ricroch A (2019). Global developments of genome editing in agriculture. Transgenic Research 28(2):45-52. https://doi.org/10.1007/s11248-019-00133-6
Rouillon C, Zhou M, Zhang J, Politis A, Beilsten-Edmands V, Cannone G, White MF (2013). Structure of the CRISPR interference complex CSM reveals key similarities with cascade. Molecular Cell 52(1):124-134. https://doi.org/10.1016/j.molcel.2013.08.020
Sansbury BM, Hewes AM, Kmiec EB (2019). Understanding the diversity of genetic outcomes from CRISPR-Cas generated homology-directed repair. Communications Biology 2(1):1-10. https://doi.org/10.1038/s42003-019-0705-y
Savary S, Willocquet L, Pethybridge SJ, Esker P, McRoberts N, Nelson A (2019). The global burden of pathogens and pests on major food crops. Nature Ecology and Evolution 3(3):430-439. https://doi.org/10.1038/s41559-018-0793-y
Savic N, Ringnalda F, Bargsten K, Li Y, Berk C, Hall J, Schwank G (2017). Covalent linkage of the DNA repair template to the CRISPR/Cas9 complex enhances homology-directed repair. BioRxiv https://doi.org/10.1101/218149
Schenke D, Cai D (2020). Applications of CRISPR/Cas to Improve Crop Disease Resistance: Beyond Inactivation of Susceptibility Factors. Iscience 23(9):101478. https://doi.org/10.1016/j.isci.2020.101478
Schmidt C, Pacher M, Puchta H (2019). DNA break repair in plants and its application for genome engineering. Methods in Molecular Biology 1864:237-266. https://doi.org/10.1007/978-1-4939-8778-8_17
Sharma S, Kaur R, Singh A (2017). Recent advances in CRISPR/Cas mediated genome editing for crop improvement. Plant Biotechnology Reports 11(4):193-207. https://doi.org/10.1007/s11816-017-0446-7
Shen H, Strunks GD, Klemann BJPM, Hooykaas PJJ, de Pater S (2017). CRISPR/Cas9-induced double-strand break repair in Arabidopsis nonhomologous end-joining mutants. G3: Genes, Genomes, Genetics 7(1):193-202. https://doi.org/10.1534/g3.116.035204
Shimada T (1978). Plant regeneration from the callus induced from wheat embryo. The Japanese Journal of Genetics 53(5):371-374. https://doi.org/10.1266/jjg.53.371
Shmakov S, Abudayyeh OO, Makarova KS, Wolf YI, Gootenberg JS, Semenova E, Koonin EV (2015). Discovery and Functional Characterization of Diverse Class 2 CRISPR-Cas Systems. Molecular Cell 60(3):385-397. https://doi.org/10.1016/j.molcel.2015.10.008
Shmakov S, Smargon A, Scott D, Cox D, Pyzocha N, Yan W, Koonin EV (2017a). Diversity and evolution of class 2 CRISPR-Cas systems. Nature Reviews Microbiology 15(3):169-182. https://doi.org/10.1038/nrmicro.2016.184
Shmakov S, Smargon A, Scott D, Cox D, Pyzocha N, Yan W, Koonin EV (2017b). Diversity and evolution of class 2 CRISPR-Cas systems. Nature Reviews Microbiology 15(3):169-182. https://doi.org/10.1038/nrmicro.2016.184
Siritunga D, Sayre RT (2003). Generation of cyanogen-free transgenic cassava. Planta 217(3):367-373. https://doi.org/10.1007/s00425-003-1005-8
Stinson BM, Moreno AT, Walter JC, Loparo JJ (2020). A Mechanism to Minimize Errors during Non-homologous End Joining. Molecular Cell 77(5):1080-1091.
Symington LS, Gautier J (2011). Double-strand break end resection and repair pathway choice. Annual Review of Genetics 45:247-271. https://doi.org/10.1146/annurev-genet-110410-132435
Tang XD, Gao F, Liu MJ, Fan QL, Chen DK, Ma WT (2019). Methods for enhancing clustered regularly interspaced short palindromic repeats/Cas9-mediated homology-directed repair efficiency. Frontiers in Genetics 10:551.https://doi.org/10.3389/fgene.2019.00551
Tashkandi M, Ali Z, Aljedaani F, Shami A, Mahfouz MM (2018). Engineering resistance against Tomato yellow leaf curl virus via the CRISPR/Cas9 system in tomato. Plant Signaling and Behavior 13(10):1-7. https://doi.org/10.1080/15592324.2018.1525996
Tomlinson KR, Bailey AM, Alicai T, Seal S, Foster GD (2018). Cassava brown streak disease: historical timeline, current knowledge and future prospects. Molecular Plant Pathology 19(5):1282-1294. https://doi.org/10.1111/mpp.12613
Tsai SQ, Zheng Z, Nguyen NT, Liebers M, Topkar VV, Thapar V, Joung JK (2015). GUIDE-seq enables genome-wide profiling of off-target cleavage by CRISPR-Cas nucleases. Nature Biotechnology 33(2):187-198. https://doi.org/10.1038/nbt.3117
Tyagi S, Kumar R, Kumar V, Won SY, Shukla P (2021). Engineering disease resistant plants through CRISPR-Cas9 technology. GM Crops and Food 12(1):125-144. https://doi.org/10.1080/21645698.2020.1831729
Ueta R, Abe C, Watanabe T, Sugano SS, Ishihara R, Ezura H, Osakabe K (2017). Rapid breeding of parthenocarpic tomato plants using CRISPR/Cas9. Scientific Reports 7(1):1-8. https://doi.org/10.1038/s41598-017-00501-4
Veley KM, Okwuonu I, Jensen G, Yoder M, Taylor NJ, Meyers BC, Bart RS (2021). Gene tagging via CRISPR-mediated homology-directed repair in cassava. G3 Genes|Genomes|Genetics 11(4)::jkab028 https://doi.org/10.1093/g3journal/jkab028
Walsh RM, Hochedlinger K (2013). A variant CRISPR-Cas9 system adds versatility to genome engineering. Proceedings of the National Academy of Sciences of the United States of America 110(39):15514-15515. https://doi.org/10.1073/pnas.1314697110
Wang M, Wang S, Liang Z, Shi W, Gao C, Xia G (2018). From Genetic Stock to Genome Editing: Gene Exploitation in Wheat. Trends in Biotechnology 36(2):160-72. https://doi.org/10.1016/j.tibtech.2017.10.002
Wang W, Pan Q, He F, Akhunova A, Chao S, Trick H, Akhunov E (2018). Transgenerational CRISPR-Cas9 Activity Facilitates Multiplex Gene Editing in Allopolyploid Wheat. The CRISPR Journal 1(1):65-74. https://doi.org/10.1089/crispr.2017.0010
Watters K (2018). The CRISPR Revolution: Potential Impacts on Global Health Security. Retrieved from http://ebot.gmu.edu/handle/1920/11338
Williams BO, Warman ML (2017). CRISPR/CAS9 Technologies. Journal of Bone and Mineral Research 32(5):883-888. https://doi.org/10.1002/jbmr.3086
Chhotaray C, Tan Y, Mugweru J, Islam MM, Hameed HA, Wang S, Lu Z, Wang C, Li X, Tan S, Liu J (2018). Advances in the development of molecular genetic tools for Mycobacterium tuberculosis. Journal of Genetics and Genomics 45(6):281-297. https://doi.org/10.1016/j.jgg.2018.06.003
Ye L, Wang C, Hong L, Sun N, Chen D, Chen S, Han F (2018). Programmable DNA repair with CRISPRa/i enhanced homology-directed repair efficiency with a single Cas9. Cell Discovery 4(1):1-12 https://doi.org/10.1038/s41421-018-0049-7
Yin K, Han T, Liu G, Chen T, Wang Y, Yu AYL, Liu Y (2015). A geminivirus-based guide RNA delivery system for CRISPR/Cas9 mediated plant genome editing. Scientific Reports 5:1-10. https://doi.org/10.1038/srep14926
Young K, Gasior SL, Jones S, Wang L, Navarro P, Vickroy B, Barrangou R (2019). The repurposing of type I-E CRISPR-Cascade for gene activation in plants. Communications Biology 2(1):1-7. https://doi.org/10.1038/s42003-019-0637-6
Zaidi SSeA, Mukhtar MS, Mansoor S (2018). Genome Editing: Targeting Susceptibility Genes for Plant Disease Resistance. Trends in Biotechnology 36(9):898-906. https://doi.org/10.1016/j.tibtech.2018.04.005
Zhang Q, Xing HL, Wang ZP, Zhang HY, Yang F, Wang XC, Chen QJ (2018). Potential high-frequency off-target mutagenesis induced by CRISPR/Cas9 in Arabidopsis and its prevention. Plant Molecular Biology 96(4-5):445-456. https://doi.org/10.1007/s11103-018-0709-x
Zhang ZT, Jiménez-Bonilla P, Seo SO, Lu T, Jin YS, Blaschek HP, Wang Y (2018). Bacterial genome editing with CRISPR-Cas9: Taking clostridium beijerinckii as an example. Methods in Molecular Biology 1772:297-325. https://doi.org/10.1007/978-1-4939-7795-6_17
Zhou H, Liu B, Weeks DP, Spalding MH, Yang B (2014). Large

chromosomal deletions and heritable small genetic changes induced by CRISPR/Cas9 in rice. Nucleic Acids Research 42(17):10903-10914. https://doi.org/10.1093/nar/gku806

ZHOU W, MA Q, ZHANG P, WANG L, WANG H, XU J, YANG J (2013). Key Scientific Questions and Recent Advances in Cassava Molecular Breeding. Scientia Sinica Vitae 43(12):1082-1089. https://doi.org/10.1360/052013-320

Zuo Z, Zolekar A, Babu K, Lin VJ, Hayatshahi HS, Rajan R, Liu J (2019). Structural and functional insights into the bona fide catalytic state of Streptococcus pyogenes Cas9 HNH nuclease domain. Elife 8:e46500.

Vol. 20(6), pp.251-255, June, 2021
DOI: 10.5897/AJB2020.17225
Article Number: 59507E467113
ISSN: 1684-5315

http://www.academicjournals.org/AJB

ACADEMIC JOURNALS
expand your knowledge

African Journal of Biotechnology

Full Length Research Paper

Antimicrobial potentials of idiolites of endophytic fungi isolated from the leaves of *Dacryodes edulis*

Malachy C. Ugwu[1*], Dave E. Ochiaja[1], David C. Nwobodo[1], Collins Chimezie[1] and Chiamaka B. Ugwu[2]

[1]Department of Pharmaceutical Microbiology and Biotechnology, Faculty of Pharmaceutical Sciences, Nnamdi Azikiwe University, Awka, Anambra State, Nigeria.
[2]Department of Pharmacology and Toxicology, Faculty of Pharmaceutical Sciences, Nnamdi Azikiwe University, Awka, Anambra State, Nigeria.

Received 17 August, 2020; Accepted 17 November, 2020

The growing levels of antimicrobial resistance have triggered interest in the search for alternative compounds to wage the war against it. Plants have been shown to harbor endophytic fungi that produce bioactive idiolites, which have potential lead compounds in the development of new drugs. This study evaluated the antimicrobial activity of endophytic fungi isolated from leaves of *Dacryodes edulis.* Endophytic fungi associated with healthy leaves of *D. edulis* were isolated using standard methods. The fungi were subjected to solid-state fermentation on rice media at 28°C for 21 days and the idiolites extracted using ethylacetate. The extracts of the endophytic fungi were evaluated for antimicrobial properties using agar well diffusion method against selected human pathogens. The endophytic fungi isolates were also characterized using macroscopy and microscopy (photomicrograph). A total of six (6) endophytic fungi (LB2, LB3, MR1, MR2, MR3, and MR4) were isolated from leaves of *D. edulis.* The extracts of isolated endophytic fungi displayed varying antimicrobial activities, with inhibition zone diameters ranging from 4 to 12 mm. The MR3 extract was the most effective metabolite and showed broad spectrum antimicrobial activity against *Staphylococcus aureus, Salmonella* typhi*, Escherichia coli, Pseudomonas aeruginosa* and *Candida albicans.* Endophytic fungi isolated from the leaves of *D. edulis* have antimicrobial activity and could be a hopeful source antimicrobial agent.

Key words: Endophytic fungi, antimicrobial, idiolites, *Dacryodes edulis*.

INTRODUCTION

The initial discovery of antimicrobials transformed humans, resulting in improved survival for both humans and their livestock. However, this health achievement was immediately dominated by the abilities of bacteria to modify themselves to resist against antimicrobials and spread these resistance traits among others. Bacterial resistance to clinically applied antibiotics has been recognized as a serious public threat worldwide and necessitates the search for new drugs to counter the problems. Thus, there is a constant and high demand for

*Corresponding author. E-mail: mc.ugwu@unizik.edu.ng.

new drugs that might help to overcome this alarming scenario of resistance development and spread. Endophytic fungi constitute a relatively unstudied and promising source for such new antibacterial agents (Nwobodo et al., 2020a; Debbab et al., 2011). Endophytic fungi are polyphyletic microorganisms that establish mutualistic associations with their host plants without causing disease symptoms (Nicoletti and Fiorentino, 2015). They are found in virtually all plants and have multiple activities on the host plants and their survival, which are exerted via varied pathways. Such pathway is via the production of idiolites, also known as secondary metabolites.

The mutual relationships between endophytes and their host plants are believed to result in survival benefits for both partners (Khare et al., 2018). The endophytes may provide protection and survival conditions to their host plant by producing a plethora of substances which, once isolated and characterized, may also have potential for use in industry, agriculture, and medicine (Verma et al., 2016). This group of microorganisms has been regarded as one of the most creative groups of secondary metabolites that play important biological roles and are potential sources of novel natural agents for exploitation in the pharmaceutical industry (Nwobodo et al., 2017; Selim et al., 2012). It is estimated that about 5% of the fungi population have been studied and the rest remain unexplored for their contribution to human welfare (Qadri et al., 2013).

Natural products from endophytic fungi have been reported to inhibit or kill a wide variety of pathogenic microorganism (Nwobodo et al., 2020a; Chirlei et al., 2012). Endophytic fungi isolated from Nigerian medicinal plants have been reported to possess broad spectrum activity against pathogenic fungi and bacteria (Nwobodo et al., 2020b; Akpotu et al., 2017; Okezie et al., 2017). The plant *Dacryodes edulis* has a long history in African traditional medicine for the treatment of various ailments (Okwu and Nnamdi, 2008). Olasunkanmi and Adeniyi (2017) reported that the leaf extract possesses broad spectrum antibacterial activity. The leaves are employed to cure skin diseases, disorders of the digestive tract, toothache and ear ache (Hassan-Olajokun et al., 2020). In the present study, crude metabolites produced by endophytic fungi isolated from sterile leaflet of *D. edulis* were evaluated for their antimicrobial activity.

MATERIALS AND METHODS

Plant collection, isolation and maintenance of endophytic fungi

Fresh leaves of *D. edulis* were collected from Agulu, Anaocha Local Government Area of Anambra State, Nigeria in June, 2019. The plant was identified and authenticated at the Department of Pharmacognosy and Traditional Medicine, Nnamdi Azikiwe University, Awka, Nigeria and Voucher specimen (PCG/19/A/045) was deposited.

Isolation of endophytic fungi from the leaves was carried out as described by Eze et al. (2018). The leaves were washed thoroughly in running tap water, and then cut into small fragments (about 1 cm^2). The leaf fragments were surface-sterilized by immersion in 2% sodium hypochlorite solution for 2 min, 70% ethanol for nearly 2 min, before a final rinse in sterile water for 5 min. These leaf fragments were transferred into malt extract agar (MEA) plates, supplemented with chloramphenicol. The Petri plates were then incubated at 27°C for 7 days. Hyphal tips of fungal colonies emerging from the leaf segments were sub-cultured on fresh MEA plates, and then single pure colony was obtained by directly picking single spores using microscopic observation (Zhang et al., 2013).

Solid state fermentation and extraction of the fungal secondary metabolites

The solid-state fermentation and extraction of the fungal metabolites were carried out using methods previously described by Okoye et al. (2013) and Nwobodo et al. (2020a). Rice medium was prepared in 1000 ml Erlenmeyer flasks as follows: approximately 200 ml of distilled water was added to 100 g of rice, and then autoclaved at 121°C for 30 min. The flasks were inoculated individually with 4 agar blocks (3 mm diameter), cut from each pure endophytic fungal culture using a sterile cork borer, and then incubated at 28°C for 21 days. After the fermentation period, the culture media and the growing mycelia were extracted using ethyl acetate, and then separated by filtration. The organic phase was vacuum-concentrated at 40°C under reduced pressure, using a rotary vacuum evaporator to obtain the crude extracts.

Antimicrobial screening

Test isolates

The microbial cultures used in this study for the antimicrobial assay were laboratory strains obtained from the Department of Pharmaceutical Microbiology and Biotechnology laboratory, Faculty of Pharmaceutical Sciences, Nnamdi Azikiwe University, Awka Nigeria. The bacterial isolates were *Staphylococcus aureus, Salmonella* typhi*, Pseudomonas aeruginosa, Escherichia coli,* and a yeast, *Candida albicans.* The bacterial isolates were identified using the standard morphological and biochemical characteristics of the bacteria according to Bergey's Manual of Determinative Bacteriology (Bergey and Holt, 2000).

Agar well diffusion assay

Antimicrobial activity of the endophytic fungal extracts was carried out using the agar well diffusion assay method as described by Akpotu et al. (2017). A stock concentration of 2 mg/ml of the fungal extracts was prepared by dissolving in dimethyl sulphoxide (DMSO 100% v/v). From the stock concentration, the working concentration of 1 mg/ml was prepared to determine the efficacy of the fungal extract. 0.1 ml standardized concentration (McFarland 0.5) of overnight cultures of the test bacteria and fungi were spread aseptically onto the surface of Mueller Hinton Agar (MHA) and Sabouraud dextrose agar (SDA) plates, for bacterial and fungal isolates, respectively. All plates were allowed to dry for about 5 min, and then agar wells were made by using a sterile cork-borer (6 mm in diameter). These wells were individually inoculated with 20 µl of each of the fungal extracts and the controls. The plates were then kept at room temperature for 1 h to allow the substances/ compounds to diffuse into the agar. The MHA plates were incubated at 37°C for 24 h, and SDA plates incubated at 25°C for 48 h. Ciprofloxacin (5 µg) and Miconazole (50 µg) served as the positive controls for the bacteria and fungi, respectively, while

Table 1. Endophytic fungi isolated from different segments of *Dacryodes edulis* leaves.

S/N	Fungal isolates	Segment of isolation
1	MR 1	Midrib
2	MR 2	Midrib
3	MR 3	Midrib
4	MR 3	Midrib
5	LB 2	Leaf Blade
6	LB 3	Leaf Blade

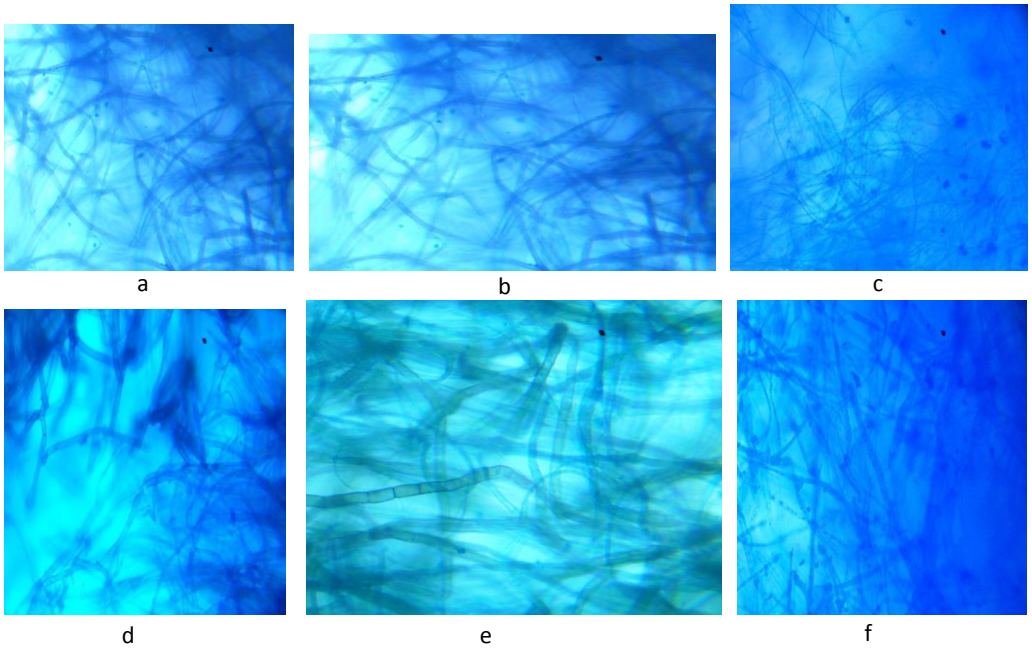

Figure 1. A photomicrograph of the endophytic fungi isolatesat 100X magnification

DMSO (100% v/v) served as the negative controls. The inhibition zones diameters (IZDs) were measured using a calibrating ruler. The assay was conducted in triplicates, and repeated twice.

Statistical analysis

Data obtained were presented as mean for experiments carried out in triplicates. The mean inhibition zones diameter of the fungal extracts against the various test microbes were compared using one-way ANOVA. Statistical significance was considered at $p \leq 0.05$. Analysis of data and graph were made using Microsoft Excels 2013 software and SPSS version 20.

RESULTS AND DISCUSSION

Multi-drug resistant pathogenic microorganisms have become a global health challenge. Endophytic fungi metabolites are indispensable as lead compounds in the search for novel antibiotics with new mechanisms of action and less toxic effects (Chirlei et al., 2012). Endophytes are known to be a rich source of idolites with several biological properties including antimicrobial activities (Nwobodo et al., 2020a; Eze et al., 2018; Kusari et al., 2008).

D. edulis has been constantly used in African traditional medicine, and the leaf extracts have been reported to exhibit antimicrobial and antioxidant activities (Okunomo and Egho, 2010). In this study, six (6) endophytic fungi were isolated. Four of the endophytic fungi were isolated from the plant leaf midrib (MR 1-4), while two where isolated from the leaf blade (LB 1 and 2) (Table 1). Thus, based on our results, fungal community appeared to be higher in the leaf midrib than in the leaf blade. The results of the morphological characterization are as shown in Figure 1.

In this study, the idiolites of the endophytic fungi from *D. edulis* exhibited antimicrobial activity at varying degrees at a concentration of 1 mg/ml. Table 2 represents

Table 2. Result of antimicrobial assay of endophytic fungal extracts showing the inhibition zone diameters (IZDs) produced against test isolates.

Test organism	IZD of fungal crude extracts (mm)						Positive control ciprofloxacin (5 µg)
	MR4	MR2	LB2	MR1	MR3	LB2	
Staphylococcus aureus	10.0±3.9	9.0±3.6	8.0±3.6	10.0±3.4	12.0±4.8	11.0±4.6	17*
Escherichia coli	0	0	7.0±3.5	0	10.0±3.8	8.0±3.6	16*
Salmonella typhi	10.0±3.9	5.0±2.2	0	0	9.0±3.6	0	21*
Pseudomonas aeruginosa	0	7.0±2.8	12.0±5.2	8.0±2.8	12.0±5.2	0	22*
Candida albicans	8.5±2.5	4.0±2.1	5.0±2.3	10.0±4.3	12.0±5.0	11.0±4.3	17*

Values are represented as Mean ± Standard Deviation of experiments in triplicates. *Statistically significant at P< 0.05. Miconazole (50 µg) was used as positive control for *Candida albicans*.

the result of the antibacterial activities of the tested fungal extracts. Extract MR3 exhibited the best antibacterial activity against 100% of the test microorganisms employed in this study. The endophytic fungal extract MR3 was not only observed to be active against all tested bacteria strains, but also displayed the highest inhibition zone diameter values of 12.0±5.2 and 12.0±5.2 against *S. aureus* and *P. aeruginosa*, respectively. However, there is a significant difference ($P < 0.05$) when compared with the values of the positive control (Table 2). The extract MR4 demonstrated the best activity against *Salmonella* typhi (IZD = 10.0±3.9 mm), but was totally resisted by *E. coli* and *P. aeruginosa*. This is not surprising as the findings of Kibret and Abera (2011) stated that the antimicrobial resistance in *E. coli* has been reported worldwide. The increasing rates of resistance among *E. coli* are a growing concern both in the developed and developing countries. Several previous studies of Marilyn et al. (2012), Nwobodo et al. (2020b), and Egbujor et al. (2020) reported that resistance development in *P. aeruginosa* is multifactorial, with mutations in several genes contributing for resistance to β-lactams, carbapenems, aminoglycosides, fluoro-quinolones and sulphonamides. *S. aureus* was sensitive to all tested extracts, while *E. coli* was sensitive to only 50% of the tested extracts (Table 2). There was a complete resistance by *P. aeruginosa* to two (MR4 and LB2) of the six extracts tested. Similarly, in a recent study, Mordi et al. (2019) reported the resistance of *P. aeruginosa* to the seed oil extract of *D. edulis*. The mean values of the zones of inhibition obtained for the fungal extracts are statistically not significant as $p > 0.05$. However, when compared with the positive control, $p < 0.001$.

Also, the extract MR3 displayed the best antifungal activity against *C. albicans* (12.0±5.0), followed by the extract of LB2 (11.0±4.3). There was no significant difference in values obtained in the antifungal assay, across all extracts and organisms ($P>0.05$).

The ability of the fungal extracts to inhibit both Gram positive and Gram negative organisms, denotes the broad spectrum potentials of the fungal metabolic extracts. These findings indicate the potentials of idolites of endophytic fungi isolated from *D. edulis* as potential value as starting point in the development of new broad spectrum antibacterial and antifungal agents. To the best of the authors' knowledge, this is the first study on the endophytic fungi isolated from *D. edulis*, hence, there are limited information on this area. However, several authors have isolated endophytic fungi from plants of this same botanical family (Burseraceae). A high diversity of fungal species was also found in leaves and stems of *Boswellia sacra* (Fierro-Cruz et al., 2017). Similarly, Guerrero and Dalisay (2018) isolated 15 fungal endophytes from *Canarium ovatum* fruit.

Conclusion

In this study, the endophytic fungal extracts of *D. edulis* were found to possess potential broad-spectrum antimicrobial activities against clinical human pathogens. It could be of much relevance to the development of new antimicrobials or chemotherapeutic drugs to address the ever increasing problems of drug resistance, which is fast encroaching, even to the last line antimicrobials.

CONFLICT OF INTERESTS

The authors have not declared any conflict of interests.

REFERENCES

Akpotu MO, Eze PM, Abba CC, Nwachukwu CU, Okoye FBC, Esimone CO (2017). Metabolites of endophytic fungi isolated from *Euphorbia hirta* growing in Southern Nigeria. Chemical Science Review Letters 21:12-19.

Bergey DH, Holt JG (2000). Bergey's manual of determinative bacteriology. 9th ed. Philadelphia: Lippincott Wiliams and Wilkins. Little, Christopher R, Carol M, Stiles LMC (2014). Introduction to Fungi. https://doi.org/10. 1094/PHI-I-2012-0426-01

Chirlei G, Fabiana T, Josiane GF, Daiani S, Vania AV, Beatriz HLN, Sales M, Yvelise MP (2012). Antimicrobial activity of endophytes from Brazilian medicinal plants. INTECH 239-254.

Debbab A, Aly AH, Chaidir C (2011). Bioactive secondary metabolites from endophytes and associated marine derived fungi. Fungal Diversity 49(1):1-12.

Egbujor MC, Nwobodo DC, Egwuatu PI, Abu IP, Ezeagu CU (2020).

Sulphonamidedrugs and *Pseudomonas aeruginosa* resistance: A review. International Journal of Modern Pharmaceutical Research 4(1):78-83.
Eze PM, Ojimba NK,Abonyi DO, Chukwunwejim CR, Abba CC, Okoye FBC, Esimone CO (2018). Antimicrobial activity of metabolites of an endophytic fungus isolated from the leaves of *Citrus jambhiri* (Rutaceae). Tropical Journal of Natural Product Research 2(3):145-149.
Fierro-Cruz JE, Jiménez P, Coy-Barrera E (2017). Fungal endophytes isolated from *Protium heptaphyllum* and *Trattinnickia rhoifolia* as antagonists of *Fusariumoxysporum*. Revista Argentina de Microbiología 49(3):255-263.
Guerrero JJG, Dalisay TU (2018). Fungal endophytes across tissue layers of Canarium ovatum (Burseraceae) fruit. Australian Journal of Mycology 27:11-21.
Hassan-Olajokun RE, Deji-Agboola AM, Olasunkanmi OO, Banjo TA, Olaniran O (2020). Antimicrobial activity of fractioned components from *Dacryodesedulis*: *Invitro* Study. European Journal of Medicinal Plants 31(9):71-82.
Khare E, Mishra J, Arora NK (2018). Multifaceted interactions between endophytes and plant: Developments and prospects. Frontiers Microbiology 15:1-17.
Kibret M, Abera B (2011). Antimicrobial susceptibility of *E.coli* from clinical sources in northeast Ethiopia. African Health Sciences 11(1):40-45.
Kusari S, Lambshoft M, Zuhike S, Spiteller M (2008). An endophytic fungus from Hypericumperforatum that produces hypericin. Journal of Natural Products 71(2):159-162.
Marilyn PG, José VB, Santiago NC (2012). Overview of Multidrug-Resistant *Pseudomonasaeruginosa* and novel therapeutic approaches. Journal of Biomaterials and Nanobiotechnology 3:519-527.
Mordi RC, Olasehinde GI, Okedere AP, Elegwule AN, Ayo-ajayi JI, Johnathan HO, Onibokun AE, Ajayi AA, Uchenna DO (2019). Antibacterial activity of moderately volatile components of the oil extracted from the seeds of *Dacryodes edulis*g. LAM. Asian Journal of Pharmaceutical and Clinical Research 12(3):246-249.
Nicoletti R, Fiorentino A (2015). Plant bioactive metabolites and drugs produced by endophytic fungi of Spermatophyta. https://doi.org/10.3390/agriculture5040918
Nwobodo DC, Ihekwereme CP, Ugwu MC, Okoye FBC (2017). Screening of endophytic fungal secondary metabolites from *Garcinia kola* and *Cola nitida*for antioxidant properties. Open Access Journal of Pharmaceutical Research 1(6):1-8.
Nwobodo DC, Ihekwereme CP, Ikem CJ, Okoye FBC (2020a). The anti-pseudomonal potentials of metabolites from some endophytic fungi isolated from Garcinia kola leaves. Novel Research in Microbiology Journal 4(3):845-855.
Nwobodo DC, Ihekwereme CP, Okoye FBC (2020b). Screening of endophytic fungal secondary metabolites from *Cola nitida*leaves for antimicrobial activities against clinical isolates of *Pseudomonas aeruginosa*. The EuroBiotech Journal 4(3):161-166.
Okoye FBC, Lu S, Nworu CS, Esimone CO, Proksch P, Chaldi A, Debbab A (2013). Depsidone and diaryl ether derivatives from the fungus *Corynesporacassiicola*, an endophyte of *Gongronemalatifolium*. Tetrahedron Letters 54:4210-4214.
Okezie UM, Eze PM, Okoye FBC, Ikegbunam MN, Ugwu MC, Esimone CO (2017). Biologically active metabolites of an endophytic fungus isolated from *Vernoni aamygdalina.* African Journal of Pharmaceutical Research and Development 9(1):24-26.
Okunomo K, Egho EO (2010). Economic importance of some underexploited tree species in Nigeria: Urgent need for separate research centers. Continental Journal of Biological Sciences 3:16-32.
Okwu DE, Nnamdi FU (2008). Evaluation of the chemical composition of *Dacryodesedulis* and *Raphiahookeri* Mann exudates used in herbal medicine in South Eastern Nigeria. African Journal of Traditional and Complementary Alternative Medicine 5(2):194-200.
Olasunkanmi OO, Adeniyi PO (2017). Antibacterial and antioxidant activities of *D.edulis*methanolic leaf extract. Journal of Advances in Medical and Pharmaceutical Sciences 14(1):1-11.
Qadri M, Johri S, Shah BA, Khajuria A, Sidiq A, Lattoo SK, Abdin MZ, Riyaz-Ul-Hassan S (2013). Identification and bioactive potential of endophytic fungi isolated from selected plants of the Western Himalayas. Springer Plus 2(8):1-14.
Selim K, El-beih A, Abdel-rahman T, El-diwany A (2012). Biology of Endophytic Fungi. Current Research in Environmental and Applied Mycology 2(1):31-82.
Verma SK, Kumar A, Lal M, Debnath M (2016). Antimicrobial activity of extract from endophytic fungus in *Calotropisprocera* root. Research in Environment and Life Sciences 9(2):212-216.
Zhang K, Su Y, Cai L (2013). An Optimized Protocol of Single Spore Isolation for Fungi. Mycologie 34(4):349-356.

Vol. 20(6), pp.256-265, June, 2021
DOI: 10.5897/AJB2021.17353
Article Number: F4C866B67115
ISSN: 1684-5315

http://www.academicjournals.org/AJB

ACADEMIC JOURNALS
expand your knowledge

African Journal of Biotechnology

Full Length Research Paper

Efficacy of thymol and eugenol against bacterial wilt bacterium *Ralstonia solanacearum*

George Oluoch[1*], Edward George Mamati[2], Viviene Matiru[3] and Moses Nyongesa[4]

[1]Institute for Basic Sciences Technology and Innovation, Pan African University, Kenya.
[2]Department of Horticulture and Food Security, Jomo Kenyatta University of Agriculture and Technology, Kenya.
[3]Department of Botany, Jomo Kenyatta University of Agriculture and Technology, Kenya.
[4]National Potato Research Centre, Kenya Agricultural and Livestock Research Organization, Kenya.

Received 28 April, 2021; Accepted 10 June, 2021

Bacterial wilt caused by *Ralstonia solanacearum* is a major constraint to production of potatoes (*Solanum tuberosum* L). To date, there are no known conventional bactericides which provide effective control of this soil borne pathogen. This study aimed at investigating the antibacterial activity of eugenol and thymol which are the major components of thyme and clove essential oils, respectively against *R. solanacearum.* The pathogen was isolated from potato tubers exhibiting bacterial wilt symptoms. The inhibitory effect of these compounds was assayed by disc diffusion and minimal inhibition concentration (MIC) methods. Combinational test was also performed using chequerboard assay. At a concentration of 100 mg mL^{-1}, thymol and eugenol had inhibition zones of 27 and 17 mm, respectively. The MIC of eugenol and thymol were determined as 275 and 175 µg mL^{-1}, respectively and both had bactericidal effect against *R. solanacearum.* Combinational test revealed an additive effect indicating that their combined use does not significantly enhance inhibition. Both compounds have a potential to be exploited as antibiotic for the management of bacterial wilt disease albeit thymol at a lower concentration. Exploitation of these volatile compounds *in vivo* however faces challenges which can be overcome through nanoencapsulation by an appropriate nanocarrier.

Key words: Essential oils, inhibitory effect, combinational test, chequerboard assay, bactericidal effect.

INTRODUCTION

Potato (*Solanum tuberosum* L.) is one of the most important food crops which provides a greater potential for food security and incomes around the world (Gildemacher et al., 2009). The productivity of the crop is however limited by both biotic and abiotic stresses. Major biotic stresses affecting potato yield are diseases which include bacterial wilt, late blight and early blight (Muthoni and Nyamongo, 2009). Out of these, bacterial wilt has no known bactericide commercially released for use which can efficiently manage to control the disease and it leads to high reduction in crop yields. This is caused by *Ralstonia solanacearum*, a Gram-negative bacterium which not only causes bacterial wilt disease in potato but also on more than 200 other plant species that include tomato, eggplant, tobacco, geranium, pepper and banana (Aguk et al., 2018; Hayward, 1991; Meng, 2013; Muthoni

*Corresponding author. E-mail: george.caas@gmail.com.

et al., 2014). *R. solanacearum* is mainly spread through infected seed stocks but can also spread from infested to healthy fields by farm equipment, irrigation water and plant-to-plant through the rhizosphere (Patil et al., 2012). Damaged roots arising from wounds caused by soil borne organisms like the nematodes or wounds formed by the emergence of lateral roots can also spread *R. solanacearum* by acting as an avenue for infection (Karim and Hossain, 2018). Once it gets into the roots, it colonizes the xylem in the vascular bundles and blocks water uptake resulting in wilting and eventual death (Meng, 2013). The bacteria can survive in water and in residues of infected plants for a long period of time making its control very difficult (Pradhanang et al., 2000).

Despite concerted efforts to control the disease, bacterial wilt continues to cause serious economic challenges in many countries in the world (Aguk et al., 2018; Karim and Hossain, 2018). Worldwide, the pathogen infestation in potatoes has been reported to lead to yield losses of between 33 and 90% and up to $1 billion yearly in lost revenue (Elphinstone, 2005). In Kenya, the disease has been reported to affect over 70% of all potato farms leading to yield losses of between 50 and 100% (Muthoni et al., 2014). Despite using a wide range of management practices such as use of chemical pesticides, phytosanitary measures, breeding for resistance and bio antagonists, dealing with the pathogen still remains a challenge (Karim and Hossain, 2018; Meng, 2013). These limitations may be due to the complexity of *R. solanacearum* pathogenicity which enhances its resistance to the available control methods. Essential oils however have different antibacterial mechanisms including inhibition of swarming motility, biofilm formation, cell membrane damage and cell death making it a powerful tool in reducing bacterial resistance (Chen et al., 2019). So far, there is no report on a known conventional bactericide which has shown effective control of this soil borne pathogen. Therefore, there is need to explore other biologically sustainable control methods which can form part of the integrated management system of the pathogen. Previously, *R. solanacearum* species complex was known to include a number of phenotypically diverse strains which were grouped into five biovars and five pathogenic races. It was later reclassified into Phylotypes I, II, III and IV based on sequence analysis. In the recent taxonomic revision, the *R. solanacearum* species complex has been reclassified into three distinct species which include *R. solanacearum* (Phylotype II) which causes potato brown rot (Bacterial wilt), *Ralstonia pseudosolanacearum* (Phylotype I and III) and *Ralstonia syzygii* (Phylotype IV) (Paudel et al., 2020).

Plants produce more than 100,000 known secondary metabolites some of which function in protecting plants against predators while others act against pathogens such as viruses, bacteria and fungi (Bassolé and Juliani, 2012). Eos are secondary metabolites whose antimicrobial activity against *R. solanacearum* have been reported in several studies (Ji et al., 2005; Oboo et al., 2014). Previous studies have revealed that EOs containing major components such as citral, carvacrol, cinnamaldehyde, thymol or eugenol have the highest activity against pathogenic microbes (Bassolé and Juliani, 2012). However, the inhibitory activity of some of these compounds including eugenol against *R. solanacearum* has not been investigated.

Among the components of clove EO, eugenol accounts for up to 95% of the oil (Nurdjannah and Bermawie, 2012). The antibacterial effect of clove EO has been attributed to the presence of its major component, eugenol (Chaieb et al., 2007). Eugenol is mainly concentrated in the buds and flowers of clove (*Zingiber aromaticum*). A part from clove, eugenol is also found in herbal plants such as thyme, ginger and turmeric (Charan et al., 2015; Khalil et al., 2017). Chemically, the IUPAC name of eugenol is 4-Allyl-2-methoxyphenol and it belongs to a class of phenylpropanoids ($C_{10}H_{12}O_2$) and hence can be produced commercially. It is also known as caryophyllic acid, allylguaiacol or 4-allylcatechol-2-methyl ether (Charan et al., 2015). Thymol is a phenol compound and a major volatile component of EO extracted from medicinal plants thyme, basil and oregano. It is a colorless crystalline compound whose IUPAC name is 2-isopropyl-5-methylphenol and can also be commercially synthesized. Thyme EO has been shown to inhibit the growth of *Aspergillus niger* and *Aspergillus tubingensis* both of which are fungal infections in grapes (Císarová et al., 2016). Thymol also has inhibitory effect on pathogenic plant bacterial species *Erwinia carotovora* and *Xanthomonas compestris* (Nesrollahi and Razavi, 2017).

When major components of EOs interact, they may have additive, antagonistic or synergistic antibacterial effects (Mourey and Canillac, 2002). Bassolé and Juliani (2012) reported that the efficacy of several combinations of EOs and their components were shown to increase when combined which took advantage of their additive and synergistic effects. Pei et al. (2009) reported a synergistic effect against *Escherichia coli* when eugenol and thymol was combined in the ration of 1:4, respectively. This significantly lowered the effective concentration of the components by 50% than when each component was used alone. The effect of combining eugenol and thymol against *R. solanacearum* has however not been studied. The present study therefore aimed at investigating the antibacterial activity of individual and mixed fractions of eugenol and thymol against *R. solanacearum*.

MATERIALS AND METHODS

Eugenol ≥98% (E51791) and thymol ≥99% (16254) were obtained from Sigma-Aldrich (St. Louis, MO, USA). Other chemicals, such as triphenyl tetrazolium chloride (TZC) peptone, glucose, casamino-

acid and agar were purchased from Legacy Lab. Africa.

Isolation and detection of *R. solanacearum*

R. solanacearum was isolated in October 2020 from potato samples exhibiting bacterial wilt symptoms collected from field grown crops in Nyandarua County in Kenya. The procedure for isolation and purification was according to Mutimawurugo et al., (2019). The isolates were grown on triphenyl tetrazolium chloride (TZC) media (peptone 10 g, glucose 2.5 g, casamino-acid 1 g, agar 18 g, TZC 50 mg in 1 L of distilled water). The TZC medium was used to differentiate cultures of *R. solanacearum* into virulent and avirulent colony types as described by Champoiseau et al., (2009). Polymerase chain reaction (PCR) was used to confirm the identity of the virulent isolates using primer pair (Nmult:21:2F/Nmult:22:RR) which is specific to *R. solanacearum* species (Fegan and Prior, 2005).

Evaluation of the antibacterial activity of eugenol and thymol

The antibacterial activity of eugenol, thymol and their combinations were evaluated using disc diffusion and broth microdilution methods as described subsequently. Dimethylsulfoxide (DMSO) alone was used as vehicle control in all the assays (Valliammai et al., 2020).

Evaluation of the antibacterial activity by disc diffusion

Antibacterial activity of thymol and eugenol against *R. solanacearum* was confirmed by disc diffusion test also known as the Kirby-Bauer assay method (Bauer et al., 1966) as described by Ambrosio et al. (2019). The test was performed in sterile 90 mm diameter Petri dishes containing solid and sterile casamino acids-peptone-glucose (CPG) nutrient agar medium. Before being tested, the solubility of thymol and eugenol were enhanced by dissolving them in DMSO. Thymol and eugenol were tested at six levels: 1000, 800, 600, 400, 200 and 100 mg mL^{-1} concentrations in DMSO. Sterile 6 mm diameter filter paper discs (Whatman paper No. 5) were impregnated with 10 µl/disk of eugenol or thymol at the different concentrations. The discs were then placed on the surface of the medium which had been flood inoculated with 100 µL of overnight microbial suspension (10^8 CFU mL^{-1}) using a sterile swab. The overnight culture of the bacterium was prepared by diluting to 10^8 CFU mL^{-1} using a spectrophotometer (Jenway 6305, UK) at a wavelength of 625 nm. A negative control included was a filter disc soaked in 10 µl of DMSO, while the positive control consisted of gentamycin antibiotic discs (10 µg/disk). After 24-h incubation at 28°C without lighting, the antibacterial activity of the antimicrobials was evaluated by measuring the diameter of the inhibition zone in mm. Each experiment had three replicates and the mean diameter of the inhibition zone was recorded.

Minimum inhibitory concentration (MIC) and minimum bactericidal concentration (MBC)

MIC was determined by micro broth dilution assay using resazurin test (Elshikh et al., 2016). Stock solutions of eugenol and thymol were prepared separately by dissolving each in DMSO to make a stock concentration of 800 µg mL^{-1} then serial two-fold dilution were prepared to reach final concentrations ranging from 400 to 200 µg mL^{-1} (400, 375, 350, 325, 300, 275, 250, 225 and 200) for eugenol and 200 to 100 µg mL^{-1} (200, 187.5, 175, 162.5, 150, 137.5, 125, 112.5 and 100) for thymol, respectively. The ranges were determined from a pre-experiment using a standard two-fold micro broth dilution. A volume of 100 µL of sterilized CPG medium was distributed from the 1st to the 9th well in each row. The same volume (100 µL) of each stock concentration was transferred to the first well microtitre plate in triplicate. Then, 100 µL of the thymol/eugenol-broth mixture was transferred from the 1st well to the 2nd well in the next row and so on till the 8th well and the last 100 µL of the antibiotic broth mixture discarded. A suspension (10 µL) of *R. solanacearum* at the concentration of 10^8 CFU mL^{-1} was then added to each of the wells. MIC was then determined after incubation for 24-h at 28°C using resazurin test. This was performed by adding 20 µL of resazurin solution at 0.015% m/v per well and the results recorded after further incubation at 28°C for 1 h. Each experiment had two treatments (thymol and eugenol) with a positive and negative control. For the positive control, 10 µL of *R. solanacearum* was added to 100 µL of nutrient broth lacking the test compound (essential oil) to check the growth of incubated bacteria. A well containing only 100 µL of broth was prepared as a negative control to check for sterility of the medium (Hasani and Hasani, 2018). Each experiment was carried out in triplicate and in three independent repeats and the results expressed as mean ± standard deviation. For wells showing inhibitions, 20 µL of the mixture were transferred to TZC agar plates. Then MBC was determined as the lowest concentration where no growth was observed on the TZC plates after 24-h incubation at 28°C (Xue and Knoxville, 2015). MBC/MIC ratio of 1-2 and 4-16 was considered bactericidal and bacteriostatic, respectively (Oulkheir et al., 2017).

Effect of combined eugenol and thymol on the inhibition of *R. solanacearum*

The interaction between thymol and eugenol on their antibacterial effectiveness against *R. solanacearum* was performed based on the fractional inhibitory concentration (FIC) index obtained through checkerboard assay using 96-well microtitre plates (Sarah and Lobna, 2017). The test concentration range for the synergy test was between 0 and 400 µg mL^{-1}. The final volume in each well was 100 µL comprising 50 µL of each diluted compound. Subsequently, 10 µL of bacterial suspension containing 1 × 10^8 CFU/mL of *R. solanacearum* was added to each well. The microtitre plate was incubated at 28°C for 24-h and MIC was read as the lowest concentration of the agent at which no visible growth occurred. The MIC of the combinations was determined using resazurin test. Positive control was prepared by adding 10 µL of *R. solanacearum* in a well containing 100 µL of nutrient broth while negative control had only 100 µL of broth (Hasani and Hasani, 2018). For comparison of MIC and FIC values, tests were made in triplicate and repeated three times. FIC index was then calculated for the thymol/eugenol combination using the following standard equations (Odds, 2003):

$$\text{FIC index} = FIC_A + FIC_B$$

$$FIC_A = \frac{MIC_A \text{ in combination}}{MIC_A \text{ alone}}$$

$$FIC_B = \frac{MIC_B \text{ in combination}}{MIC_B \text{ alone}}$$

where FIC_A and FIC_B (where A and B are thymol and eugenol respectively) are the minimum concentrations that inhibited the bacterial growth for antibacterial compounds A and B, respectively. Results were provided in tabular form. The results of the FIC index were interpreted as Synergy (FIC index value of ≤0.5), Additive (FIC index value of 0.5 < FIC ≤ 4), or Antagonism (FIC index value of FIC > 4) (Odds, 2003).

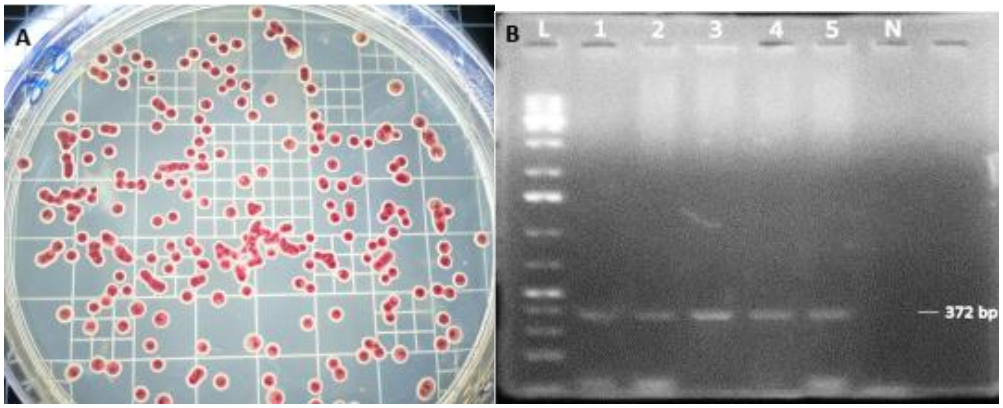

Figure 1. Colonies of virulent pure culture of *R. solanacearum* on TZC media (A); *R. solanacearum* species validation for isolates 1-5 with Nmult21:2F/Nmult22:RR primer pair (amplification of a 372bp amplicon); L-1kb plus DNA ladder; N-Negative control (B).

RESULTS

Isolation and identification of *R. solanacearum*

Morphological and molecular tests were used to ascertain the identities of the suspected *R. solanacearum* isolates. After 48-h incubation, TZC agar differentiation test was used to distinguish virulent from avirulent isolates. The virulent isolates were identified based on their characteristic red center and whitish margin (Figure 1). The identity of the virulent isolates was further confirmed by PCR using primers specific to *R. solanacearum* species (Figure 1) (Fegan and Prior, 2005).

Evaluation of the antibacterial activity by disc diffusion

The antimicrobial activity of thymol against *R. solanacearum* was higher than that of eugenol for all the ranges of concentrations (Figure 2). At the concentration of 100 mg mL^{-1}, thymol exhibited a zone of inhibition of 26 ± 0.6 mm against *R. solanacearum* in comparison to eugenol and gentamycin which had inhibition zones of 17 ± 0.4 and 20 ± 0.5 mm, respectively (Figure 3).

Minimum inhibitory concentration and minimum bactericidal concentration

The MIC and MBC was used to evaluate the antibacterial activity of eugenol and thymol in relation to virulent *R. solanacearum* isolate. After 24-h incubation, the MIC was determined as the lowest concentration where inhibition occurred (blue resazurin colour remained unchanged) (Figure 4). For the MBC, 20 µl of the contents of the wells where inhibition occurred were plated on CPG medium and incubated at 28°C for 24-h. The MIC value was determined as 175 and 275 mg mL^{-1} for thymol and eugenol, respectively. For the MBC, there was no growth in all the wells where inhibition occurred. The lowest concentration for each of the compounds was therefore taken as the MBC. Thymol and eugenol were found to have bactericidal effect on *R. solanacearum* (Table 1).

Effect of combined eugenol and thymol on the inhibition of *R. solanacearum*

Checkerboard assay was performed to study the antibacterial interaction between thymol and eugenol against *R. solanacearum*. The lowest concentration which inhibited the growth of bacteria was found when 100 mg mL^{-1} of thymol combined with 200 mg mL^{-1} of eugenol (Figure 5). The FIC value for the most effective combination was determined as 0.57 and 0.73 for thymol and eugenol which resulted to a FIC index of 1.3 (Table 2).

DISCUSSION

The potato bacterial wilt pathogen, *R. solanacearum* was successfully isolated and identified by both morphological and molecular means. The isolation was done using TZC medium which is useful in distinguishing *R. solanacearum* among other bacteria during isolation, and for distinguishing virulent colonies from avirulent mutant ones during purification of cultures (Kelman, 1954). The virulent colonies were identified based on their characteristic fluidal and white with pink centers as reported by Aley and Elphinstone (1995). The morphologically determined virulent isolates were further confirmed to belong to *R. solanacearum* species (previously classified as phylotype II) using species specific primers (Nmult21:2F/Nmult22:RR) which

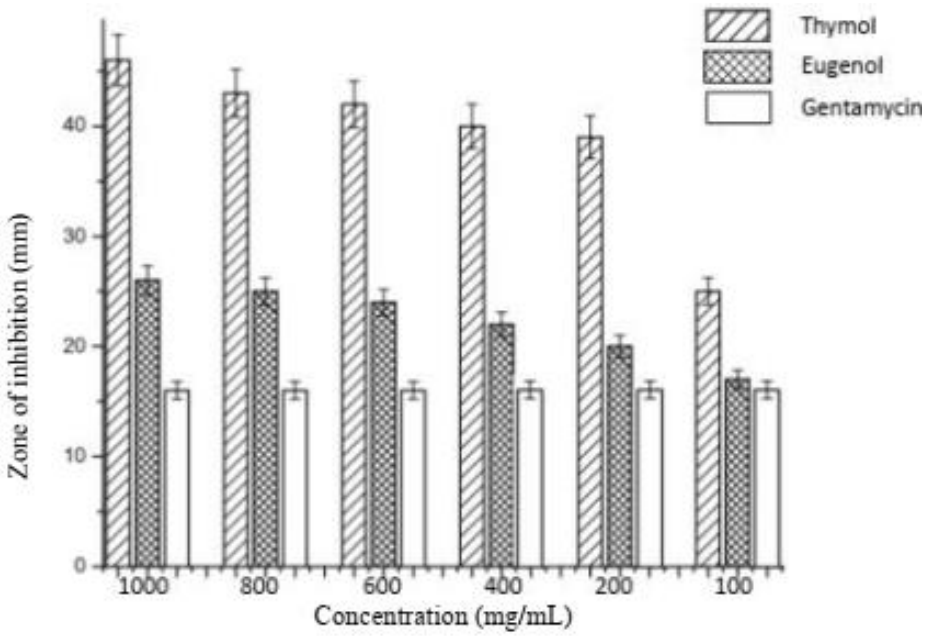

Figure 2. Zones of inhibition measured for thymol and eugenol (10 µg/disk) against *R. solanacearum*; Gentamycin disc (10 µg/disk). Error bars indicate standard errors (n = 3).

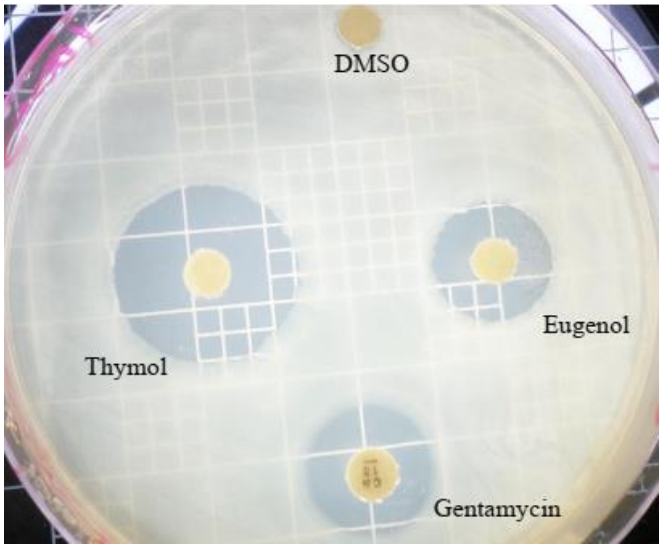

Figure 3. Antibacterial activities of thymol and eugenol (100 µg mL^{-1}; 10 µg/disk) against *R. solanacearum*. Negative control (disc impregnated with DMSO), positive control (gentamycin disc (10 µg/disk).

amplified a 372 bp in the intergenic spacer region between the 16S and 23S rRNA genes (Fegan and Prior, 2005).

The methods used in assessing the antimicrobial activity of EOs include agar dilution, disc diffusion and broth dilution (Perricone et al., 2015). Using the disc diffusion assay, thymol was shown to have the highest inhibition zones in all the tested concentrations in comparison to both eugenol and gentamycin which was used as a positive control (Figure 2). There was no growth inhibition in the disc impregnated with DMSO, an indication that it has no activity against *R. solanacearum*.

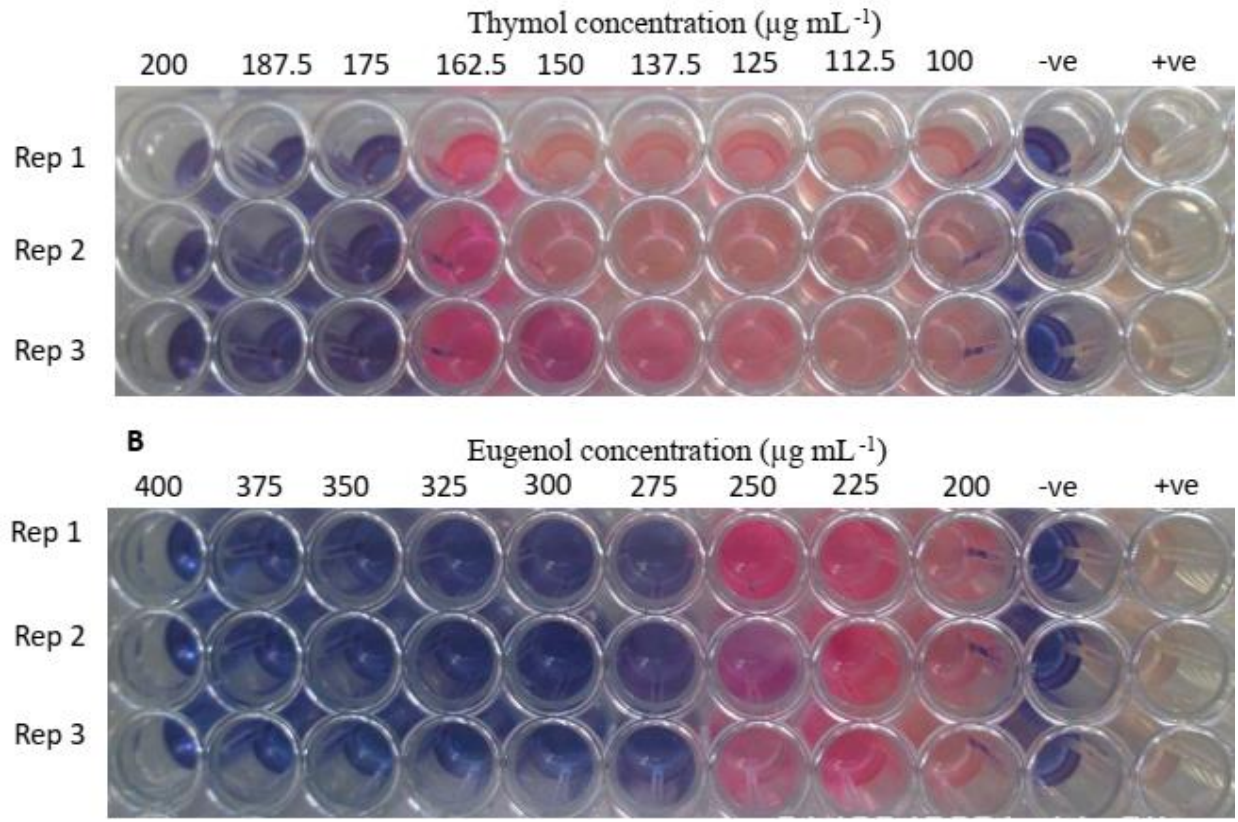

Figure 4. Minimum inhibitory concentration of thymol (A) and eugenol (B) against *R. solanacearum* using resazurin aided microdilution; (-ve) negative control (broth only); (+ve) positive control (broth + *R. solanacearum*).

Table 1. The antibacterial effect of thymol and eugenol against *R. solanacearum*.

Compound	MIC (µg mL^{-1})	MBC (µg mL^{-1})	MBC/MIC	Antibacterial effect
Thymol	175	175	1	Bactericidal
Eugenol	275	275	1	Bactericidal

Similar observation was reported previously by Li et al. (2016). In the previous study using agar diffusion, a strong antibacterial activity of thyme oil was reported against 120 clinical strains of bacteria of the genera *Escherichia*, *Enterococcus*, *Pseudomonas* and *Staphylococcus* (Sienkiewicz et al., 2012). Using disc diffusion test to study the antibacterial and antifungal activity of eugenol, Pavesi et al. (2018) reported inhibition zones of 12.1, 4.2 and 3.2 mm for *Candida albicans, E. coli* and *Staphylococcus aureus*, respectively. This variation in results may be due to the disc size, amount of compound impregnated into the disc and the volume of agar used. Disc diffusion test provides only qualitative results and neither quantification of the antimicrobial response nor distinguishing bacteriostatic from bactericidal effect of the antimicrobial is possible with this method (Nasir et al., 2015). In addition to the disc diffusion test, it has been recommended that the MIC or cidal concentration values of the test compound be established (Orchard and Van Vuuren, 2017).

The antimicrobial activities of eugenol and thymol were evaluated for their MIC and MBC using micro broth dilution assay (Figure 5). The MIC of thymol and eugenol was determined as 175 mg mL^{-1} and 275mg mL^{-1} respectively using the resazurin indicator dye. Resazurin dye is a redox indicator and has been used to determine the MIC of a number of antibacterial compounds (Elshikh et al., 2016; Kokina et al., 2019). In the presence of active bacterial cells, blue non-fluorescent resazurin is reduced to pink fluorescent resorufin which can further be reduced to uncolored nonflourescent hydroresorufin and hence can give a direct measure of the metabolic activity of the bacteria (O'Brien et al., 2000). The MIC of thymol was significantly lower than that of eugenol indicating that

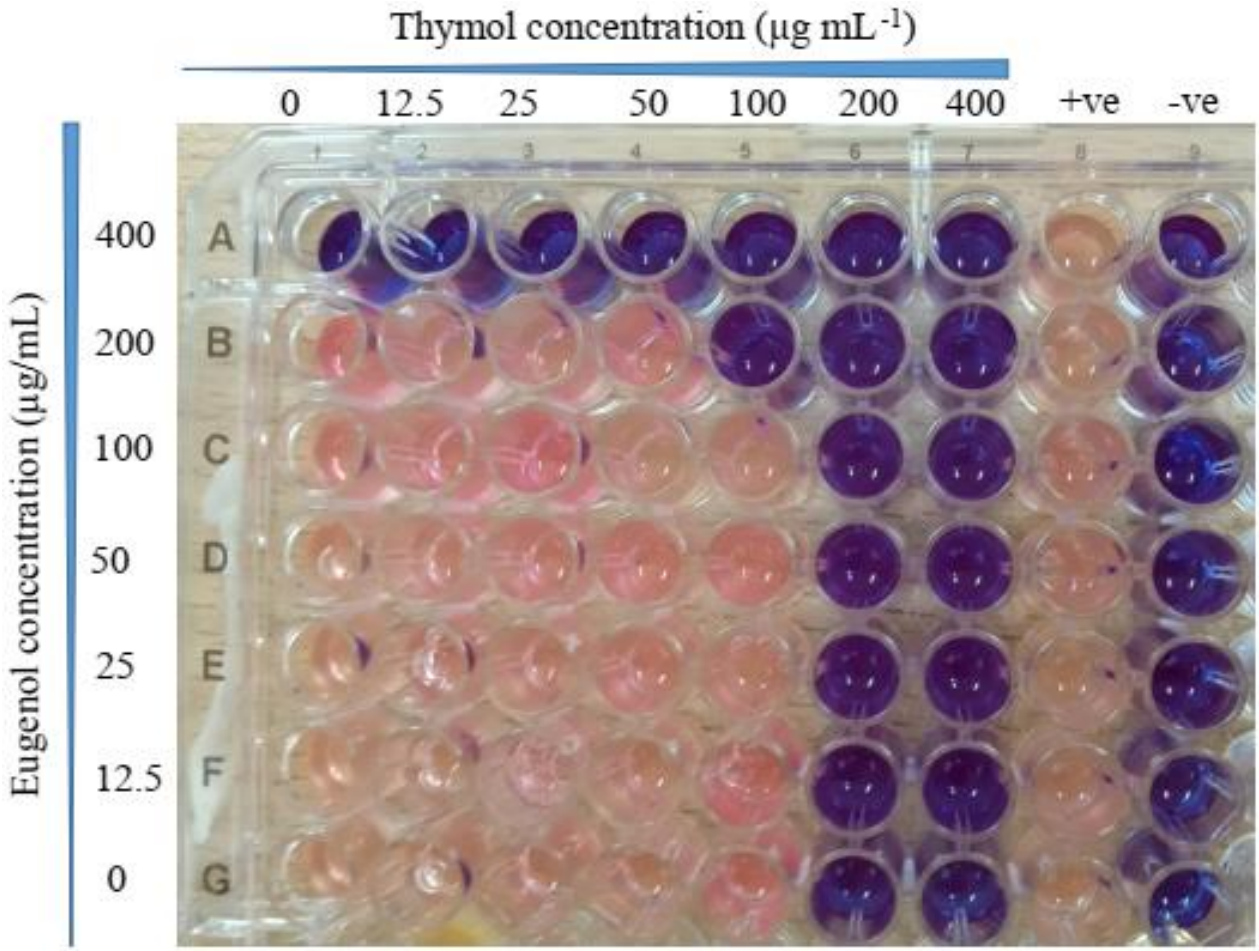

Figure 5. Checkerboard method for the determination of the effect of combination of eugenol and thymol on *R. solanacearum*; (+ve) positive control (broth + *R. solanacearum*); (-ve) negative control (broth only).

Table 2. Effect of treatment with combined thymol and eugenol on the growth of *R. solanacearum* culture in µg mL^{-1} according to the FIC index.

Compound	Alone MIC (µg mL^{-1})	Combined MIC (µg mL^{-1})	FIC value	FIC index
Thymol	175	100	0.57	1.3
Eugenol	275	200	0.73	

it has a higher antibacterial activity against *R. solanacearum*. The high antibacterial activity of thymol in comparison to eugenol has also been reported against *E. coli* (Pei et al., 2009). This results were in the same range with a previous study by Sarah and Lobna (2017) which reported the MIC values (128 to 256 µg mL^{-1}) of thymol against different isolates of *S. aureus* (Sarah and Lobna, 2017). However in a different study to evaluate the antibacterial effect of eugenol and thymol against *E. coli* using two-fold micro broth dilution, the MIC was determined as 1600 and 400 mg mL^{-1}, respectively (Pei et al., 2009). This difference in results with the current study can be attributed to the different microbes tested and the different experimental conditions used. The MIC of eugenol against a number of other pathogens have also been reported including *S. aureus*, *Salmonella enterica* and fungi including *Cladosporium* (MIC: 100 µg mL^{-1}), *Aspergillus* (MIC:100 µg mL^{-1}) and *Cladosporium* species (MIC: 350 µg mL^{-1}) (Kit-Kay et al., 2019). This is however the first study in which the MIC of eugenol has been reported against *R. solanacearum*. A study by Jeyakumar and Lawrence (2021) on the mechanism of action of eugenol against *E. coli* demonstrated that it alters membrane permeability of the bacteria which then

leads to leakage of intracellular contents and hence death of the bacteria. Thymol on the other hand inhibits the bacterial growth by increasing the permeability of its cytoplasmic membrane to adenosine triphosphate leading to the release of lipopolysaccharides (Pei et al., 2009).

The lowest concentration of the sample that resulted to ≥99.9% kill of the initial inoculum was considered as MBC as described by Oulkheir et al. (2017) and was determined as 175 and 275 mg mL^{-1} for thymol and eugenol, respectively. This was similar to their respective MIC's which indicated that both thymol and eugenol has bactericidal effect against *R. solanacearum* and hence both can be considered as potential candidates for use in controlling *R. solanacearum*. Determination of both MIC and MBC of these compounds is important in the determination of the effective concentration *in vitro*, which in turn will help in recommending the dosage and to assess the potential for using these compounds for crop protection in agriculture (Cai et al., 2018).

The antibacterial efficacy can be enhanced if two EO components get mixed together or with other known antimicrobials (Kalemba and Synowiec, 2019). When EO compounds interact, they may lead to additive, antagonistic, or synergistic effects (Odds, 2003). The antimicrobial properties of a number EO components and their combinations have been reported in several studies (Bassolé and Juliani, 2012). For example, eugenol was reported to exhibit a synergistic antibacterial activity against *E. coli* when in combination with thymol (Charan et al., 2015). The checkerboard assay in this study revealed an additive effect when thymol was combined with eugenol against *R. solanacearum* (FIC =1.3) (Table 2). This meant that the sum of the individual effect of eugenol and thymol is equal to their combined effect. A similar combination against *E. coli* was however synergistic (Pei et al., 2009). Lambert et al. (2001) reported an additive effect when carvacrol and thymol were combined against *Pseudomonas aeruginosa* and *S. aureus* and they showed that the overall inhibition could be attributed mainly to the additive antimicrobial action of those two compounds. This variation in the effect is because the effect of combining antibacterial compounds is dependent on the combination of the components tested and the microbe to which it is tested against (Bassolé et al., 2010). The effective concentration of thymol when in combination with eugenol was however reduced by 43% against *R. solanacearum* while that of eugenol was reduced by 27%. This additive effect of thymol/eugenol may be due to the fact that thymol disintegrated the outer membrane of *R. solanacearum*, making it easier for eugenol to enter the cytoplasm and combine with proteins (Pei et al., 2009).

The utilization of EO compounds in controlling soil borne phytopathogens in the field is limited by their instability when exposed to environmental and physiological factors which may lead to the loss of their potency (Kit-Kay et al., 2019). In order therefore to utilize eugenol and thymol in controlling *R. solanacearum* in potato farms, there is need for a proper delivery system. Studies have shown that encapsulating EOs in biodegradable polymer shells has a potential of protecting them from volatilization and sustenance of their antioxidant and antimicrobial properties (Jamil et al., 2016).

Conclusion

This study has shown that both eugenol and thymol have antibacterial properties against *R. solanacearum*. The MIC of thymol (175 µg mL^{-1}) was however found to be lower than that of eugenol (275 µg mL^{-1}). Combinational test using checkerboard assay revealed an additive effect when the two compounds were mixed against *R. solanacearum* indicating that their combined use does not enhance inhibition. The use of these essential oil compounds in controlling *R. solanacearum in vivo* may however be limited due to their volatility, hydrophobicity, rapid degradation as well as poor solubility in water. These challenges can be overcome through nano-encapsulating them into lipid or polymer based organic nanocarriers.

CONFLICT OF INTERESTS

The authors have not declared any conflict of interests.

ACKNOWLEDGEMENTS

The authors acknowledge the financial support from the African Union through the Pan African University, Institute for Basic Sciences and Technology.

REFERENCES

Aguk JA, Karanja N, Schulte-Geldermann E, Bruns C, Kinyua Z, Parker M (2018). Control of bacterial wilt (*Ralstonia solanacearum*) in potato (*Solanum tuberosum*) using rhizobacteria and arbuscular mycorrhiza fungi. African Journal of Food, Agriculture, Nutrition and Development 18(2):13371-13387. https://doi.org/10.18697/ajfand.82.16905

Aley E, Elphinstone J (1995). Culture media for Ralstonia solanacearum isolation, identification and maintenance. Fitopatologia 30:126-130.

Ambrosio CM, Ikeda NY, Miano AC, Saldaña E, Moreno AM, Stashenko E, Contreras-Castillo CJ, Da Gloria EM (2019). Unraveling the selective antibacterial activity and chemical composition of citrus essential oils. Scientific Reports 9(1):1-13. https://doi.org/10.1038/s41598-019-54084-3

Bassolé IHN, Juliani HR (2012). Essential oils in combination and their antimicrobial properties. Molecules 17(4):3989-4006. https://doi.org/10.3390/molecules17043989

Bassolé IHN, Lamien-Meda A, Bayala B, Tirogo S, Franz C, Novak J, Nebié RC, Dicko MH (2010). Composition and Antimicrobial Activities of Lippia multiflora Moldenke, Mentha x piperita L. and *Ocimum basilicum* L. Essential Oils and Their Major Monoterpene Alcohols Alone and in Combination. Molecules 15(11):7825-7839. https://doi.org/10.3390/molecules15117825

Bauer AW, Kirby WMM, Sherris JC, Turck M (1966). Antibiotic

Susceptibility Testing by a Standardized Single Disk Method. American Journal of Clinical Pathology 45(4):493-496. https://doi.org/10.1093/ajcp/45.4_ts.493
Cai L, Chen J, Liu Z, Wang H, Yang H, Ding W (2018). Magnesium oxide nanoparticles: Effective agricultural antibacterial agent against *Ralstonia solanacearum*. Frontiers in Microbiology 9(4):1-19. https://doi.org/10.3389/fmicb.2018.00790
Chaieb K, Hajlaoui H, Zmantar T, Kahla-Nakbi AB, Rouabhia M, Mahdouani K, Bakhrouf A (2007). The chemical composition and biological activity of clove essential oil, Eugenia caryophyllata (*Syzigium aromaticum* L. Myrtaceae): a short review. Phytotherapy Research 21(6):501-506. https://doi.org/10.1002/ptr.2124
Champoiseau PG, Jones JB, Allen C (2009). *Ralstonia solanacearum* Race 3 Biovar 2 Causes Tropical Losses and Temperate Anxieties. Plant Health Progress 10(1):35. https://doi.org/10.1094/php-2009-0313-01-rv
Charan RMR, Srinivasan V, Selvaraj S, Mahapatra SK (2015). Versatile and Synergistic Potential of Eugenol: A Review. Pharmaceutica Analitica Acta 6(6):1-6. https://doi.org/10.4172/21532435.1000367
Chen J, Mao S, Xu Z, Ding W (2019). Various antibacterial mechanisms of biosynthesized copper oxide nanoparticles against soilborne *Ralstonia solanacearum*. RSC Advances 9(7):3788-3799. https://doi.org/10.1039/c8ra09186b
Císarová M, Tančinová D, Medo J (2016). Antifungal activity of lemon, eucalyptus, thyme, oregano, sage and lavender essential oils against *Aspergillus niger* and *Aspergillus tubingensis* isolated from grapes. Potravinarstvo 10(1):83-88. https://doi.org/10.5219/554
Elphinstone J (2005). Edited by Allen C, Prior P, Hayward AC. St. Paul, MN: APS Press. In The current bacterial wilt situation: a global overview. In: Bacterial wilt disease and the *Ralstonia solanacearum* species complex. Edited by Allen C, Prior P, Hayward AC. St. Paul, MN: APS Press.
Elshikh M, Ahmed S, Funston S, Dunlop P, McGaw M, Marchant R, Banat IM (2016). Resazurin-based 96-well plate microdilution method for the determination of minimum inhibitory concentration of biosurfactants. Biotechnology Letters 38(6):1015-1019. https://doi.org/10.1007/s10529-016-2079-2
Fegan M, Prior P (2005). How complex is the "*Ralstonia solanacearum* species complex". Bacterial wilt disease and the *Ralstonia solanacearum* species complex 1:449-461.
Gildemacher PR, Kaguongo W, Ortiz O, Tesfaye A, Woldegiorgis G, Wagoire WW, Kakuhenzire R, Kinyae PM, Nyongesa M, Struik PC, Leeuwis C (2009). Improving potato production in Kenya, Uganda and Ethiopia: A system diagnosis. Potato Research 52(2):173-205. https://doi.org/10.1007/s11540-009-9127-4
Hasani M, Hasani S (2018). Nano-encapsulation of thyme essential oil in chitosan-Arabic gum system: Evaluation of its antioxidant and antimicrobial properties. Journal of Food Biochemistry 2(2):75-82. https://doi.org/10.1111/jfbc.12913
Hayward AC (1991). Biology and Epidemiology of Bacterial Wilt Caused by *Pseudomonas solanacearum*. Annual Reviews Phytopathology 29:65-87. https://doi.org/10.1146/annurev.py.29.090191.000433
Jamil B, Abbasi R, Abbasi S, Imran M, Khan SU, Ihsan A, Bokhari H (2016). Encapsulation of cardamom essential oil in chitosan nano-composites: In-vitro efficacy on antibiotic-resistant bacterial pathogens and cytotoxicity studies. Frontiers in Microbiology 7(1580):1-10. https://doi.org/10.3389/fmicb.2016.01580
Jeyakumar GE, Lawrence R (2021). Mechanisms of bactericidal action of Eugenol against *Escherichia coli*. Journal of Herbal Medicine 26:100406. https://doi.org/10.1016/j.hermed.2020.100406
Ji P, Momol MT, Olson SM, Pradhanang PM, Jones JB (2005). Evaluation of thymol as biofumigant for control of bacterial wilt of tomato under field conditions. Plant Disease 89(5):497-500. https://doi.org/10.1094/PD-89-0497
Kalemba D, Synowiec A (2019). Agrobiological Interactions of Essential Oils of Two Menthol Mints: *Mentha piperita* and *Mentha arvensis*. Molecules 25(1):1-33. https://doi.org/10.3390/molecules25010059
Karim Z, Hossain M (2018). Management of Bacterial Wilt (*Ralstonia solanacearum*) of Potato: Focus on Natural Bioactive Compounds. Journal of Biodiversity, Conservation and Bioresouce Management 4(1):1-10.
Kelman A (1954). The relationship of pathogenecity in *Pseudomonas solanacearum* to colony appearance on a tetrazolium medium. Phytopathology 44(12):693-695.
Khalil AA, Rahman UU, Khan MR, Sahar A, Mehmood T, Khan M (2017). Essential oil eugenol: Sources, extraction techniques and nutraceutical perspectives. RSC Advances 7(52):32669-32681. https://doi.org/10.1039/c7ra04803c
Kit-Kay M, Masnah BK, Sunday BA, Raghavendra S, Yew-Beng K, Kavitha M, Madhu KB, Sazali HA, Mallikarjuna RP (2019). A Comprehensive Review on Eugenol's Antimicrobial Properties and Industry Applications: A Transformation from Ethnomedicine to Industry. Pharmacognosy Reviews 13(25):1-9. https://doi.org/10.4103/phrev.phrev
Kokina M, Salevic A, Kaluševic A, Levic S, Pantic M, Dejan P, Šavikin K, Shamtsyan M, Nikšic M, Nedovic V (2019). Characterization, antioxidant and antibacterial activity of essential oils and their encapsulation into biodegradable material followed by freeze drying. Food Technology and Biotechnology 57(2):282-289. https://doi.org/10.17113/ftb.57.02.19.5957
Lambert RJW, Skandamis PN, Coote PJ, Nychas GJE (2001). A study of the minimum inhibitory concentration and mode of action of oregano essential oil, thymol and carvacrol. Journal of Applied Microbiology 91(3):453-462. https://doi.org/10.1046/j.1365-2672.2001.01428.x
Li S, Yu Y, Chen J, Guo B, Yang L, Ding W (2016). Evaluation of the antibacterial effects and mechanism of action of protocatechualdehyde against *Ralstonia solanacearum*. Molecules 21(6):754 https://doi.org/10.3390/molecules21060754
Meng F (2013). Ralstonia Solanacearum Species Complex and Bacterial Wilt Disease. Journal of Bacteriology and Parasitology 04(02):2-5. https://doi.org/10.4172/2155-9597.1000e119
Mourey A, Canillac N (2002). Anti-Listeria monocytogenes activity of essential oils components of conifers. Food Control 13(4-5):289-292. https://doi.org/10.1016/S0956-7135(02)00026-9
Muthoni J, Kabira J, Shimelis H, Melis R (2014). Spread of Bacterial Wilt Disease of Potatoes in Kenya: Who is to Blame? International Journal of Horticulture 4(3):10-15 https://doi.org/10.5376/ijh.2014.04.0003
Muthoni J, Nyamongo DO (2009). A review of constraints to ware Irish potatoes production in Kenya. A Journal of Horticulture and Forestry 1(7):98-102. https://doi.org/10.1007/BF00259576
Mutimawurugo MC, Wagara IN, Muhinyuza JB, Ogweno JO (2019). Virulence and characterization of isolates of potato bacterial wilt caused by *Ralstonia solanacearum* (Smith) in Rwanda. African Journal of Agricultural Research 14(6):311-320. https://doi.org/10.5897/AJAR2018.13686
Nasir B, Fatima H, Ahmad M, Ihsan-ul-Haq (2015). Recent Trends and Methods in Antimicrobial Drug Discovery from Plant Sources. Austin Journal of Microbiology 1(1):1-12. http://austinpublishinggroup.com/microbiology/fulltext/ajm-v1-id1002.php
Nesrollahi P, Razavi SM (2017). Herbicidal and Anti Pathogenic Potential of Thymol. Scholars Academic Journal of Biosciences 5(3):183-186. https://doi.org/10.21276/sajb.2017.5.3.9
Nurdjannah N, Bermawie N (2012). 11-Cloves. In Handbook of Herbs and Spies. (Second E. Peter (Ed.), Woodhead Publishing Series in Food Science, Technology and Nutrition 1:197-215 Woodhead Publishing. https://doi.org/https://doi.org/10.1533/9780857095671.197
O'Brien J, Wilson I, Orton T, Pognan F (2000). Investigation of the Alamar Blue (resazurin) fluorescent dye for the assessment of mammalian cell cytotoxicity. European Journal of Biochemistry 267(17):5421-5426. https://doi.org/10.1046/j.1432-1327.2000.01606.x
Oboo H, Muia A, Kinyua Z (2014). Effect of Essential Oil Plant Extracts on in vitro Growth of *Ralstonia solanacearum*. Egerton Journal of Science and Technology 14(2073):141-160.
Odds FC (2003). Synergy, antagonism, and what the chequerboard puts between them. The Journal of Antimicrobial Chemotherapy 52(1):1 https://doi.org/10.1093/jac/dkg301
Orchard A, VanVuuren S (2017). Commercial Essential Oils as Potential Antimicrobials to Treat Skin Diseases. In Evidence-based Complementary and Alternative Medicine 2017.

https://doi.org/10.1155/2017/4517971
Oulkheir S, Aghrouch M, El-Mourabit F, Dalha F, Graich H, Amouch F, Ouzaid K, Moukale A, Chadli S (2017). Antibacterial Activity of Essential Oils Extracts from Cinnamon, Thyme, Clove and Geranium Against a Gram Negative and Gram Positive Pathogenic Bacteria. Journal of Diseases and Medicinal Plants 3(1):1-5. https://doi.org/10.11648/j.jdmp.s.2017030201.11
Patil VU, Gopal J, Singh BP (2012). Improvement for Bacterial Wilt Resistance in Potato By Conventional and Biotechnological Approaches. Agricultural Research 1(4):299-316. https://doi.org/10.1007/s40003-012-0034-6
Paudel S, Dobhal S, Alvarez AM, Arif M (2020). Taxonomy and Phylogenetic Research on *Ralstonia solanacearum* Species Complex: A Complex Pathogen with Extraordinary Economic Consequences. Pathogens 9(11):886 https://doi.org/10.3390/pathogens9110886
Pavesi C, Banks LA, Hudaib T (2018). Antifungal and antibacterial activities of eugenol and non-polar extract of *Syzygium aromaticum* L. Journal of Pharmaceutical Sciences and Research 10(2):337-339.
Pei RS, Zhou F, Ji BP, Xu J (2009). Evaluation of combined antibacterial effects of eugenol, cinnamaldehyde, thymol, and carvacrol against E. coli with an improved method. Journal of Food Science 74(7):M379-M383. https://doi.org/10.1111/j.1750-3841.2009.01287.x
Perricone M, Arace E, Corbo MR, Sinigaglia M, Bevilacqua A (2015). Bioactivity of essential oils: A review on their interaction with food components. Frontiers in Microbiology 6(2):1-7. https://doi.org/10.3389/fmicb.2015.00076
Pradhanang PM, Elphinstone JG, Fox RTV (2000). Sensitive detection of *Ralstonia solanacearum* in soil: A comparison of different detection techniques. Plant Pathology 49(4):414-422. https://doi.org/10.1046/j.1365-3059.2000.00481.x
Sarah MA, Lobna SEH (2017). Combined efficacy of thymol and silver nanoparticles against *Staphylococcus aureus*. African Journal of Microbiology Research 11(11):450-457. https://doi.org/10.5897/ajmr2016-8387
Sienkiewicz M, Łysakowska M, Denys P, Kowalczyk E (2012). The antimicrobial activity of thyme essential oil against multidrug resistant clinical bacterial strains. Microbial Drug Resistance 18(2):137-148. https://doi.org/10.1089/mdr.2011.0080
Valliammai A, Selvaraj A, Yuvashree U, Aravindraja C, Karutha Pandian S (2020). sarA-Dependent Antibiofilm Activity of Thymol Enhances the Antibacterial Efficacy of Rifampicin Against *Staphylococcus aureus.* Frontiers in Microbiology 11(7):1-13. https://doi.org/10.3389/fmicb.2020.01744
Xue J, Knoxville U (2015). Essential Oil Nanoemulsions Prepared with Natural Emulsifiers for Improved Food Safety. Doctoral Dissertations University of Tennessee, 194 pp.http://trace.tennessee.edu/cgi/viewcontent.cgi?article=4730&context=utk_graddiss%5Cnhttp://trace.tennessee.edu/utk_graddiss/3381

Vol. 20(6), pp.266-274, June, 2021
DOI: 10.5897/AJB2016.15696
Article Number: 85DA99067135
ISSN: 1684-5315

http://www.academicjournals.org/AJB

ACADEMIC JOURNALS
expand your knowledge

African Journal of Biotechnology

Review

Imaging from anatomic to molecular and atomic resolution scales: A review

Kamweru, Paul Kuria

Department of Physical Sciences, Chuka University, P. O. Box 109-60400, Chuka, Kenya.

Received 23 September, 2016; Accepted 19 January, 2017

Imaging may be referred to as the 'eyes of science' as it provides scientists with highly informative multi-dimensional and multi-parameter data usually invisible to the naked eye. As instrumentation technologies and genetic engineering advances, it's possible in modern times to observe and image highly dynamic biochemistry processes. This paper reviews positron emission tomography (PET), magnetic resonance imaging (MRI), computed tomography (CT), ultrasound, visible light microscopy, bioluminescence (BLI) and fluorescence mediated tomography (FMT) imaging techniques, highlighting the principles behind the operation of each technique, their major strengths and drawbacks. With the enhancement of the existing techniques and evolution of new ones, the future possibility of refined view of systems invisible to naked human eye is promising. More so is when two or more techniques are combined in biological systems analysis.

Key words: Optical, imaging, microscopy, resolution, fluorescence.

INTRODUCTION

Imaging, whether macroscopic, microscopic or nanoscopic plays a unique role in sciences in that it aids to collect data that can be analyzed to provide useful insights during experimentation and postexperiment. In that respect, imaging may be referred to as the 'eyes of science'. Imaging provides scientists with highly informative multi-dimensional and multi-parameter data. Examples of physical parameters that could be imaged/measured are concentration e.g. of water (Pircher et al., 2003) and oxygen (Kurokawa et al., 2015; Papkovsky and Dmitriev, 2012a, b), tissue properties (Gao, 1996), surface area (Eils and Athale, 2003), molecular architecture (Fridman et al., 2012), protein binding dynamics (Marsh and Teichmann, 2015), protein diffusion rates (Day and Schaufele, 2008) and many others, all of which provide an insight on temporal biological functions. Traditionally imaging has been done using various techniques that for example freezes biological specimens during sample preparations, but with the recent advances in high-resolution microscopy and genetically engineered fluorescent probes that are fusible to cellular proteins (Day and Schaufele, 2008), live cell imaging is now possible, that is very useful to observe the highly dynamic cellular multi-parameters. In other words, events or parameters occurring on a large scale of time scales can be obtained in minimally invasive

E-mail: pkamweru@gmail.com, pkkamweru@chuka.ac.ke.

Table 1. Imaging from anatomical to atomic scales.

Imaging technique	Spatial resolution	Depth limit	Scan Time	Key use	References
PET/MicroPET/MicroSPECT	1-2 mm	No limit	Minutes	Metabolic imaging of molecules such as glucose, thymidine, imaging of probes such as antibodies, peptides etc.	Weissleder, 2002; Park et al., 2007; Koba et al., 2013; Moore et al., 2000; Jang, 2013
MRS	≈ 2 nm	-	Minutes-Hours	Detection of metabolites	Gabbay et al , 2007; Müller et al., 2014; Strobel et al., 2008
fMRI	≈ 1 nm	No limit	Seconds-Minutes	Functional imaging of brain activity	Kriegeskorte and Bandettini, 2007; Ciobanu and Pennington, 2004
MRI/MicroMRI	4-100 µm,	No limit	Minutes-Hours	Anatomical Imaging	Weissleder, 2002; Ciobanu and Pennington, 2004; Singh et al., 2002
CT/MicroCT	12-50 µm	No limit	Minutes	Lung and bone tumor imaging	Weissleder, 2002; Koba et al., 2013; Jang, 2013; Meng et al , 2006.
Ultrasound	≈ 50 µm	Millimeters	Seconds	Vascular and interventional imaging	Weissleder, 2002, Jang, 2013.
Visible Microscopy (various modern techniques are summarized in Table 2)					
Bioluminescence (BLI)	Several mm	cm	Minutes	Gene expression and cell tracking	Sadikot and Blackwell, 2005; Keyaerts et al., 2012)
Fluorescence mediated tomography (FMT)	1-2 mm	< 1 cm	Seconds-Minutes	Quantitative imaging of targeted fluorochromes in deep tumors	Ntziachristos et al., 2002; Ntziachristos and Weissleder, 2003
Atomic force microscopy	10-20 nm	-	Minutes	Mapping cell surface	Leonenko et al., 2007; Binnig et al , 1986.
Electron microscopy	≈ 5 nm	-	Seconds	Discerning protein structure	Murphy and Jensen, 2007

optical based techniques. Obtained parameters in biological systems are useful and applied to allow both therapeutic and diagnostic applications (Alivisatos et al., 2005; Michalet et al., 2005; Loo et al., 2004). In addition data acquired from imaging procedures forms the foundation for mathematical modeling e.g. of protein kinetics and biochemical signaling networks (Chen and Murphy, 2004). Imaging data can also be utilised to test computational models developed in computational biology (Kherlopian et al., 2008).

IMAGING ON MULTIPLE SCALES

In contemporary times, using several techniques such as positron-emission tomography, magnetic resonance imaging, and optical coherence tomography, imaging is possible in a wide large of spatial resolution, ranging between 1 mm and 10 µm. Even much higher spatial resolutions at the molecular or at atomic levels (< 10 nm) are now possible with electron microscopy and scanning probe techniques, as summarized in Table 1.

Between these two resolutions extremes lies the resolving power of optical microscopy (that is, 10 nm to 1 mm) that utilizes visible light (≈ 400 to 700 nm). A summary of various modern visible range imaging techniques are summarized in Table 2. Imaging within this electromagnetic spectra region is beneficial since the radiation energy strikes a balance between being energetic enough to view fluorescent probes and fair enough to be minimally invasive, thus enabling live cell imaging.

However, a major drawback arises from the limits to spatial resolution that is famously represented by the Abbes equation (Abbe, 1873):

$$d = \frac{\lambda}{2\, n \sin\, \theta} \equiv \frac{\lambda}{2NA} \quad (1)$$

where λ is the radiation wavelength, n is the refractive index of the medium, θ is the half angle over which the objective can gather light radiation, NA is the numerical aperture of the objective. A direct implication of Equation 1, with $NA \approx 1.4 - 1.6$ possible with modern optics is that, the spatial resolution $d \approx \frac{1}{2}\lambda$, meaning that for green light of around 500 nm $d = \lambda/2 = 250$ nm (0.25 µm). In

Table 2. Modern innovative techniques that overcomes the Abbes resolution limit.

Visible microscopic technique	Principle	Resolution	Scan time	References
Near-Field (NSOM) -Scanning near-field optical microscopy -Wide-field near-field optical microscopy	Done by placing the detector very close to the specimen surface	20 nm (Lateral), 2–5 nm (axial)		Dürig et al., 1986; Oshikane et al., 2007: Novotny et al., 1995
-Photo-activated light microscopy (PALM) -Fluorescence PALM (FPALM) -Stochastic optical reconstruction (STORM)	Photoactivation/photo switching and localization of single fluorescent molecules	10-40 nm (Lateral) ~ 10-50 nm (Axial)	Seconds	Hess et al., 2006; Betzig et al 2006; Rust et al., 2006; Heilemann et al., 2008; Huang et al., 2008; Shtengel et al., 2009
Stimulated emission depletion (STED)	PSF shrinking by stimulated emission depletion	30-50 nm (Lateral) 30-600 nm (Axial)		Betzig et al., 2006; Rust et al., 2006; Donnert et al., 2006; Hell and Wichmann, 1994
Saturated structured illumination (SSIM)	Moiré pattern by spatially structured illumination	~ 100 nm (Lateral) < 300 nm (Axial)	Seconds	Gustafsson, 2000; Burnette et al., 2011; Andersson, 2008;
Ground state depletion (GSD)	Depletion of ground-state energy of out-of-focus molecules	~ 15 nm (Lateral)	Minutes	Hell and Kroug, 1995
4Pi and I^{5}M	Coherent addition of spherical wavefronts of two opposing high aperture angle lenses	~ 100 nm (Axial)		Bewersdorf et al., 2006; Egner et al., 2002; Egner et al., 2004; Egner and Hell, 2005; Geisler, 2009
Confocal microscopy	actively suppressing any signal coming from out-of-focus planes e.g. by use of a pinhole in front of the detector			Robert et al., 1996
Widefield and TIRF (total internal reflection fluorescence) Microscopy	Formation of evanescence excitation field as light is total internally reflected at an interface between a high- and a low-index medium	~ 100 nm		Chung et al., 2006
Optical coherence tomography	Use of low-coherence interferometry to produce a 2D image of optical scattering from internal tissue microstructures	Few µm	Minutes	Huang et al., 1991

addition, the limit implies that radiation of much lower wavelengths e.g. x-rays, can achieve higher resolutions, but this leads to the loss of the aforementioned advantage of visible light, that is, minimal invasiveness. As a consequence of tireless research, several techniques to innovatively overcome the Abbes resolution limit has been developed, as summarized in Table 2. Principles underlying the working of these techniques laid out in Table 2, have been presented in different articles and reviews (Weisenburger and Sandoghdar, 2015; Won, 2009; Hell et al., 2009).

IMAGING TECHNIQUES

It is projected that in the coming years, improvement in both spatial and lateral resolution combined with time-based sampling will be on the increase. In addition, more techniques will improve the ability to image highly dynamic molecular and cellular substructures. These innovative techniques will most probably lie on improvement of the existing microscopy methods, ultrasound, computed tomography (CT), magnetic resonance I maging (MRI), positron emission

Table 3. Comparison of micro-, mini- and clinical-scale CT.

Parameter	Suitable for	Resolution μm)	Transaxial scan field-of-view	Time of scan	References
CT	Large animals up to humans	> 450	> 20 cm	Few seconds	Weissleder, 2002; Meng et al., 2006; Thomasson et al., 2004.
Mini-CT	Mice, primates, rats , rabbits	100-450	5-20 cm	Sub seconds to few seconds	Meng et al., 2006; Ritman, 2011.
Micro-CT	Tissue samples , insects, mice and rats	5-100	1-5 cm	Seconds to hours	Meng et al., 2006; Ritman, 2011.

tomography (PET), microCT, microMRI, fMRI, MicroPET among others. This review paper briefly discusses in this section the imaging techniques across a multiple resolution scale, giving a summary of each technique's underlying principles and discussion of their advantages and limitations.

PET/MICROPET/MICROSPECT

Positron emission tomography (PET) is an imaging technique that enables performance of *in vivo* measurements of the anatomical distribution and rates of specific biochemical reactions (Phelps and Mazziotta, 1985). In this technique, radioactive decaying nuclides such as ^{15}O, ^{13}N, ^{11}C, ^{18}F, ^{124}I and ^{94m}Tc are incorporated into metabolically active molecules and then intravenously injected into the animal (Massoud and Gambhir, 2003; Kherlopian et al., 2008; Weissleder, 2002). These metabolically active molecules diffuse in the target tissue, after a brief window period and the nuclides begin to decay, emitting positrons that collide with free electrons. This interaction of positrons and free electrons results to the conversion of matter into two 511 keV γ-rays emerging in opposite directions (Nelson et al., 2002; Phelps et al., 2002) which are detected and observed by detector rings. By using radioactive tracers, reconstruction of 3-D images to show the concentration and locations of metabolic molecules of interest is made possible (Gambhir, 2002). For example, molecular events in the course of Cancer development, during therapy or recurrence can be monitored (Phelps et al., 2002; Gambhir, 2002) by PET. Applied that way, PET is a highly sensitive and minimally-invasive technology. An additional strength of PET is that quantitative kinetic data of highly dynamic biochemistry can be acquired repetitively. However, due to the same decay type of the different radioactive tracers, it is only possible to trace one molecular species in a given imaging experiment or clinical scan. Single photon emission tomography (SPECT) also involves the detection and quantification of gamma-emitting radionuclides. This technique is commonly used in experimental oncology to track individual molecules or cells. The molecule or cell of interest is labelled with a gamma-ray-emitting nuclide such as, ^{99m}Tc, ^{111}In, ^{123}I or ^{125}I, injected into an animal and followed using sodium iodide gamma cameras or solid-state cadmium-zinc telluride (CZT) detectors (Groch, 2001). Gamma emitting nuclides are cheap and differ in their decay time, energy and mode of attachment and hence different nuclides are used for different applications. By placing Lead collimators between the animal and detectors, spatial information is obtained, which when obtained in various projections are finally tomographicaly reconstructed.

MRI/MICROMRI AND FMRI

When imaging an object by Magnetic Resonance Imaging (MRI), the object is placed in a strong magnetic field. This magnetic field aligns the spins of the hydrogen nuclei, predominantly in water and fat, in a direction parallel to the field. Then using a radio frequency pulse, the sample's protons spins can be made to tilt and precess (Nazarian et al., 2013). A radio frequency receiver records the resulting signal, which is can readily be constructed to produce detailed pictures of organs, soft tissues, bone and virtually all other internal body structures (Curie et al., 2013). At much higher magnetic field strengths, which improves resolution, the method is referred to as MicroMRI. Functional magnetic resonance imaging or functional MRI (fMRI) is a functional neuroimaging procedure based on MRI, and used to image brain activity in response to specified stimuli. When a stimuli requires a response in a particular area of the brain, metabolism and hence demand for blood flow and more oxygenated hemoglobin increases in that area. The ratio of oxygenated and deoxygenated brain is altered in

that region and hence an image taken will have a different contrast, especially when compared with the baseline measurements (Parrish et al., 2000).

ULTRASOUND

Detection of reflected sound waves (20-60 MHz; 2-10 MHz in humans) as echoes by probes forms the basis of ultrasound imaging. A handheld probe that sends pulses of sound into a patient's body is moved over the body using water-based gels. The gels are used to avoid intense sound reflections at the borderlines between ultrasonic probe and the patient's skin resulting from air pockets. The depth of the tissue reflecting the sound waves is inferred from the time it takes for the echo to travel back to the probe. Computer Algorithms are then used to interpret these echo waveforms to construct an image (Jensen, 2007). Ultrasound major strengths are that it is less expensive compared to other techniques, it is more patient friendly e.g. there is no claustrophobia, and it is dynamic making real time observation possible which makes artifacts detection easier than in other techniques (Lento and Primack, 2008). A major drawback arises due to techniques' dependence on body's general constitution; resolution is compromised in obese and muscular patients for example (Lento and Primack, 2008). However, improvement of visualization and resolution of deeper structures is improving with recent refinement of tissue harmonics (Rosenthal et al., 2001).

CT/MICROCT AND MINI-CT

X-ray computed tomography (CT) measures the absorption of X-rays as they pass through tissues. Intrinsic differences in absorption between bone, fat, air and water result in high-contrast images of anatomical structures in CT. Due to the CT relatively poor soft-tissue contrast and inability to differentiate between tumors and surrounding tissue, iodinated contrast agents, which perfuse different tissue types at different rates, are commonly used to delineate organs and tumors. Practically, a low X-ray source and a detector rotate around the subject, acquiring volumetric data.

The detectors are typically charged coupled devices (CCD) and act to photo transduce incoming X-rays (Kalender, 2006). Micro- and mini-CT are scaled down CT-imaging modalities for small animals, which in principle provide the same information about morphology and disease status or disease progression for animals as clinical-scale CT does for humans. However, several major differences compared to clinical CT scanning exist as reviewed by Bartling et al. (2007). For animal studies, microCT machines can be used which typically operate with higher energy X-rays when compared to human scanners. The increase in energy improves resolution, but exposes the specimen to more ionizing radiation which has adverse health effects. A comparison of the three is shown in the Table 3.

A key advantage of CT is its high spatial resolution, 12 to 50 µm (Weissleder, 2002; Meng, 2006) which is needed to visualize fine anatomical details. CT can also be combined with functional imaging technologies that provide dynamic and metabolic information. The radiation dose of CT, however, is not negligible and this limits repeated imaging in human studies due to health risks (Thomasson et al., 2004).

OPTICAL MICROSCOPY APPROACHING TO NANOSCOPY

Optical microscopy could be regarded as the most significant tool to visualize objects that are usually invisible to the naked eye. It's a technique with the capability to measure surface morphology and localize molecular and protein distributions *in vivo*. Through microscopy, our knowledge about the 'micro-world' has been greatly enhanced. Technological improvement, coupled with the advent of green fluorescent protein (GFP) leading to rise of fluorescence microscopy has been a major step forward in the study of living cells. Traditional fluorescence microscopy suffered from the need to use high energetic laser light, hence photobleaching the samples and detection of out of focus excitations, further impairing the resolution already limited by Abbes equation. Improvement of traditional fluorescence microscopy, has led to development of new microscopy techniques such as multi-photon and confocal and microscopy to deal with the two drawbacks of traditional microscopy respectively (Yuste, 2005). Following continuous and ongoing research, in effort to break the diffraction barrier, other techniques like stimulated emission depletion (STED) (Betzig et al., 2006), photo-activated localized microscopy (PALM) (Hess et al., 2006; Betzig et al., 2006) and stochastic optical reconstruction microscopy (STORM) (Rust et al., 2006) has been developed. These methods have improved resolution to, 30 to 50 nm for STED and 10 to 40 nm for PALM/STORM (Heilemann et al., 2008, Huang, 2008; Meyer et al., 2008). In STED microscopy two pulsed lasers are used, one laser pulse is chosen to have the wavelength that excites fluorophores, and a second donut shaped laser pulse that depletes fluorescence follows instantaneously. The wavelength of the second laser is tuned to be longer than the fluorescence emission. Consequently, photons from the second laser induce electrons to drop to a lower energy level (stimulated emission) averting typical fluorescence, and hence achieving emission depletion. The final result would be a very small area (center of the donut shaped depleting beam) from where the fluorescence is detected. This area is smaller than a diffraction-limited spot. The

principle behind STORM and PLAM is the ability to stochastically switch on and off (Huang et al*.,* 2009; Huang et al*.,* 2010) a small subset of fluorescent molecules, the only difference is that PALM uses photo-activatable fluorescent proteins and STORM uses photo-switching of pairs of cyanine dyes (Bates et al., 2007; Rust et al., 2006; Heilemann et al., 2008). If the number of activated fluorophores is kept low enough so that the distance between the molecules is larger than the resolution limit, each fluorophore molecule can be localized. A super-resolved image is then obtained by the superposition of many wide-field images containing information on the location of different single molecules (Hess et al*.,* 2006; Betzig et al*.,* 2006; Rust et al*.,* 2006).

An additional innovative microscopic technique that achieves resolution at the nano-scale (< 10 nm) is the Förster Resonance Energy Transfer (FRET). The technique has been reviewed extensively by Sekar and Periasamy (2003), and Roy et al. (2008) among others. The technique is based on resonance energy transfer whereby, an excited donor fluorophore in close proximity (< 10 nm) to an acceptor fluorophore, whose absorption spectrum overlaps with the emission spectrum of the donor, non-radiatively transfers some of its excited state energy to the acceptor in a manner dependent on dipole-dipole resonance coupling (Pietraszewska and Gadella, 2010). Hence a positive FRET occurrence estimates that the two fluorophores are within 10 nm (Berney and Danuser, 2003). With a confocal microscope, one way FRET is performed is by acceptor-bleaching method as described in earlier publications by former colleagues (Orthaus et al., 2008; Orthaus et al., 2009) in use to study the structure of the human Kinetochore. Recently, the technique has demonstrated, to be a valuable tool in our study the centromeric chromatin (Llères et al., 2009). This is the chromatin site where the kinetochore structure is anchored by the presence of CENP-A histone and longer links made possible by the CENP-C terminal tails as we have reported in Abendroth et al. (2015). A combination of the STORM and FRET in the study kinetochore structure and centromeric chromatin is expected to be a major breakthrough in understanding of these highly dynamic structures in the cell cycle.

BIOLUMINESCENCE IMAGING

Bioluminescence imaging (BLI) is a technique similar to Fluorescence Optical imaging, the difference is that here, the few photons being measured emanate from cells that have been genetically engineered to express luciferases (Sato et al*.,* 2004). Luciferases are enzymes that catalyze the oxidation of a substrate to release photons of light (Greer and Szalay, 2002). These enzymes are isolated from a variety of species for example, luciferase from the firefly catalyze the oxidation of luciferin, whereas luciferase from the sea pansy *Renilla reniformis* catalyze the oxidation of coelenterazine causing the release of a photon (Sadikot and Blackwell, 2005). Because mammalian tissues do not naturally emit bioluminescence, *in vivo* BLI has considerable appeal because images can be generated with very little back-ground signal. Credit to genetic engineering, a number of luciferases that results to a spectral shift of released photons have been created (Loening et al*.,* 2010). This, coupled with high sensitive optical filters, imaging of two or more cellular proteins, or their mutants can be tracked simultaneously. BLI is inexpensive, a good alternative of PET imaging, however, it is not likely to be used in a clinical setting, because it can only monitor transgenically modified tumour cells and because it is difficult to detect photons released from deep tissues (Weissleder, 2002).

FLUORESCENCE-MEDIATED TOMOGRAPHIC IMAGING

In this technique, fluorescently labeled probe of interest is exposed to light from different sources. The resultant fluorescence is detected by various detectors positioned in a spatially defined order in an imaging chamber. The obtained information is reconstructed using an algorithm, giving a 3-D reconstructed tomographic image that makes it useful for clinical measurements. The potential of FMT for laboratory use is great since it does not require radioactive labeling and it can make use of the increasing number of fluorescent tags (Ntziachristos and Weissleder, 2003). As a major strength of this technique, it has been demonstrated that a combination of measurements of fluorescent and of intrinsic contrast can provide self-calibrated tomographic data that could yield absolute fluorochromes concentration reconstructions (Ntziachristos et al., 2002). In addition the technique can do in vivo observations (Ntziachristos et al., 2002).

CONCLUSION

A review of the diverse imaging techniques used for diagnosis and research has been presented though the list is not exhaustive. It is very clear that no single technique can achieve everything that needs to be observed, each technique has its own strengths as well as limitations. These unique strengths and drawbacks dictate where and when to apply a technique e.g. ultrasound for its low associated risks is applied in viewing fetus, but it is of no use to image lungs and bones for example because of the very high reflections at air-tissue and bone-tissue interfaces. Another major factor that makes each technique unique is the resolution. This is a consequence of biological systems being complex, and so is the radiation interaction with these systems. Infact there is a resolution gap between techniques that are suitable for experimental research

and clinical imaging, that is, there is a gap between anatomic and microscopic scales. To address the resolution gaps, a combination of imaging techniques is recommended and indeed these combinations are being tried out. For example there have been successful attempts to bridging fluorescence microscopy and electron microscopy. Another example is the combination of PET and CT scanners which makes it possible to acquire metabolic information recorded with higher resolution anatomical CT images.

CONFLICT OF INTERESTS

The authors have not declared any conflict of interests.

REFERENCES

Abbe E (1873). Beiträge zur Theorie des Mikroskops und der mikroskopischen Wahrnehmung. Arch. Mikroskop. Anat. 9:413-418.

Abendroth C, Hofmeister A, Hake SB, Kamweru PK, Miess E, Dornblut C, Küffner I, Deng W, Leonhardt H, Orthaus S, Hoischen C, Diekmann S (2015). The CENP-T C-Terminus Is Exclusively Proximal to H3.1 and not to H3.2 or H3.3. International Journal of Molecular Sciences 16(3):5839-5863.

Alivisatos AP, Gu W, Larabell C (2005). Quantum dots as cellular probes. Annual Review of Biomedical Engineering 7:55-76.

Andersson S (2008). Localization of a fluorescent source without numerical fitting. Optics Express 16:18714-18724.

Bartling HS, Stiller W, Semmler W, Kiessling F (2007) Small animal computed tomography imaging. Current Medical Imaging Reviews 3:45-59.

Bates M, Huang B, Dempsey GT, Zhuang X (2007). Multicolor super-resolution imaging with photo-switchable fluorescent probes. Science 317:1749-1753.

Berney C, Danuser G (2003). FRET or No FRET: A Quantitative Comparison. Biophysical Journal 84:3992-4010.

Betzig E, Patterson GH, Sougrat R, Lindwasser OW, Olenych S, Bonifacino JS, Davidson MW, Lippincott-Schwartz J, Hess HF (2006). Imaging intracellular fluorescent proteins at nanometer resolution. Science 313:1642-1645.

Bewersdorf J, Schmidt R, Hell SW (2006). Comparison of I^5M and 4Pi-microscopy. Journal of Microscopy 222:105-117.

Binnig G, Quate CF, Gerber Ch (1986). Atomic force microscope. Physical Review Letters 56:930

Burnette DT, Sengupta P, Dai Y, Lippincott-Schwartz J, Kachar B (2011). Bleaching/blinking assisted localization microscopy for superresolution imaging using standard fluorescent molecules. Proceedings of the National Academy of Sciences USA 108:21081-21086.

Chen X, Murphy RF (2004). Location proteomics: determining the optimal grouping of proteins according to their subcellular location patterns as determined from fluorescence microscope images. In. Signals, Systems and Computers, 2004. Conference Record of the Thirty-Eighth Asilomar Conference on Nov 7. IEEE. 1:50-54.

Chung E, Kim D, So PTC (2006). Extended resolution wide-field optical imaging: objective-launched standing-wave total internal reflection fluorescence microscopy. Optics Letters 31:945-947.

Ciobanu L, Pennington CH (2004). 3D micron-scale MRI of single biological cells. Solid State Nuclear Magnetic Resonance 25(1-3):138-141.

Curie S, Hoggard N, Craven IJ, Hadjivassiliou M, Wilkinson ID (2013). Understanding MRI: basic MR physics for physicians. Postgraduate Medical Journal 89:209-223.

Day RN, Schaufele F (2008). Fluorescent protein tools for studying protein dynamics in living cells: a review. Journal of Biomedical Optics13(3):031202.

Donnert G, Keller J, Medda R, Andrei MA, Rizzoli SO, Lührmann R, Jahn R, Eggeling C, Hell SW (2006). Macromolecular - scale resolution in biological fluorescence microscopy. Proceedings of the National Academy of Sciences USA 103:11440-11445.

Dürig U, Pohl DW, Rohner F (1986). Near-field optical scanning microscopy. Journal of Applied Physics59(10):3318-3327.

Egner A, Hell SW (2005). Fluorescence microscopy with super-resolved optical sections. Trends in Cell Biology15:207-215.

Egner A, Jakobs S, Hell SW (2002). Fast 100-nm resolution three-dimensional microscope reveals structural plasticity of mitochondria in live yeast. PNAS 99:3370-3375.

Egner A, Verrier S, Goroshkov A, Soling HD, Hell SW (2004). 4Pi-microscopy of the Golgi apparatus in live mammalian cells. Journal of Structural Biology 147:70-76.

Eils R, Athale C (2003). Computational imaging in cell biology. Journal of Cell Biology 161(3):477-481.

Fridman K, Mader A, Zwerger M, Elia N, Medalia O (2012). Innovation: Advances in tomography: probing the molecular architecture of cells. Nature Reviews Molecular Cell Biology 13:736-742.

Gabbay V, Hess DA, Liu S, Babb JS, Klein RG, Gonen O (2007). Lateralized caudate metabolic abnormalities in adolescent major depressive disorder: a proton MR spectroscopy study. Australian Journal of Pharmacy 164(12):1881-1889.

Gambhir SS (2002). Molecular imaging of cancer with positron emission tomography. Nature Reviews Cancer 2:683-693.

Gao L, Parker KJ, Lerner RM, Levinson SF (1996). Imaging of the elastic properties of tissue-A review. Ultrasound in Medicine and Biology 22(8): 959-977.

Geisler C (2009). Fluorescence nanoscopy in three dimensions. Göttingen: University of Göttingen.

Greer LF, Szalay AA (2002). Imaging of light emission from the expression of luciferases in living cells and organisms: a review. Luminescence 17:43-74.

Groch MW, Erwin WD (2001). Single-photon emission computed tomography in the year 2001: instrumentation and quality control. Journal of Nuclear Medicine Technology 29:12-18.

Gustafsson MG (2000). Surpassing the lateral resolution limit by a factor of two using structured illumination microscopy. Journal of Microscopy 198:82-87.

Heilemann M, Van De Linde S, Schüttpelz M, Kasper R, Seefeldt B, Mukherjee A, Tinnefeld P, Sauer M (2008). Sub-diffraction-resolution fluorescence imaging with conventional fluorescent probes Angewandte Chemie 47:6172-6176.

Hell SW, Schmidt R, Egner A (2009). Diffraction-unlimited three-dimensional optical nanoscopy with opposing lenses. Nature Photonics 3:381-387.

Hell SW, Wichmann J (1994). Breaking the diffraction resolution limit by stimulated emission: stimulated-emission-depletion fluorescence microscopy. Optics Letters 19:780-782.

Hell SW, Kroug M (1995). Ground-state-depletion fluorescence microscopy: A concept for breaking the diffraction resolution limit. Applied Physics B 60(5):495-497.

Hess ST, Girirajan TP, Mason MD (2006). Ultra-high resolution imaging by fluorescence photoactivation localization microscopy. Biophysical Journal91:4258-4272.

Huang B, Babcock H, Zhuang X (2010). Breaking the diffraction barrier: super-resolution imaging of cells. Cell 143:1047-1058.

Huang B, Bates M, Zhuang X (2009). Super-resolution fluorescence microscopy. Annual Review of Biochemistry. 78:993-1016.

Huang B, Wang W, Bates M, Zhuang X (2008). Three-dimensional super-resolution imaging by stochastic optical reconstruction microscopy. Science 319:810-813.

Huang D, Swanson EA, Lin CP, Schuman JS, Stinson WG, Chang W, Hee MR, Flotte T, Gregory K, Puliafito CA, Fujimoto JG (1991). Optical Coherence Tomography. Science 254(5035):1178-1181.

Jang BS (2013). MicroSPECT and MicroPET Imaging of Small Animals for Drug Development. Toxicology Research29 (1):1-6.

Jensen JA (2007). Medical ultrasound imagingProgress in Biophysics & Molecular Biology 93(1-3):153-165.

Kalender WA (2006). X-ray computed tomography. Physics in Medicine & Biology 51(13):R29-43.

Keyaerts M, Caveliers V, Lahoutte T (2012). Bioluminescence imaging:

looking beyond the light. Trends in Molecular Medicine18(3):164-172.
Kherlopian AR, Song T, Duan Q, Neimark MA, Po MJ, Gohagan JK, Laine AF (2008). A review of imaging techniques for systems biology. BMC Systems Biology 2(1):74.
Koba W, Jelicks LA, Fine EJ (2013). MicroPET/SPECT/CT imaging of small animal models of disease. The American Journal of Pathology 182(2):319-24.
Kriegeskorte N, Bandettini P (2007). Analyzing for information, not activation, to exploit high-resolution fMRI. Neuroimage 38(4):649-662.
Kurokawa H, Ito H, Inoue M, Tabata K, Sato Y, Yamagata K, Kizaka-Kondoh S, Kadonosono T, Yano S, Inoue M, Kamachi T (2015). High resolution imaging of intracellular oxygen concentration by phosphorescence lifetime. Scientific Reports 5:1-13.
Lento PH, Primack S (2008). Advances and utility of diagnostic ultrasound in musculoskeletal medicine. Current Reviews in Musculoskeletal Medicine 1(1):24-31.
Leonenko ZV, Finot E, Cramb DT (2007). Atomic force microscopy to study interacting forces in phospholipid bilayers containing general anesthetics. Methods in Molecular Biology 400:601-609.
Llères D, James J, Swift S, Norman DG, Lamond AI (2009). Quantitative analysis of chromatin compaction in living cells using FLIM–FRET. Journal of Cell Biology 187(4):481-496.
Loening AM, Dragulescu-Andrasi A, Gambhir SS (2010). A red-shifted Renilla luciferase for transient reporter-gene expression. Nature Methods 7:5-6.
Loo CH, Min-Ho L, Hirsch LR, West JL, Halas NJ, Drezek RA (2004). Nanoshell bioconjugates for integrated imaging and therapy of cancer. In. Proc SPIE - Int Soc Opt Eng 1st edition. San Jose, CA, USA , SPIE - The International Society for Optical Engineering Pp.1-4.
Marsh JA, Teichmann SA (2015). Structure, Dynamics, Assembly, and Evolution of Protein Complexes. Annual Review of Biochemistry 84:551-575.
Massoud TF, Gambhir SS (2003). Molecular imaging in living subjects: seeing fundamental biological processes in a new light. Genes & Development17:545-580.
Meng Y, Shaw CC, Liu X, Altunbas MC, Wang T, Chen L, Tu SJ, Kappadath SC, Lai CJ (2006). Comparison of two detector systems for cone beam CT small animal imaging: a preliminary study. In. Medical Imaging Mar 2. International Society for Optics and Photonic. Pp. 614245-614245.
Meyer L, Wildanger D, Medda R, Punge A, Rizzoli SO, Donnert G, Hell SW (2008). Dual-color STED microscopy at 30-nm focal-plane resolution. Small 4(8):1095-1100.
Michalet X, Pinaud FF, Bentolila LA, Tsay JM, Doose S, Li JJ, Sundaresan G, Wu AM, Gambhir SS, Weiss S (2005). Quantum dots for live cells, in vivo imaging, and diagnostics. Science 307(5709):538-544.
Moore AH, Osteen CL, Chatziioannoll AF, Hovda DA, Cherry SR (2000). Quantitative Assessment of Longitudinal Metabolic Changes In vivo After Traumatic Brain Injury in the Adult Rat Using FDG-MicroPET. Journal of Cerebral Blood Flow & Metabolism 20:1492-1501.
Müller C, Kong X, Cai JM, Melentijević K, Stacey A, Markham M, Twitchen D, Isoya J, Pezzagna S, Meijer J, Du JF (2014). Nuclear magnetic resonance spectroscopy with single spin sensitivity. Nature Communications 5:1-6.
Murphy GE, Jensen GJ (2007). Electron cryotomography. Biotechniques 43(4):413-417.
Nazarian S, Beinart R, Halperin HR (2013). Magnetic Resonance Imaging and Implantable Devices. Circulation: Arrhythmia and Electrophysiology 6:419-428.
Nelson SJ, Graves E, Pirzkall A, Li X, Antiniw Chan A, Vigneron DB, McKnight TR (2002). In vivo molecular imaging for planning radiation therapy of gliomas: an application of 1H MRSI. Journal of Magnetic Resonance Imaging 16(4):464-476.
Novotny L, Pohl DW, Hecht B (1995). Scanning near-field optical probe with ultrasmall spot size. Optics Letters 20:970-972.
Ntziachristos V, Graves E, Weissleder R (2002). Advantages of fluorescence-mediated tomography, a prelude to molecular interrogations in deep tissues. In. Biomedical Topical Meeting 2002 Apr 7 (p. MF4). Optical Society of America.
Ntziachristos V, Weissleder R (2003). Fluorescence-mediated molecular tomography, Patent no. 2003: US 6615063 B1.
Ntziachristos V, Ripoll J, Weissleder R (2002). Would near-infrared fluorescence signals propagate through large human organs for clinical studies? Optics Letters 27(5).333-335.
Orthaus S, Biskup C, Hoffmann B, Hoischen C, Ohndorf S, Benndorf K, Diekmann S (2008). Assembly of the inner kinetochore proteins CENP-A and CENP-B in living human cells. Chembiochem 9:77-92.
Orthaus S, Klement K, Happel N, Hoischen C, Diekmann S (2009). Linker Histone H1 is present in centromeric chromatin of living human cells next to inner kinetochore proteins. Nucleic Acids Research 37:3391-3406.
Oshikane Y, Kataoka T, Okuda M, Hara S, Inoue H, Nakano M (2007). Observation of nanostructure by scanning near-field optical microscope with small sphere probe. Science and Technology of Advanced Materials 8(3): 181.
Papkovsky DB, Dmitriev RI (2013). Biological detection by optical oxygen sensing. Chemical Society Reviews 42(22):8700-8732.
Papkovsky DB, Dmitriev RI (2012). Optical probes and techniques for O_2 measurement in live cells and tissue. Cellular and Molecular Life Sciences 69(12):2025-2039.
Park SJ, Rogers WL, Huh S, Kagan H, Honscheid K, Burdette D, Chesi E, Lacasta C, Llosa G, Mikuz M, Studen A (2007). A prototype of very high resolution small animal PET scanner using silicon pad detectors. Nuclear Instruments and Methods in Physics Research A 570(3):543-555.
Parrish TB, Gitelman DR, LaBar KS, Mesulam MM (2000). Impact of signal to-noise on functional MRI. Magnetic Resonance in Medicine 44(6):925-932.
Phelps ME, Chatziioannou A, Cherry S, Gambhir S (2002). Molecular Imaging of Biological Processes from MicroPET in Mice to PET in Patients. IEEE International Symposium on Biomedical Imaging.1:1-9.
Phelps ME, Mazziotta JC (1985). Positron emission tomography: human brain function and biochemistry. Science 228(4701):799-809.
Pietraszewska A, Gadella TWJ (2010). FRET microscopy: from principle to routine technology in cell biology. Journal of Microscopy 241(2):111-118
Pircher M, Götzinger E, Leitgeb R, Fercher AF, Hitzenberger CK (2003). Measurement and imaging of water concentration in human cornea with differential absorption optical coherence tomography. Optics Express 11(18):2190-2197.
Ritman EL (2011). Current Status of Developments and Applications of Micro-CT. Annual Review of Biomedical Engineering 13:531-552.
Robert HW (1996). Confocal optical microscopy. Reports on Progress in Physics 59:427.
Rosenthal SJ, Jones PH, Wetzel LH (2001). Phase inversion tissue harmonic sonographic imaging: a clinical utility study. American Journal of Roentgenology176:1393-1398.
Roy R, Hohng S, Ha T (2008). A practical guide to single-molecule FRET. Nature Methods 5:507-516.
Rust MJ, Bates M, Zhuang X (2006). Sub-diffraction-limit imaging by stochastic optical reconstruction microscopy (STORM). Nature Methods 3:793-795.
Sadikot RT, Blackwell TS (2005). Bioluminescence Imaging. Proceedings of the American Thoracic Society 2:537-540.
Sato A, Klaunberg B, Tolwani R (2004). *In vivo* bioluminescence imaging. Comparative Medicine 54(6):631-634.
Sekar RB, Periasamy A (2003). Fluorescence resonance energy transfer (FRET) microscopy imaging of live cell protein localizations. Journal of Cell Biology 160(5):629-633.
Shtengel G, Galbraith JA, Galbraith CG, Lippincott-Schwartz J, Gillette JM, Manley S, Sougrat R, Waterman CM, Kanchanawong P, Davidson MW, Fetter RD (2009). Interferometric fluorescent super-resolution microscopy resolves 3D cellular ultrastructure. Proceedings of the National Academy of Sciences USA 106:3125-3130.
Singh D, Febbo PG, Ross K, Jackson DG, Manola J, Ladd C, Tamayo P, Renshaw AA, D'Amico AV, Richie JP, Lander ES (2002). Gene expression correlates of clinical prostate cancer behavior. Cancer Cell 1(2):203-209.

Strobel K, van den Hoff J, Pietzsch J (2008). Localized proton magnetic resonance spectroscopy of lipids in adipose tissue at high spatial resolution in mice in vivo. Journal of Lipid Research 49(2):473-480.
Thomasson DM, Gharib A, Li KCP (2004). A Primer on Molecular Biology for Imagers. Academic Radiology 11(10):1159-1168.
Weisenburger S, Sandoghdar V (2015). Light Microscopy: An ongoing contemporary revolution. Contemporary Physics56 (2):123-143.
Weissleder R (2002). Scaling down imaging: Molecular mapping of cancer in mice. Nature Reviews Cancer 2(1):11-18.
Won R (2009). Eyes on super-resolution. Interview to Moernet W.E. about, 'Advanced imaging techniques have evolved to see beyond the diffraction limit. Nature Photonics 3:368-369.
Yuste R (2005). Fluorescence microscopy today. Nature Methods 2(12):902-904.

Vol. 20(6), pp.275-286, June, 2021
DOI: 10.5897/AJB2021.17357
Article Number: 9E8610067152
ISSN: 1684-5315

http://www.academicjournals.org/AJB

ACADEMIC JOURNALS
expand your knowledge

African Journal of Biotechnology

Full Length Research Paper

Vigna radiata (mung bean) acid phosphatase is difficult to purify and may have a role as a vegetative Storage protein

Hailey Elizabeth Lightle, Sarah Anne Fosco, Rachel Nicole Giles, Jordyn Marie Meekma, Nicole Marie Moore, Megan Vawn Palacio and Suzanne Elisabet Williams*

Department of Chemistry, Northern Michigan University, 1401 Presque Isle Avenue, Marquette, MI, 49855, USA.

Received 7 May, 2021; Accepted 8 June, 2021

Acid phosphatase from mung bean (*Vigna radiata*) germinated seeds was partially purified via ammonium sulfate precipitation and fully purified via gel excision and heat denaturation, yielding a 29 kDa protein. Using 4-nitrophenylphosphate as a substrate, V_{max} and K_m values of 0.10 µmol/min and 0.27 mM, respectively, were obtained. The acid phosphatase was heat resistant, enhanced by the presence of Fe^{2+} and Mn^{2+} salts, and inhibited by the presence of citrate. Mung bean acid phosphatase reacted immunologically with primary antibodies against *Solanum tuberosum* acid phosphatase, while polymerase chain reaction (PCR) analyses suggest there are some common sequences between mung bean acid phosphatase DNA and that of *Arabidopsis thaliana* acid phosphatase vegetative storage protein. This suggests plant acid phosphatases are structurally as well as functionally related.

Key words: Acid phosphatase, mung bean, *Vigna radiata*, vegetative storage protein.

INTRODUCTION

Phosphatases (3.1.3) are a diverse group of enzymes found in most living systems. Historically, they have been less well studied than protein kinases, but recently there has been more interest in both protein and genetic characterization and regulation (Bheri et al., 2021; Schweighofer and Meskiene, 2015; Brautigan, 2013; Uhrig et al., 2013; Anand and Srivastava, 2012; Moorman and Brayton, 2021). In plants, phosphatases appear to have the important roles of liberating and securing phosphates for growth, especially in germinating seeds (Duff et al., 1994; Anand and Srivastava, 2012). These enzymes are abundant and robust enough that their extraction and analyses are routinely used as a laboratory experiment in undergraduate biochemistry courses (Moorman and Brayton, 2021) as done in Northern Michigan University. Acid phosphatases, which are optimally active at acidic pH, and are the focus of this paper, often appear to catalyze reactions with a broad spectrum of substrates, such as 4-nitrophenyl phosphate, ATP, pyridoxal-5'-phosphate, creatine phosphate, etc. (Verjee, 1969; Joyce and Grisolia, 1960). Several subclasses of acid phosphatase (AP) enzymes include purple acid phosphatases (PAP) which contain a chromogenic iron center (Anand and Srivastava, 2012; Tran et al., 2010; Schenk et al., 2000), tartarate-resistant acid phosphatases which are not affected by tartrate,

*Corresponding author. E-mail: swilliam@nmu.edu. Tel: 906-362-1125.

vegetative storage proteins (VSP) which, in addition to phosphatase activity, also store essential amino acids for growing plants (Staswick, 1994), and DXDXT phosphatases which all share the aspartate, aspartate, and threonine consensus sequence (Collet et al., 1998). Some of these DXDXT phosphatases also have other consensus sequences such as GDXXXD (Thaller et al., 1998); clearly aspartate is an important amino acid for these enzymes. *Arabidopsis thaliana* (thale cress) is a model organism for plants; this means its genome is well-studied and it is often used as a blueprint for plant studies. According to genetic analyses of the *A. thaliana*, putative PAP are the most abundant AP (The Arabidopsis Genome Initiative, 2000; Li et al., 2002), while the actual number of AP enzymes present in a species is related to its polyploidy. A number of studies have been done on plants deprived of phosphate and AP expression increases during times of low phosphate, but the expression varies among plant tissue type, that is, roots vs. leaves (Li et al., 2002; Mission et al., 2005; Wu et al., 2003; Bargaz et al., 2013; Baldwin et al., 2001; Tejera Garcia et al., 2004).

Vegetative storage proteins (VSPs) are thought to be used by plants as a depot for essential amino acids and are metabolized when the need arises, such as during times of growth and injury (Staswick, 1994). At least one of the *A. thaliana* VSPs, VSP2, has been shown to have not only phosphatase activity at acidic pH, but also functions as an anti-insect protein (Liu et al., 2005).
Furthermore, the anti-insect activity, or defense role, is tied to the phosphatase activity as deletion of a critical aspartate in the DXDXT consensus sequence results in loss of both activities. To date sequence analysis of the *A. thaliana* genome suggests over 40 putative AP proteins with no specific functions assigned (The Arabidopsis Genome Initiative, 2000; Li et al., 2002), therefore much remains to be sorted out for this interesting and diverse group of enzymes.

A number of years have been spent using acid phosphatase from *Vigna radiata* (mung bean) sprouts to examine kinetics and protein purification. It is simple to germinate mung bean seeds and the AP activity is easily assayed with 4-nitrophenylphosphate. However, in our hands, the enzyme does not purify with ion exchange chromatography. This is in contrast to the many literature protocols for isolating AP from plants such as common bean (Tejera Garcia et al., 2004), wheat germ (Waymack and Van Etten, 1991), and yellow lupin (Olczak et al., 1997) using anion exchange resins, while protocols for AP isolation from other plants such as soybean (Hegeman and Grabau, 2001), and peanut (Gonnety et al., 2006) employ both anion and cation exchange resins over multiple steps. Nadir et al. (2012) reported using anion exchange chromatography in their partial purification of a 29 kD acid phosphatase protein from germinated mung bean seeds (Nadir et al., 2012), while in 2014 this same research group described the purification of another 29 kD acid phosphatase from the leaves of germinating mung bean seeds using cation exchange chromatography (Saeed et al., 2014). Clearly these reports and numerous isolation procedures suggest that there are several AP isoenzymes in plants and purification is not straight-forward. Surchandra et al. (2012) published a report that described an essentially one-step purification of mung bean AP with ammonium sulfate precipitation; however, after several years of trying, these results could not be duplicated. The current paper describes two methods of isolating mung bean AP, (1) using heat denaturation and (2) using band excision from an SDS polyacrylamide gel. A partial gene was also isolated for mung bean AP using DNA primers based on the sequence of an *A. thaliana* VSP2 acid phosphatase and compared its expression at two different temperatures.

MATERIALS AND METHODS

Chemicals and reagents

All chemicals and reagents, unless otherwise noted, were of research grade and obtained from commercial chemical vendors.

Growth of seedlings

Organic mung bean seeds were obtained from a local food cooperative. The seeds were soaked overnight in water, drained, spread out on paper towels, and covered with aluminium foil to ensure darkness for germination. The seeds were allowed to germinate at room temperature or at 37°C for an average of four days.

Extraction of protein from germinated seedlings

Sprouted seeds (20 to 10 g) were either chopped in a small food processor or mashed thoroughly with a mortar and pestle, and then mixed with cold 0.1 M sodium acetate, pH 5.2 (2.5 mL extraction buffer per gram seed mass). After filtering through cheesecloth the resulting filtrate was centrifuged for 30 min at 12,000 x g, 4°C. The pellet was discarded and the supernatant labeled as “the crude extract”.

Ammonium sulfate precipitation of crude extract

The crude extract was made about 30% in (NH4)2SO4 (0.166 g/mL) and incubated on ice for 30 min. After centrifuging for 30 min at 12,000×g, 4°C, the resulting supernatant was brought to about 70% in (NH4)2SO4 (0.253 g/mL) and incubated for an additional 30 min on ice. The final centrifugation was for 30 min at 17,400×g, 4°C. The pellet was resuspended in 2 mL of cold 0.1 M sodium acetate, pH 5.2 and dialyzed against the same over two days at 4°C in a total of 8 L with one exchange after 24 h.

Assay of acid phosphatase activity

The activity of acid phosphatase was measured using 4-nitrophenylphosphate (4NPP). Assays were conducted at room temperature with 0.1 to 12 mM of substrate, 0.1 M sodium acetate, pH 5.2, buffer in a final volume of 3.0 mL. Termination of the

enzyme activity was done with NaOH (0.1 mL of 8 M yielding a final concentration of 0.27 M). An aliquot of enzyme (usually 0.1 mL or 0.05 mL) was used to initiate the reaction and it was terminated either at 3.0 or 10.0 min with NaOH. Concentration of the product, 4-nitrophenol, was measured spectrophotometrically at 410 nm. The spectrophotometer was blanked for each concentration of PNPP with the same assay concentrations and conditions except that water was used in place of the enzyme. Rates were calculated in µmol/min using 19.3 $mM^{-1}cm^{-1}$ as the molar absorptivity of 4-nitrophenol determined with pure 4-nitrophenol in 0.1 M sodium acetate, pH 5.2.

Determination of Km and Vmax

Maximum velocity (Vmax) and the Michaelis-Menten constant (Km) were calculated over a range of substrate from 0.1 to 12 mM for a 10 min assay. Data were plotted and curve-fitted with Origin graphing software using the Hill function, $Vmax(X^n/K^n + X^n)$ where n = number of binding sites and was set to 1. The data were also analyzed linearly in Lineweaver-Burk, Eadie-Hofstee and Hanes-Woolf plots (Copeland, 2000) and parameters averaged.

SDS- PAGE analysis

Samples were run under denaturing conditions (2-mercaptoethanol) on BioRad 4-20% tris-glycine mini-gels (Laemmli, 1970). Running buffer contained tris, glycine, and SDS; gels were run at 150 V for about 1 h. All gels were stained with 0.1% w/v Coomassie Blue R250 in 50% methanol, 7.5% acetic acid, and 42.5% water, and destained with methanol/acetic acid/water in a 25:10:65 ratio.

Band excision of AP protein from SDS polyacrylamide gel

Samples were run under non-denaturing (no 2-metcaptoethanol) conditions on a BioRad 4 to 20% tris-glycine mini-gel. All of the individual wells were removed from the gel and it was run as one large well in which 160 µL of protein sample plus non-reducing tracking dye were added. The gel was run at 150 V for about 1 h and not stained. The bands (horizontal bands running the width of the gel) of the partially-purified acid phosphatase were cut out of the gel with a clean razor blade and crushed up in 0.1 M sodium acetate, pH 5. The gel fragments were incubated in the sodium acetate buffer overnight at 4°C, physically removed from the buffer the following day. The buffer was concentrated and exchanged with fresh 0.1 M sodium acetate, pH 5.0 using Amicon 10 centrifuge filters.

Heat denaturation studies

Dialyzed mung bean protein was heated to various temperatures for 15 to 30 min. Samples were consequently centrifuged at 10,000×g in a microcentrifuge for 3 to 5 min to remove precipitate.

Western blot analysis

Gels were run as described earlier under non-denaturing (no 2-mercaptoethanol). Instead of staining and fixing gels, they were subjected to electrical transfer in 20 mM tris, 192 mM glycine, and 20% (v/v) methanol at 4°C overnight. Antibodies used were either a primary rabbit antibody against *Solanum tuberosum* (potato) acid phosphatase (Agrisera) followed by a goat anti-rabbit peroxidase conjugate secondary (Rockland), or a rabbit anti-potato acid phosphatase peroxidase conjugate (Rockland) that did not require a secondary antibody. All antibodies were used at vendor recommended dilutions. Incubation buffer was a tris-buffered saline that contained 2% (w/v) instant dry milk, and 0.05 to 0.1% (v/v) tween 20.

Agarose gel analysis

All DNA analyses were performed on 1to 2% (w/v) agarose gels with tris-borate-EDTA running buffer at 80 to 150 V for 1 h (Davis et al., 1994). Detection was with ethidium bromide.

DNA extraction from mung bean sprouts

Mung bean sprouts were germinated at room temperature as specified earlier, frozen in liquid N2, ground, and extracted with the Promega Wizard or the QIAGEN Genomic DNA Purification kits using the plant protocol. Purity and size of DNA was checked by agarose gel electrophoresis.

Polymerase chain reaction (PCR) of mung bean DNA

Primer sets were designed to amplify a region of chromosome 5 of *A. thaliana*. The region of chromosome 5 corresponded to the VSP2 acid phosphatase gene (NCBI database accession# AB006778.1) and comprised 8,500275 to 8,500,296 bp for the forward primer and 8,502,218 to 8,502,242 bp for the reverse primer. The two primer sets, #1 and #2, differed only by an additional nucleotide at one end, and were designed by the primer choosing feature of the NCBI's BLAST program.

Lyophilized primers (25 nmol) were obtained from Integrated DNA Technologies, Inc. The ribulose-1,5-bisphosphate carboxylase/oxygenase enzyme (Rubisco; rbcL) primer was obtained from the Carolina Biological Supply Company. PCR reactions were run using commercially available 10 mM nucleotide mix, 25 mM $MgCl_2$, amplification grade water, Promega's GoTaq polymerase (5U/µL) and green GoTaq buffer, and 6 pm of each primer. A Perkin Elmer 480 thermal cycler was used for amplification with 35 cycles of 94°C for 30 s, 54°C for 45 s, and 72°C for 45 s, after a hot start of 94°C for 5 min.

Reverse transcriptase procedure

Total RNA was isolated from mung bean seeds germinated at room temperature by crushing them in liquid nitrogen and following vendor protocols in the RNAqueous-4PCR total RNA Isolation Kit (Ambion/ThermoFisher Scientific). RNA was quantitated via UV spectroscopy and then subjected to reverse transcription using a GoScript Reverse Transcription System A5000 (Promega). The cDNA was then subjected to PCR as described earlier.

RESULTS AND DISCUSSION

Purification of acid phosphatase

Following the protocol outlined in Surchandra et al. (2012), ammonium sulfate was used in a two-step process to partially purify acid phosphatase (AP) in order to precipitate and concentrate the protein. The Surchandra et al., (2012) process was to use a 30% cut with ammonium sulfate first followed by a 70% cut. A variety of ammonium sulfate concentrations and steps

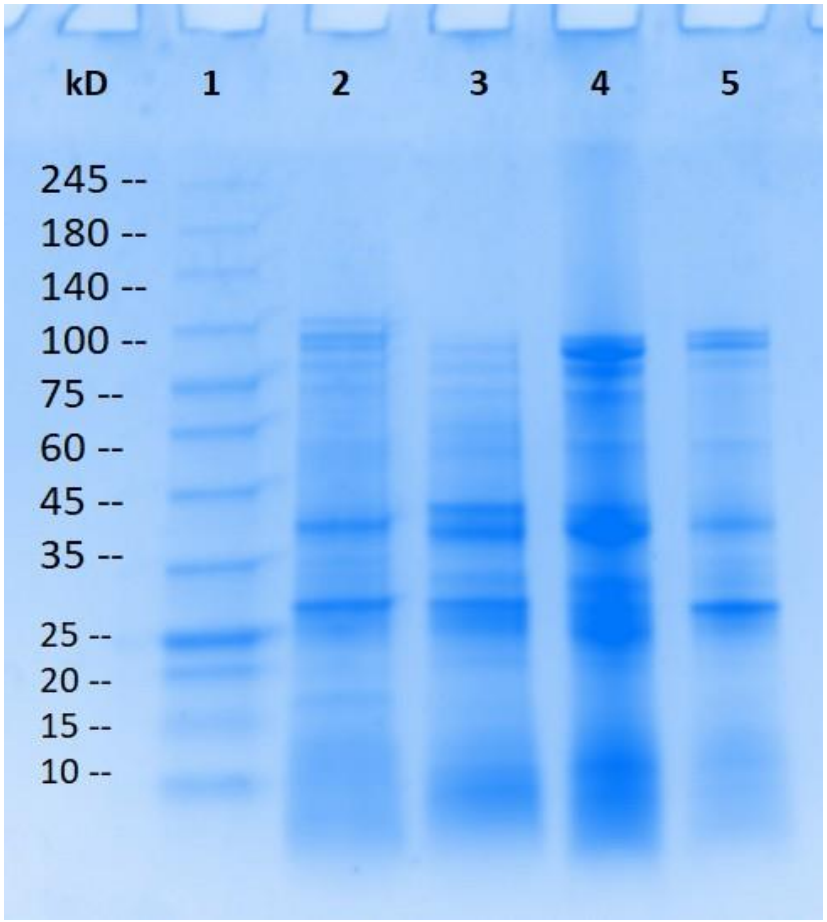

Figure 1. SDS polyacrylamide analysis (4-20% gradient tris-glycine gel) of extracted mung bean protein. Lane 1: GeneTex Trident molecular weight markers, Lanes 2 and 5: two different samples of crude extract (no ammonium sulfate) and Lanes 3 and 4: two different samples of partially purified protein subjected to ammonium sulfate precipitation followed by dialysis.

including single cuts of 50 to 80% ammonium sulfate and two-step cuts having final values of salt at 50 to 90% was also experimented with. It was found that an ammonium sulfate cut of 70% led to the best AP activity, but there was not a drastic difference between the other salt values in terms of activity or purity (data not shown). For purposes of keeping to the Surchandra et al. (2012) protocol for comparisons, most data reported in this paper involve the two step ammonium sulfate precipitation with a final ammonium sulfate cut of 70%. Figure 1 shows the SDS PAGE of ammonium sulfate precipitation followed by dialysis against buffer. Lanes 2 and 5 are two different samples of crude protein extract, while lanes 3 and 4 are two different preparations of extract that has been salted out followed by dialysis. Clearly there are a multitude of bands in the ammonium sulfate-precipitated protein (lanes 3 and 4) and the protein is not pure. In fact there is not much difference between the crude extract and the salted-out protein. This is in contrast to the gel photo reported by Surchandra et al., (2012) which showed a single band at approximately 34,500 Daltons after only ammonium sulfate precipitation.

In order to fully purify the AP enzyme, we tried column chromatography. In our hands, the dialyzed AP did not purify further with cation or anion exchange, gel filtration, or lectin chromatography (data not shown). Heat denaturation followed by centrifugation did lead to a pure protein (Figure 2A, lane 5). These results suggest that mung bean AP is quite heat stable, it remained at least partially active up until 80°C (Figure 4). Bands from a gel of a partial purification in order to obtain pure protein were also excised. After buffer exchange to remove the SDS from the gel bands, it was found that the mung bean acid phosphatase molecular weight was about 29 kDa (Figure 2B). These results are similar to the estimated 34.5 kDa reported by Surchandra et al., (2012), and also fit the putative mung bean acid phosphatase sequence deposited in the NCBI protein database (Kang et al., 2014) which suggests a protein of 31 kDa. The literature

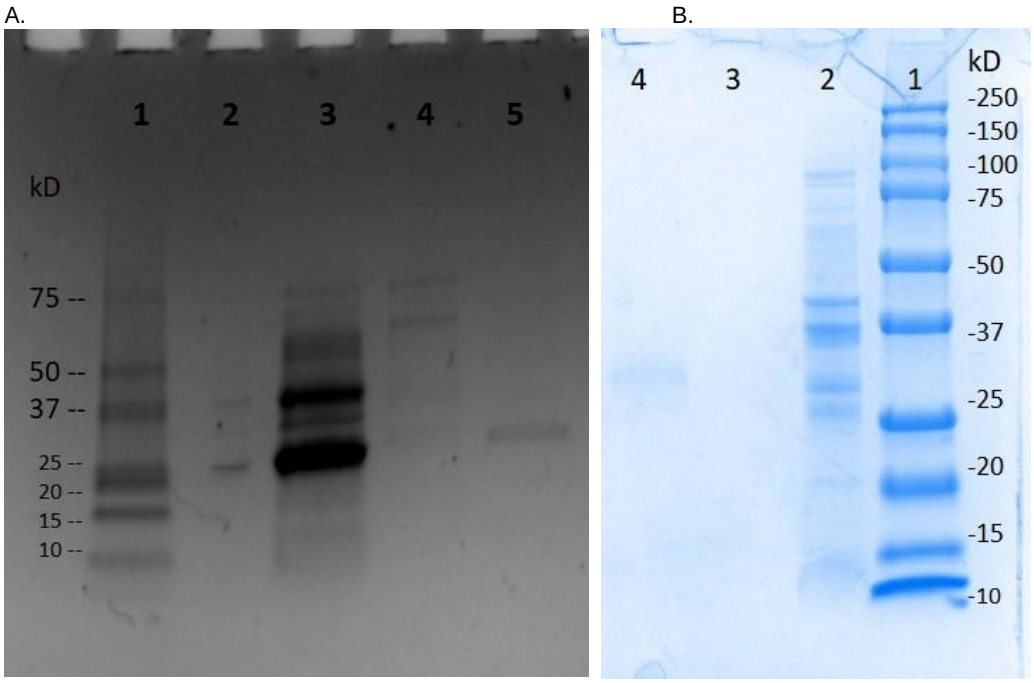

Figure 2. Purification of acid phosphatase from mung bean sprouts. A) Heat denaturation of mung bean protein after ammonium sulfate-precipitation followed by dialysis. Lane 1: BioRad Precision Plus molecular weight markers, Lane 2: empty, Lane 3: dialyzed protein that has not been heat-treated, Lane 4: resuspended protein precipitate after heat treatment, and Lane 5: protein that remained soluble after heat treatment of 15 min at 70°C. B) Band excision of AP from polyacrylamide gel. Lane 1: BioRad Precision Plus molecular weight markers. Lane 2: dialyzed protein after ammonium sulfate precipitation, Lane 3: empty, and Lane 4: band of AP excised from a previous gel after buffer exchange.

reports of acid phosphatase isolation from plants describe either a low molecular weight enzyme of around 30 kDa (Zaman et al., 2020; Saeed et al., 2014; Nadir et al., 2012; Asaduzzaman et al., 2011; Zaman et al., 2020) or a higher molecular weight enzyme around 60 kDa (Anand and Srivastava, 2014; Xie and Shang, 2018). This study produced a low molecular weight AP enzyme. Both reducing and non-reducing gels were used and yielded the same results (data not shown) suggesting the low molecular weight AP is monomeric. It is unclear as to how Surchandra et al. (2012) managed to isolate a single protein with only an ammonium sulfate precipitation. We have one plausible idea; the gel analysis by the Surchandra group may have involved depleted Coomassie blue stain. In our hands any type of Coomassie blue stain has a limited shelf life; depleted stain does not adequately stain all proteins.

Activity assays with 4-nitrophenylphosphate

Because heat denaturation or excising protein from a gel led to either low yields or some significant loss of activity, many of the kinetic assays were performed with partially purified acid phosphatase. Plotting rate versus concentration of 4-nitrophenylphosphate substrate in a saturation plot (Figure 3) showed Michaelis-Menten type kinetics as saturation was achieved and the data fit to a rectangular hyperbola. The experiment was set up in a similar manner to Surchandra et al., (2012) so that we could directly compare the kinetic parameters maximum velocity (V_{max}) and the Michaelis-Menten constant (K_m). V_{max} and K_m from the Michaelis-Menten plot (Figure 3), were 0.10 µmol/min and 0.27 mM, respectively. We also plotted these data with several linear plots (data not shown) which confirmed the experimental V_{max} and K_m.

The values of the present study agree somewhat well with those of Surchandra et al., (2012)'s V_{max} value of 1.33 µmol/min and better with their K_m value of 0.416 mM. Other mung bean AP studies reported a K_m of 0.3 mM (Nadir et al., 2012) and of 0.5 mM (Saeed et al., 2014), also which agree well with our K_m value, especially when considering some studies were done with partially purified enzyme preparations. Additionally, a large difference was noticed in reaction rates when using acetate buffer versus citrate buffer. The enzyme reaction rate was about two times higher when run in 0.1 M acetate buffer, pH 5.2, compared to 0.1 M citrate, pH 5.2. Interestingly, Surchandra et al., (2012) routinely used

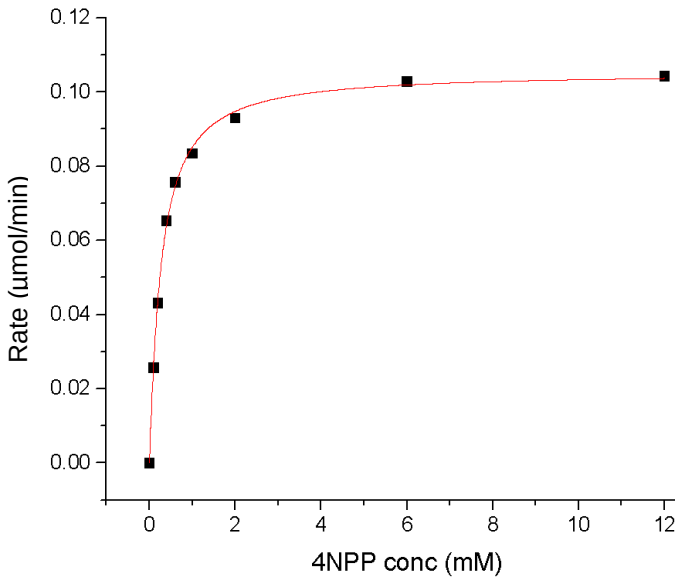

Figure 3. Effect of 4-nitrophenylphosphate (4NPP) concentration on activity of acid phosphatase. Assay was run for 10 min. Detection of the 4-nitrophenolate anion product was done by measuring absorbance at 410 nm. The Hill equation was used to curve fit the data and number of binding sites was set to 1. Origin graphing software provides an adjusted R^2 value and it was 0.998.

citrate buffers in their assays. Along with other research groups, this study performs the AP assay in acetate buffer (Nadir et al., 2012; Saeed et al., 2014) because citrate has been known to inhibit acid phosphatase since 1969 (Verjee, 1969). Another possibility for differences in Vmax values is the number used for the molar absorptivity of the product, 4-nitrophenol (4NP). This study obtained 19.3 mM^{-1} cm^{-1} which was determined by measuring pure 4 NP in 0.1 M acetate buffer, pH 5.2. Surchandra et al. (2012) does not report what molar absorptivity was used, but in our hands the molar absorptivity of 4 NP in 0.1 M citrate buffer, pH 5.2, was about 47X lower than what it is in acetate. Finally, freshly sprouted mung beans were typically used and germinating seeds were not removed; we are not sure what part of the germinating seeds other investigators used.

Heat sensitivity of acid phosphatase

It is interesting that mung bean AP is highly thermostable. Its activity was investigated at several temperatures and optimal temperature was found to be around 60°C (Figure 4), if we ran the entire assay at elevated temperatures. However, when the enzyme was heated first and then assayed there was a dramatic decrease in activity, even at the modest temperatures (Figure 4). At this point we do not have an explanation for the difference in activity. Our optimum temperature for activity of 60°C agrees well with most studies on mung bean acid phosphatase (Surchandra et al., 2012; Nadir et al., 2012; Saeed et al., 2014), but the exact optimal temperature for enzyme activity may not be a useful parameter (Almeida and Marana, 2019) and it might be better to classify enzymes as thermostable or non-thermostable.

Others have found phosphatase enzymes resistant to heat (Tagad and Sabharwal, 2018; Yenigün and Güvenilir, 2003; Wyss et al., 1998; Menichetti et al., 2015). We can speculate that naturally germinating seeds may experience extreme ranges of temperature and this heat stability trait is a survival advantage for plants.

Metal sensitivity

Some preliminary studies examining metal sensitivity show AP is activated by the presence of Mn^{2+} and Fe^{2+}, while it is inhibited by Cu^{2+}, Zn^{2+} and Ca^{2+} compared to buffer conditions (Figure 5). Metal dependence is known for certain acid phosphatases, although it is thought that the substrate is actually the moiety interacting with the metal ion rather than the enzyme itself (Brautigan, 2013).

Western blot analysis

During this study, an antibody raised against mung bean AP was not available, but two different commercial anti-AP antibodies were used to begin investigating the

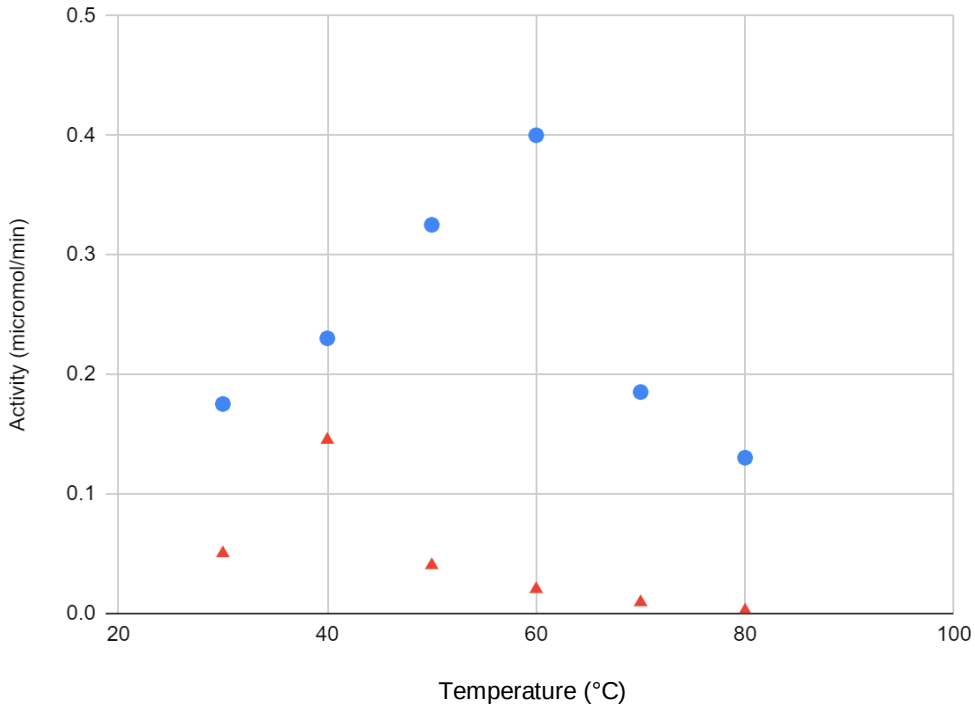

Figure 4. Enzyme activity was measured with para-nitrophenyl phosphate as a substrate in sodium acetate buffer, pH 5.2. Either the enzyme solution was kept at the depicted temperature for 3-5 min, let cool to room temperature and then assayed ("enzyme heated") or the entire assay was run at the depicted temperature for 3-5 min ("assay heated"). All data were normalized for volumes of enzyme used and time of incubation.

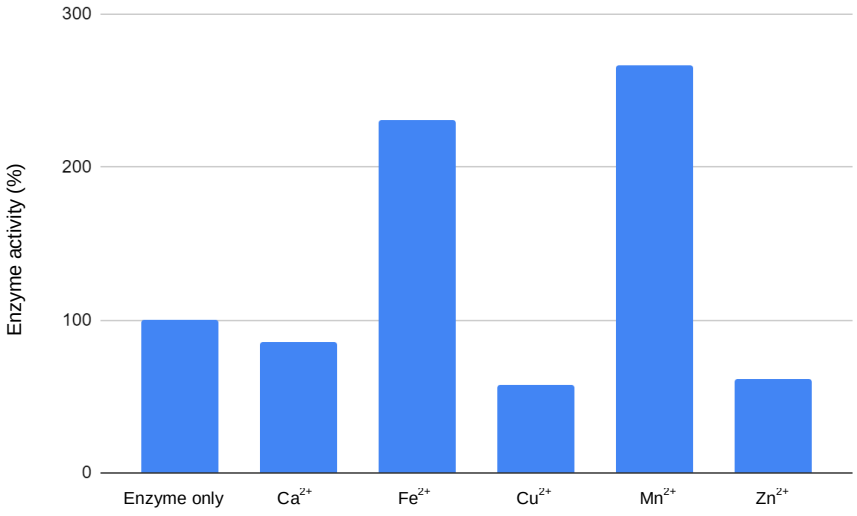

Figure 5. Relative activities of acid phosphatase in the presence of metal ions. The activity of the native enzyme without added metal ions was considered 100% active and the corresponding assays containing 1.0 mM metal ions are shown as a percentage of full activity.

structural similarities between plant acid phosphatases. Using a primary antibody against *S. tuberosum* (potato), the antibody was found to recognize several products from partially purified mung bean AP (Figure 6A, lane 2). The most recognized protein by the potato antibody is about 68 kDa and not our purified AP. Surprisingly, this

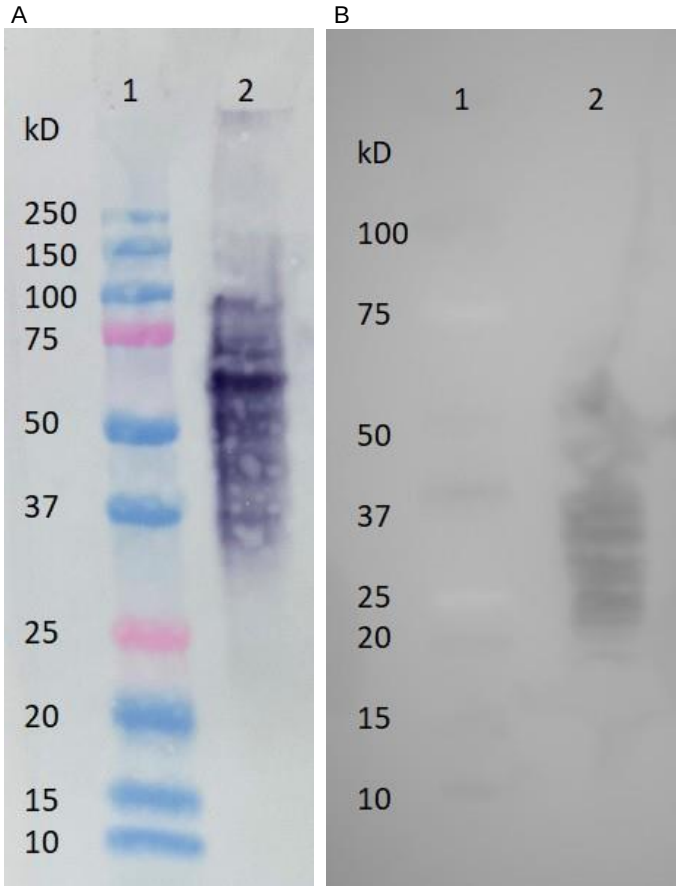

Figure 6. Western blots of mung bean acid phosphatase. Extracts of partially purified protein were run on SDS PAGE and transferred to nitrocellulose. Detection was with anti-acid phosphatase from *Solanum tuberosum* (potato) followed by peroxidase activation of 4-chloro-1-naphthol. A. Primary antibody was an anti-acid phosphatase and secondary antibody was a peroxidase conjugate. B. The primary anti-acid phosphatase antibody was conjugated directly to a peroxidase enzyme, so no secondary antibody was used.

antibody does not recognize any proteins in the molecular weight range of the mung bean AP. A different anti-potato AP antibody was used in a preliminary study (a peroxidase conjugate), and while it also recognizes many proteins, the detected proteins are in the appropriate molecular weight range (Figure 6B, lane 2). Future attempts will be made to use this antibody conjugate against the purified AP once we have obtained enough protein for it to be detectable.

Genetic analysis suggests AP may function as a vegetative storage protein

DNA primers were designed based on the nucleotide sequence of *A. thaliana* vegetative storage protein 2 (VSP2) found in the NCBI protein/gene database, because at the time of this study, no sequences for any *V. radiata* genes had been deposited. Amplification with *A. thaliana* primers (set #1) led to one major band at just under 300 bp (Figure 7, lane 2). Another set of *A. thaliana* primers (set #2) led to one much weaker band at approximately 300 bp (Figure 7, lane 3). As a positive control, a Ribulose-1,5-bisphosphate carboxylase/oxygenase enzyme (Rubisco; rbcL) commercially-available primer was also used to amplify mung DNA. The PCR product is clearly visible at approximately 600 bp (Figure 7, Lane 4). The rbcL primer produces a 600 bp PCR product for Rubisco so these results verify high quality plant DNA from our mung bean extraction.

The only difference between the two primers sets used in lanes 2 and 3 (Figure 7) was an additional nucleotide A. Both primer sets were designed to hybridize to the flanking nucleotide regions of the three exons of *A.*

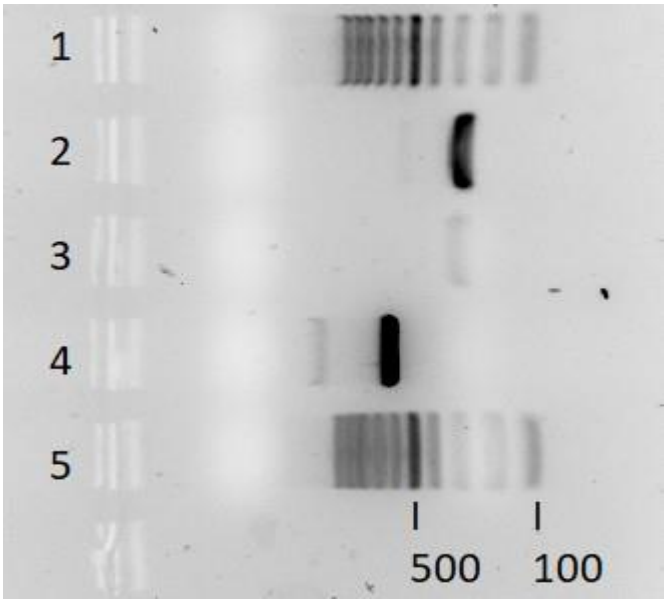

Figure 7. Inverted image of a 1.5% agarose gel at 135 V in tris-buffered EDTA (TBE). Lanes 1 and 5 are 100 bp DNA ladders—the most intense molecular weight band is 500 bp. Lanes 2 and 3 are PCR products of the amplification of mung bean DNA with *Arabidopsis thaliana* primer sets #1 and #2, respectively. Lane 4 is the PCR product of amplification of mung bean DNA with a Rubisco primer (rbcL; Carolina Biological) as a positive control for plant DNA. The same volume of PCR product was loaded into lanes 2-4.

thaliana VSP2, located on chromosome 5.

Because the mung bean DNA actually amplified with *A. thaliana* primers suggests that the VSP2 acid phosphatase gene sequence in *A. thaliana* is related to something in *V. radiata.* A PCR product of 300 bp suggests a protein of about 100 amino acids, while the *A. thaliana* VSP2 is 265 amino acids (Swarbreck et al., 2011). After our genetic results were obtained, a predicted acid phosphatase protein for mung bean was deposited in the NCBI database (accession #XP_014490817.1) (Kang et al., 2014). The translated amino acid sequence for mung bean AP contains the DXDXT consensus sequence (Collet et al., 1998) as well as an additional GDXXXD consensus sequence (Thaller et al., 1998) and has an expected mass of 30, 945 Daltons. This predicted protein fits our purified mung bean AP. Comparison of the mung bean predicted AP protein sequence with the *A. thaliana* VSP2 protein sequence shows only a 41% sequence identity, but the VSP2 protein also contains the same two AP consensus sequences of DXDXT and GDXXXD. Taken together these results suggest the mung bean AP and *A. thaliana* VSP2 are related, and that mung bean AP may have another role as a vegetative storage protein. It was a surprise that our mung bean PCR amplification did not lead to a larger product; it was well short of the 2000 bp expected due to the location of the primers (perimeter of the *A. thaliana* exons). The low sequence identity between the two proteins could explain this. It will be interesting to see what part of the mung bean exon/intron region amplified, and our next step will be to sequence our mung bean PCR product. *A. thaliana* VSP2 has also been found to exert anti-insect activity through its acid phosphatase consensus sequence of DXDXT (Liu et al., 2005). As the predicted protein for mung bean AP has this consensus sequence, it may have a third role as an anti-insect protein. Future studies will be needed to confirm these additional roles for mung bean AP.

Effect of heat on AP protein synthesis

Since mung bean AP is heat stable we were interested if expression of proteins varied during seed germination if the temperature was raised. Seeds were germinated at room temperature and at 37°C and RNA transcription was compared. With the *A. thaliana* primer set #1 we used reverse transcription to create cDNA from isolated mRNA and compared these on a gel (Figure 8). Lane 1 shows cDNA generated from *V. radiata* seed germination at 37°C. There are two distinct bands, one at about 750 bp, and the

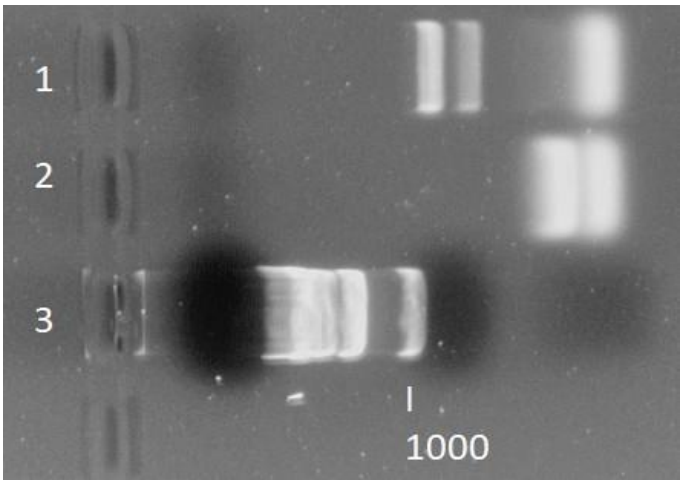

Figure 8. Agarose gel (1 %) at 100 V in tris-buffered EDTA (TBE). Lanes 1 and 2 are PCR amplification products of the cDNA made from a reverse transcriptase reaction of mung bean seed germination. The primers used were *Arabidopsis thaliana* set #1 (designed from vegetative storage protein 2 (VSP2). Lane 2 is amplification of a room temperature seed germination and lane 1 is germination at 37°C. Lane 3 is a 1000 bp DNA ladder. The same volume of PCR product was loaded into lanes 1 and 2.

lower one about 500 bp (based on multiple gels and molecular weight ladders), as well as a larger "fuzzy" band at less than 200 bp (Figure 8, Lane 1). Lane 2 of this gel picture contains the cDNA from a room temperature seed germination of *V. radiata*. Clearly, there are no higher molecular weight cDNA bands, only the lower than 200 bp "fuzzy" bands. The lower bands are indicative of primer aggregation, and do not suggest successful transcription. Because there is evidence of transcription in lane 1 (750 and 500 bp bands), it may be that mRNA transcription of a VSP2 homolog in mung bean during seed germination is induced at elevated temperatures. Thus, it was concluded that the mung bean VSP2 homolog might aid the plant during extreme temperatures.

Conclusion

An attempt was made to duplicate an ammonium sulfate precipitation purification of mung bean acid phosphatase reported previously (Surchandra et al., 2012) which led to a pure 34.5 kD enzyme. In this study, the published procedure led to a mixture of proteins which could not further be resolved by typical protein purification techniques. Mung bean acid phosphatase was purified using heat denaturation or band excision from an SDS polyacrylamide gel. Measuring V_{max} and K_m with 4-nitrophenylphosphate as the substrate on the partially purified mung bean extract yielded 0.10 µmol/min and 0.27 mM, respectively. These values are comparable to those obtained by others (Surchandra et al., 2012; Nadir et al., 2012; Saeed et al., 2014). Using primers designed against an *A. thaliana* AP-vegetative storage protein/anti-insect gene, a short *V. radiata* gene was amplified. This suggests there is at least one VSP2 homolog in mung bean, further studies will be required to determine if the mung bean protein similarly has insecticide activity. As the anti-potato antibody immunologically recognized several mung bean proteins, it is clear that plant acid phosphatases are structurally related, and additional research will address how much they are functionally-related.

The increase in mung bean mRNA during elevated temperature implies that AP thermal stability is not a coincidence and rather it is an important aspect of plant survival during potential temperature extremes. These results show that acid phosphatases are an interesting class of enzymes in plants and understanding them better may lead to advances not only in enzyme characterization, but in agricultural practices.

CONFLICT OF INTERESTS

The authors have not declared any conflict of interests.

REFERENCES

Almeida VM, Marana SR (2019). Optimum temperature may be a misleading parameter in enzyme characterization and application. PLoS ONE 14(2):e0212977.

https://doi.org/10.1371/journal.pone.0212977
Anand A, Srivastava PK (2012). A molecular description of acid phosphatase. Applied Biochemistry and Biotechnology 167(8):2174-2197. doi: 10.1007/s12010-012-9694-8
Anand A, Srivastava PK (2014). Isolation and enzymatic properties of a nonspecific acid phosphatase from *Vigna aconitifolia* seeds. Biotechnology and Applied Biochemistry 61(2):145-152. doi: 10.1002/bab.1131
Asaduzzaman AK, Rahman HM, Yeasmin T (2011). Purification and characterization of acid phosphatase from a germinating black gram (*Vigna mungo* L.) seedling. Archives of Biological Sciences 63(3):747-756.
Baldwin JC, Karthikeyan AS, Raghothama KG (2001). LEPS2, a phosphorus starvation-induced novel acid phosphatase from tomato. Plant Physiology 125(2):728-737. doi: 10.1104/pp.125.2.728
Bargaz A, Ghoulam C, Devron JJ (2013). Specific expression and activity of acid phosphatases in common bean nodules. Plant Signaling and Behavior 8(8):e25022. doi: 10.4161/psb.25022
Bheri M, Mahiwal S, Sanyal SK, Pandey GK (2021). Plant protein phosphatases: What do we know about their mechanism of action? The FEBS Journal 288(3):756-785. doi:10.1111/febs.15454
Brautigan DL (2013). Protein Ser/Thr phosphatases - the ugly ducklings of cell signalling. The FEBS Journal 280(2):324-345. doi:10.1111/j.1742-4658.2012.08609.x
Collet JF, Stroobant V, Pirard M, Delpierre G, van Schaftingen E (1998). A new class of phosphotransferases phosphorylated on an aspartate residue in an amino-terminal DXDX(T/V) motif. Journal of Biological Chemistry 273(23):14107-14112. https://doi.org/10.1074/jbc.273.23.14107
Copeland RA (2000). Enzymes, A practical introduction to structure, mechanism, and data analysis. 2nd edition, Wiley-VCH, New York, NY, pp. 40, 132, 134-135.
Davis L, Kuehl M, Battey J (1994). Basic methods in molecular biology. 2nd edition, Appleton & Lange, East Norwalk, CT, pp. 159-161, and 750.
Duff SMG, Sarath G, Plaxton WC (1994). The role of acid phosphatases in plant phosphorus metabolism. Physiologia Plantarum 90(4):781-800. https://doi.org/10.1111/j.1399-3054.1994.tb02539.x
Gonnety JT, Niamke S, Faulet BM, Kouadio EJPN, Kouame LP (2006). Purification and characterization of three low-molecular-weight acid phosphatases from peanut (*Arachis hypogaea*) seedlings. African Journal of Biotechnology 5(1):035-044.
Hegeman OCE, Grabau EA (2001). A novel phytase with sequence similarity to purple acid phosphatases is expressed in cotyledons of germinating soybean seedlings. Plant Physiology 126(4):1598-1608. doi: 10.1104/pp.126.4.1598
Joyce BK, Grisolia S (1960). Purification and properties of a nonspecific acid phosphatase from wheat germ. Journal of Biological Chemistry 235(8):2278-2281. PMID: 14408027.
Kang JY, Kim SK, Kim M, MY, Lestari P, Kim KH, Ha BK, Jun TH, Hwang WJ, Lee T, Lee J, Shim S (2014). Genome sequence of mung bean and insights into evolution within the Vigna species. Nature Communications 5(5443). https://doi.org/10.1038/ncomms6443
Laemmli UK (1970). Cleavage of structural proteins during the assembly of the head of bacteriophage T4. Nature 227(5259):680-685.
Li D, Zhu H, Liu K, Liu X, Leggewie G, Udvardi M, Wang D (2002). Purple acid phosphatases of Arabidopsis thaliana. Comparative analysis and differential regulation by phosphate deprivation. Journal of Biological Chemistry 277(31):27772-27781. doi: 10.1074/jbc.M204183200
Liu Y, Ahn JE, Datta S, Salzman RA, Moon J, Huyghues-Despointes B, Pittendrigh B, Murdock LL, Koiwa H, Zhu-Salzman K (2005). Arabidopsis vegetative storage protein is an anti-insect acid phosphatase. Plant Physiology 139(3):1545-1556. doi: 10.1104/pp.105.066837
Menichetti L, Reyes Ortigoza A, García N, Giagnoni L, Nannipieri P, Renella G (2015). Thermal sensitivity of enzyme activity in tropical soils assessed by the Q_{10} and equilibrium model. Biology and Fertility of Soils 51:299-310. doi: 10.1007/s00374-014-0976-x
Mission J, Raghothama KG, Jain A, Jouhet J, Block MA, Bligny R, Ortet P, Creff A, Somerville S, Rolland N, Doumas P, Nacry P, Herrerra-Estrella L, Nussaume L, Thibaud MC (2005). A genome-wide transcriptional analysis using Arabidopsis thaliana Affymetrix gene chips determined plant responses to phosphate deprivation. Proceedings of the National Academy of Sciences 102(33):11934-11939. https://doi.org/10.1073/pnas.0505266102
Moorman V, Brayton A (2021). Identification of individual components of a commercial wheat germ acid phosphatase preparation. PLoS ONE 16(3):e0248717. https://doi.org/10.1371/journal.pone.0248717
Nadir S, Saeed A, Naz R, Siddiqua A, Sherazi M, Wazir SM, Saeed A (2012). Isolation, purification and characterization of acid phosphatase from germinating *Vigna radiata* seeds. Journal of the Chemical Society of Pakistan 34(3):717-727.
Olczak M, Watorek W, Morawiecka B (1997). Purification and isolation of acid phosphatase from yellow lupin seeds. Biochimica et Biophysica Acta 1341(1):14-25. doi: 10.1016/s0167-4838(97)00055-1
Saeed A, Salim M, Naz R, Zaman U, Baloch AL, Nadir S, Saeed A (2014) Partial purification, characterization and some kinetic properties of low molecular weight acid phosphatase from leaves of germinating *Vigna radiata* seeds. The Journal of Animal and Plant Sciences 24(5):1466-1477.
Schenk G, Guddat LW, Ge Y, Carrington LE, Hume DA, Hamilton S, de Jersey J (2000). Identification of mammalian-like purple acid phosphatases in a wide range of plants. Gene 250(1-2):117-125. doi:10.1016/s0378-1119(00)00186-4
Schweighofer A, Meskiene I (2015). Phosphatases in plants. Methods in Molecular Biology 1306:25-46. https://doi.org/10.1007/978-1-4939-2648-0_2
Staswick PE (1994). Storage proteins of vegetative plant tissues. Annual Review of Plant Physiology and Plant Molecular Biology 45(1):303-322. https://doi.org/10.1146/annurev.pp.45.060194.001511
Surchandra T, Roy SS, Singh NR, Sahoo MR, Prakash N (2012). Partial purification and biochemical characterization of acid phosphatase from germinated mung bean (*Vigna radiata*) seeds. African Journal of Biotechnology 11(103):16777-16782. doi: 10.5897/AJB12.2552
Swarbreck D, Lamesch P, Wilks C, Huala E (2011). Direct submission to Arabidopsis TAIR10 release. The Arabidopsis Information Resource, Department of Plant Biology, Carnegie Institution, Stanford, CA, 2011.
Tagad CK, Sabharwal SG (2018). Purification and characterization of acid phosphatase from *Macrotyloma uiflorum* seeds. Journal of Food Science Technology 55(1):313-320. doi: 10.1007/s13197-017-2941-9
Tejera Garcia NA, Olivera M, Iribarne C, and Lluch C. (2004) Partial purification and characterization of a non-specific acid phosphatase in leaves and root nodules of *Phaseolus vulgaris*. Plant Physiology and Biochemistry 42(7-8):585-591. doi: 10.1016/j.plaphy.2004.04.004
Thaller MC, Schippa S, Rossolini GM (1998). Conserved sequence motifs among bacterial, eukaryotic, and archaeal phosphatases that define a new phosphohydrolase superfamily. Protein Science 7(7):1647. doi: 10.1002/pro.5560070722
The Arabidopsis Genome Initiative (2000). Analysis of the genome sequence of the flowering plant *Arabidopsis thaliana.* Nature 408:796-815. https://doi.org/10.1038/35048692
Tran HT, Hurley BA, Plaxton WC (2010). Feeding hungry plants: The role of purple acid phosphatases in phosphate nutrition. Plant Science 179(1-2):14-27. https://doi.org/10.1016/j.plantsci.2010.04.005
Uhrig GR, Labandera AM, Moorhead GB (2013). Arabidopsis PPP family of serine/threonine protein phosphatases: many targets but few engines. Trends in Plant Science 18(9):505-513. http://dx.doi.org/10.1016/j.tplants.2013.05.004
Verjee ZHM (1969). Isolation of three acid phosphatases from wheat germ. European Journal of Biochemistry 9(3):439-444. doi: 10.1111/j.1432-1033.1969.tb00628.x
Waymack PP, Van Etten RL (1991). Isolation and characterization of a homogeneous isoenzyme of wheat germ acid phosphatase. Archives of Biochemistry and Biophysics 288(2):621-633. doi:10.1016/0003-9861(91)90245-e
Wu P, Ma L, Hou X, Wang M, Wu Y, Liu F, Deng XW (2003). Phosphate starvation triggers distinct alterations of genome expression in Arabidopsis roots and leaves. Plant Physiology 132(3):1260-1271. doi: 10.1104/pp.103.021022
Wyss M, Pasamontes L, Rémy R, Kohler J, Kusznir E, Gadient M, Müller

F, van Loon AP (1998). Comparison of the thermostability properties of three acid phosphatases from molds: *Aspergillus fumigatus* phytase, A. niger phytase, and A. niger pH 2.5 acid phosphatase. Applied Environmental Microbiology 64(11):4446-4451. doi: 10.1128/AEM.64.11.4446-4451.1998

Xie L, Shang Q (2018). Genome-wide analysis of purple acid phosphatase structure and expression in ten vegetable species. BMC Genomics 19:646. doi: 10.1186/s12864-018-5022-1

Yenigün B, Güvenilir Y (2003). Partial purification and kinetic characterization of acid phosphatase from garlic seedling. Applied Biochemistry and Biotechnology 105-108:677-87. doi:10.1385/ABAB:107:1-3:677

Zaman U, Naz R, Khattak NS, ur Rehman K, Iqbal A, Ahmad S, Shah LA (2020). Investigating the thermodynamic and kinetics properties of acid phosphatase extracted and purified from seedlings of *Chenopodium murale*. International Journal of Biological Macromolecules 165:1475-1481. https://doi.org/10.1016/j.ijbiomac.2020.10.041

Related Journals: